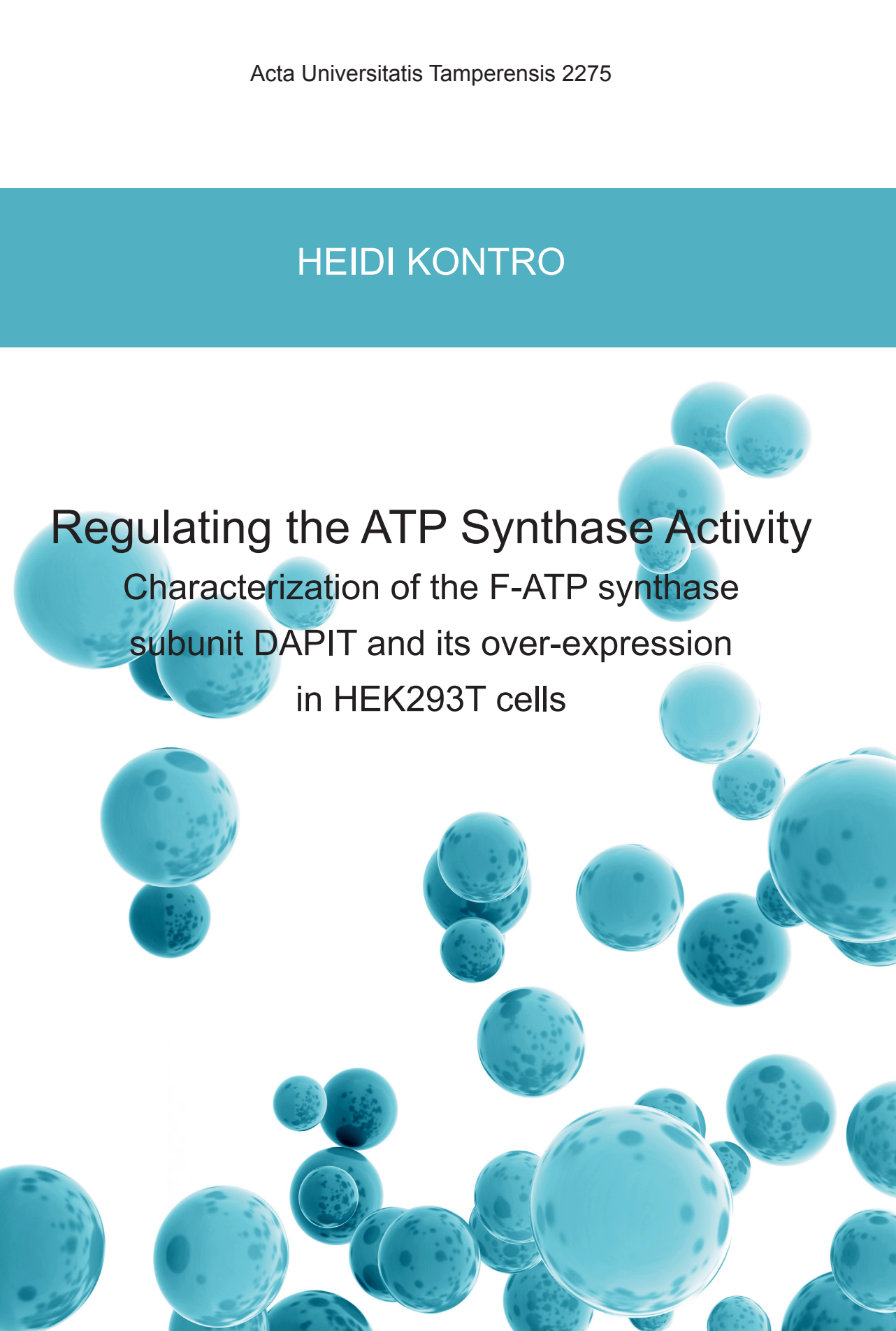


HEIDI KONTRO



Regulating the ATP Synthase Activity

Characterization of the F-ATP synthase
subunit DAPIT and its over-expression
in HEK293T cells



HEIDI KONTRO

Regulating the ATP Synthase Activity

Characterization of the F-ATP synthase
subunit DAPIT and its over-expression
in HEK293T cells



ACADEMIC DISSERTATION

To be presented, with the permission of
the Faculty council of the Faculty of Medicine and Life Sciences
of the University of Tampere,
for public discussion in the Jarmo Visakorpi auditorium
of the Arvo building, Lääkärintäti 1, Tampere,
on 19 May 2017, at 12 o'clock.

UNIVERSITY OF TAMPERE

HEIDI KONTRO

Regulating the ATP Synthase Activity

Characterization of the F-ATP synthase
subunit DAPIT and its over-expression
in HEK293T cells

Acta Universitatis Tamperensis 2275
Tampere University Press
Tampere 2017

ACADEMIC DISSERTATION

University of Tampere, Faculty of Medicine and Life Sciences
Finland

Supervised by

Professor Heikki Kainulainen
University of Jyväskylä
Finland
Professor Emeritus Markku Mäki
University of Tampere
Finland

Reviewed by

Dr. Tomáš Mráček
Institute of Physiology CAS
Czech Republic
Docent Pekka Taimen
University of Turku
Finland

The originality of this thesis has been checked using the Turnitin OriginalityCheck service in accordance with the quality management system of the University of Tampere.

Copyright ©2017 Tampere University Press and the author

Cover design by
Mikko Reinikka

Acta Universitatis Tamperensis 2275
ISBN 978-952-03-0425-6 (print)
ISSN-L 1455-1616
ISSN 1455-1616

Acta Electronica Universitatis Tamperensis 1777
ISBN 978-952-03-0426-3 (pdf)
ISSN 1456-954X
<http://tampub.uta.fi>

Suomen Yliopistopaino Oy – Juvenes Print
Tampere 2017



To my family

ABSTRACT

Type 1 diabetes (TD1) is a complex metabolic disorder accompanied by alterations in cellular physiology, metabolism and gene expression. Previously it has been shown that in type I diabetic mice several mRNAs coding the proteins of complexes in the electron transport chain in the mitochondria are down-regulated. However, it is not known how diabetes affects the composition or activity of the mitochondrial energy-producing enzyme, ATP synthase. This study discovered and characterized a supernumerary subunit, Diabetes Associated Protein in Insulin-sensitive Tissues, DAPIT, of the ATP-synthase membrane-embedded F_0 complex. In addition, the effects of over-expression of DAPIT on cellular and molecular level were characterized to clarify its consequences in type 1 diabetes.

This thesis comprises three separate studies. Study I discovered, named and characterized a novel protein, DAPIT, in the insulin-sensitive tissues of a type 1 diabetic rat by differential display (DD-PCR) methodology, sequencing, Northern blot and database search. In study II a custom-made antibody against DAPIT was characterized, the protein histological expression in several rat and human tissues was described and its mitochondrial presence at cellular level was confirmed. Furthermore, it was proposed that DAPIT could be a common component of proton pumps. Also, the protein level of DAPIT and its myofiber-type specific expression was studied in insulin-sensitive tissues of healthy and diabetic rats and the muscle calf complex of mice. Finally, in study III a gene-manipulated cell line over-expressing DAPIT was constructed and characterized at mitochondrial, metabolic, morphological and behavioral levels.

Study I revealed that DAPIT was a small membrane-spanning protein conserved in the animal kingdom. In healthy rat its mRNA was highly expressed in aerobic, including insulin-sensitive tissues. In diabetic rats the mRNA expression was down-regulated in the myocardium and skeletal muscle compared to control tissues. The results of study II showed that the antibody against the carboxy-terminal end of DAPIT recognized the protein at both cellular and tissue levels. Exploiting this antibody, mitochondrial and lysosomal expression of DAPIT was demonstrated. The antibody against the amino-terminus of the protein was not functional in all the applications used. In histochemical studies of tissues from healthy humans and rats,

DAPIT was abundant in insulin-sensitive tissues employing aerobic metabolism and in epithelium actively transporting nutrients and ions. In insulin-sensitive tissues of diabetic rats DAPIT was over-expressed in myocardium, skeletal muscle (namely gastrocnemius) and adipose tissue, but down-regulated in the liver compared to healthy rats. In comparison to mice skeletal muscle (calf complex composed of gastrocnemius, soleus and plantaris), no difference in protein expression was seen due to heterogeneity in muscle myofiber types. Finally, in a cell-line over-expressing DAPIT in study III it was shown that an increase at protein level severely impaired the mitochondria by inactivating the ATP-synthase activity regardless of active respiration of the cells. As a consequence, the mitochondria produced reactive oxygen species (ROS), which most likely up-regulated transcription factors, further regulating anaerobic metabolism and cell dedifferentiation. As a result, the epithelial type of cells transformed into mesenchymal-like and decelerated its proliferation rate. Searches in databases implicated DAPIT over-expression as being abundant in various cancer cell lines, suggesting that it could function as an oncogene when over-expressed in the presence of insulin.

The studies in this series enabled the discovery and characterization of a novel protein, DAPIT, in insulin-deficient diabetes. Its expression at cellular and tissue level in healthy and diabetic humans and rodents was characterized with a custom-made antibody. DAPIT over-expression diminished the activity of the energy-producing ATP-synthase, thereby regulating cellular metabolism to the point of aerobic glycolysis and disappearance of the epithelial characteristics of the studied cell line. As a consequence, the dedifferentiated cells showed several features of cancer stem cells, which are discussed. In addition to the DAPIT over-expressing cell line and type 1 diabetes, this over-expression, according to literature and databases, was also seen in Parkinson's disease, multiple sclerosis (MS), high weight gain, cardiac hypertrophy and arsenic-related toxicity. These findings suggest that DAPIT over-expression could be a more common phenomenon in regulating ATP-synthase and inactivity of oxidative phosphorylation in diseases where metabolic disturbances play a significant role, for example diabetes, cancer, degenerative, autoimmune, toxin and epigenetically regulated conditions. The knock-in mouse recognizing the pathologic changes in question would be of help in understanding the consequences of mitochondrial impairments due to DAPIT over-expression.

TIIVISTELMÄ

Tyypin 1 diabetes on monimutkainen metabolinen häiriötila, joka aiheuttaa muutoksia solun fysiologiaan, aineenvaihduntaan ja geenien ilmentymiseen. Insuliinin puutoksen tiedetään aiheuttavan hiiren kudoksissa geenisäätelyn häiriintymistä mm. laskemalla mitokondriaalisen elektroninsiirtoketjun proteiinien mRNA-tasoa. Sen sijaan energiaa tuottavan ATP-syntaasin rakenneyksiköiden ilmentyminen diabeteksessa on proteiinitasolla vielä tuntematonta, kuten ilmentymisen vaikutukset itse entsyymikompleksin aktiivisuuteenkin. Tässä väitöskirjatyössä on löydetty ja karakterisoitu ATP-syntaasin F_0 kompleksin rakenneproteiini Diabetes Associated Protein in Insulin-sensitive Tissues, DAPIT. Lisäksi sen yli-ilmentymisen vaikutusta solun fysiologiaan on luonnehdittu molekyylibiologisin keinoin diabeettisen ja muun tautiyhteyden selventämiseksi.

Väitöskirja koostuu kolmesta erillisestä osatyöstä. Osatyössä I DD-PCR-, sekvensointi-, Northern blot-menetelmien sekä tietokantahaun avulla löydettiin, nimettiin ja karakterisoitiin uusi proteiini, DAPIT, tyypin 1 diabeettisen rotan insuliiniherkistä kudoksista. Osatyössä II karakterisoitiin erikoisvalmisteinen, DAPITin tunnistava vasta-aine, jonka avulla proteiinin ilmentyminen havainnollistettiin immunohistokemiallisesti useissa rotan ja ihmisen kudoksissa. Lisäksi vahvistettiin DAPITin mitokondriaalinen esiintyminen solutasolla, sekä havaittiin lysosomaalinen ilmentyminen. DAPITin ilmentymistä tutkittiin myös diabeettisen rotan ja hiiren insuliiniherkissä kudoksissa, ja havainnollistettiin sen lihassäie-spesifinen esiintyminen hiiressä. Väitöskirjan osatyössä III geenimuuntelun avulla rakennettiin DAPITia yli-ilmentävä solulinja, jonka mitokondrioita, energia-aineenvaihduntaa, morfologiaa ja käyttäytymisominaisuuksia selvitettiin.

Osatyö I tuotti uuden DAPIT-proteiinin, joka osoittautui konservoituneeksi eläinkunnassa. Terveellä rotalla proteiinin lähetti-RNA ilmeni runsaana mm. insuliiniherkissä kudoksissa. Diabeettisella rotalla lähetti-RNAn ilmentyminen oli alentunut sydämessä ja lihaksessa kontrollikudokseen verrattuna. Osatyössä II DAPITin aminohapposekvenssin karboksyylipäähän suunniteltu vasta-aine tunnisti kohteensa sekä solu- että kudostasolla. Vasta-aineen avulla nähtiin DAPITin erityinen ilmentyminen mitokondrioissa ja lysosomeissa. Aminopäähän suunniteltu vasta-aine ei ollut yhtä luotettava jokaisessa sovelluksessa. Ihmisen ja rotan kudosten

immunohistokemiallisessa tutkimuksessa DAPITia esiintyi runsaasti aerobista aineenvaihduntaa hyödyntävissä insuliiniherkissä kudoksissa, sekä aktiivisesti ravinteita ja ioneja kuljettavissa epiteelirakenteissa. Diabeettisen rotan insuliiniherkkien kudosten tutkimus osoitti DAPITin proteiinitason olevan koholla, toisin kuin lähetti-RNA tasolla, sydämessä, lihaksessa ja rasvassa mutta alentunut maksassa normaaliin kudokseen verrattuna. Terveen ja diabeettisen hiiren lihaksessa eroja sen sijaan ei havaittu lihasyhdistelmän runsaan säietyyppivaihtelun vuoksi. Osatyössä III DAPITia aktiivisesti ilmentävässä solulinjassa havaittiin merkittävä mitokondriaalinen haitta proteiinin normaalia runsaamman esiintymisen seurauksena: Energiaa tuottavan ATP-syntaasin aktiivisuus laski lisääntyneestä soluhengityksestä huolimatta. Tämän seurauksena syntyi mitokondrioiden tuottamia happiradikaaleja, jotka todennäköisesti säätelivät transkriptiotekijöitä, siten edistäen anaerobista aineenvaihduntaa ja solun taantumista. Lopulta epiteelityypin solu muuntui mesenkymaaliseksi hidastaen jakautumistaan ja liikkumistaan. Geenien monistumisesta raportoiva tietokanta osoitti DAPITin lisääntyneen ilmentymisen olevan runsasta useissa syöpäsolulinjoissa ja syövässä, ehdottaen sillä olevan syöpiä edistäviä onkogeenisia ominaisuuksia.

Tämän väitöskirjan tutkimukset mahdollistivat uuden DAPIT proteiinin löytymisen insuliinipuutostilanteessa. Teetetyn vasta-aineen avulla sen ilmentyminen havainnollistettiin solu- ja kudostasolla ihmisen ja jyräjän terveissä ja diabeettisissa kudoksissa. Normaalia runsaammin ilmentyessään DAPIT aiheuttaa ATP-syntaasin aktiivisuuden heikentymistä huolimatta hengitysketjun toiminnan aktivoitumisesta. Tämän seurauksena solun aineenvaihdunta ohjautuu glykolyysiin, mikä morfologiatasolla näkyy epiteeliominaisuuden häviämisenä. Solu taantuu monella tapaa osoittaen useita syöpien kantasolujen ominaisuuksia, joista on keskusteltu. Tutkitun solulinjan ja tyypin 1 diabeteksen lisäksi kirjallisuuden ja tietokantojen perusteella DAPITin runsasta ilmentymistä lähetti-RNA tasolla esiintyy myös muissa patofysiologissa tautimalleissa ja tiloissa, kuten Parkinsonin taudissa, multippelissa skleroosissa, painon nousussa, sydämen vajaatoiminnassa ja arseenialtistumisessa. Tämä väitöskirja yhdessä kirjallisuuden kanssa viitoittavat runsaan DAPITin ilmentämisen mahdollisesti olevan yleinen ominaisuus, joka vaikuttaa ATP-syntaasin aktiivisuuteen ja siten energiantuottoon sairauksissa ja tiloissa, joihin metaboliset häiriöt osallistuvat. Näihin kuuluvat mm. diabetes, syöpä, degeneroivat ja autoimmunisairaudet, sekä myrkkujen ja epigenetiikan säätelemät tilat. Kudosten ja solutyypin patologisia muutoksia väitöskirjassa kuvatun mitokondriaalisen haitan seurauksena selventäisi geneettisellä ohjauksella DAPITia runsaasti ilmentävä hiiri,

jonka karakterisoiminen mahdollistaisi yleisemmän haitan vaikutusten tunnistamisen.

CONTENTS

ABSTRACT	5
TIIVISTELMÄ.....	7
CONTENTS.....	11
LIST OF ORIGINAL PUBLICATIONS	15
ABBREVIATIONS	16
1 INTRODUCTION.....	21
2 REVIEW OF THE LITERATURE.....	22
2.1 Type 1 diabetes.....	22
2.1.1 Streptozotocin-induced diabetes.....	22
2.1.2 Cellular regulation upon insulin deficiency	23
2.2 Mitochondria	23
2.2.1 Biogenesis, structure and protein transport	24
2.2.2 Oxidative phosphorylation (OXPHOS).....	25
2.2.2.1 Respiratory chain complexes.....	26
2.2.2.2 ATP synthase.....	27
2.2.2.2.1 Overall structure.....	28
2.2.2.2.2 Supernumerary subunits including DAPIT	29
2.2.2.2.3 Inhibitory factor 1 (IF1)	30
2.2.2.2.4 Dimerization, cristae formation and superassemblies.....	31
2.2.2.2.5 Membrane permeability.....	32
2.2.2.2.6 Membrane rearrangement in cellular ageing and stem cell differentiation	32
2.2.2.2.7 Ectopic F-ATPase.....	32
2.3 Cell metabolism and differentiation.....	33
2.3.1 Aerobic glycolysis.....	33
2.3.2 Proliferation and differentiation	35
2.3.3 Hif1a and ROS.....	35
2.3.4 Epithelial to mesenchymal transition, EMT	36

3	AIMS OF THE STUDY	37
4	MATERIALS AND METHODS	38
4.1	Animals, human samples and ethical permission (I, II).....	38
4.2	Cell lines and cell culture (II, III)	38
4.3	RNA isolation and detection methods (I, III).....	39
4.3.1	RNA isolation and DD-PCR (I).....	39
4.3.2	DNA cloning and sequence analysis (I).....	39
4.3.3	Northern hybridization (I).....	40
4.3.4	DNA constructs, transfection and semi-quantitative PCR (III)	40
4.4	Protein detection (II, III)	41
4.4.1	Total and nuclear protein isolation from tissues and cells (II, III).....	41
4.4.2	DAPIT antibodies (II)	42
4.4.3	Western blot (II, III)	42
4.4.4	Immunohistochemistry and -fluorescence of cells and tissues (II, III)	43
4.5	Mitochondrial function (III)	44
4.5.1	DNA copy number (III)	44
4.5.2	Activity of TCA cycle and respiratory chain (III).....	45
4.5.3	Mass, membrane potential and superoxide level assays (III)	45
4.5.4	Isolation of mitochondria and complex V activity (III)	46
4.6	Cell functional measurements (III)	47
4.6.1	Growth, mortality and synchronization (III)	47
4.6.2	Migration and adhesion (III)	47
4.6.3	Glucose and lactate assays (III).....	48
4.6.4	Oncomine and CCLE data-analysis (III).....	48
5	RESULTS	49
5.1	DD-PCR in diabetic rat insulin-sensitive tissues (I)	49
5.2	Molecular characterization of DAPIT (I).....	51
5.2.1	Northern blot analysis of DAPIT mRNA (I)	51
5.2.2	mRNA and protein sequence of DAPIT and its homologues (I).....	53
5.2.3	Structural analysis of DAPIT (I)	55
5.3	Localization and tissue expression of DAPIT (II).....	55
5.3.1	Specificity of DAPIT antibodies (II)	55

5.3.2	Cellular localization of DAPIT by immunofluorescence (II)	56
5.3.3	Tissue expression of DAPIT by immunohistochemistry and Western blot (II)	57
5.4	Metabolism and cell behavior of DAPIT over-expressing HEK293T cells (III)	58
5.4.1	Terminology and normalization of mitochondrial parameters (III)	58
5.4.2	Decreased mitogenesis (III)	58
5.4.3	DAPIT over-expression (III)	60
5.4.4	Metabolic activity of mitochondria (III)	61
5.4.5	Nuclear proteins (III)	63
5.4.6	Cell morphology and junction and adhesion proteins (III)	63
5.4.7	Cell growth, mortality, migration and adhesion (III)	63
5.4.8	Glucose consumption and lactate production (III)	65
5.4.9	<i>Usmg5</i> copy number in cancer cell lines (III)	66
6	DISCUSSION AND FUTURE PERSPECTIVES	67
6.1	DD- PCR (I)	67
6.2	Structural analysis and cellular localization of DAPIT (I, II)	68
6.3	Specificity of DAPIT antibodies (II)	70
6.4	Tissue expression of DAPIT by Western blot and immunohistochemistry (II)	71
6.5	Metabolism and cell behavior of DAPIT over-expressing cells (III)	72
6.5.1	Overall effects on mitochondria (III)	72
6.5.2	ATP synthase activity (III)	73
6.5.3	Aerobic glycolysis and epithelial to mesenchymal transition (III)	74
6.5.4	Morphology, migration and proliferation (III)	75
6.6	Defects and diseases of mitochondrial ATP synthase	76
6.6.1	Nuclear genetic defects	76
6.6.2	DAPIT down-regulation	76
6.6.3	DAPIT over-expression	77
6.6.3.1	Cancer cell lines, tumors and stemness	77
6.6.3.2	Type 1 diabetes, Parkinson's disease and multiple sclerosis (MS)	81
6.6.3.3	Weight-gaining, cardiac hypertrophy and arsenic metabolism	81
6.7	Strengths, limitations and future prospects	82

7	SUMMARY	84
8	ACKNOWLEDGEMENTS	86
9	REFERENCES.....	89
10	SUPPLEMENTS	107
11	ORIGINAL PUBLICATIONS.....	113

LIST OF ORIGINAL PUBLICATIONS

This thesis is based on the following original communications, which are referred to in the text by the Roman numerals I-III:

I Päivärinne H, Kainulainen H. DAPIT, a novel protein down-regulated in insulin-sensitive tissues in streptozotocin-induced diabetes. *Acta Diabetol.* 2001, 38(2):83-6.

II Kontro H, Hulmi JJ, Rahkila P, Kainulainen H. Cellular and tissue expression of DAPIT, a phylogenetically conserved peptide. *Eur J Histochem.* 2012 May 22;56(2):e18.

III Kontro H, Cannino G, Rustin P, Dufour E, Kainulainen H. DAPIT Over-Expression Modulates Glucose Metabolism and Cell Behavior in HEK293T Cells. *PLoS One.* 2015 Jul 10;10(7):e0131990.

Correction: *PLoS One.* 2015; 10(10): e0141036.

Correction: *PLoS One.* 2015; 10(11): e0143268.

The original publications are reprinted with the permission of the copyright holders.

ABBREVIATIONS

5' RNA CAP	a specially altered nucleotide on the 5' end of precursor messenger RNA
6,8 PL	6,8 kDa proteolipid
aD15C	carboxy-terminal antibody against DAPIT
aD15N	amino-terminal antibody against DAPIT
ADP	adenosine diphosphate
AMP	adenosine monophosphate
AMPK	5' adenosine monophosphate-activated protein kinase
ANT	ADP/ATP translocase
AS3MT	arsenic methyltransferase
ATCC	American Type Culture Collection
ATP	adenosine triphosphate
ATP5a1	a subunit of mitochondrial ATP synthase
ATP5e	ATP Synthase Mitochondrial F ₁ Complex, Epsilon Subunit
Atp6v0d1	ATPase, H ⁺ transporting, lysosomal V ₀ subunit D1
ATPAF2	ATP synthase, Mitochondrial F ₁ complex, Assembly Factor 2
Bak	bcl-2-like protein
Bax	bcl-2-like protein 4
BLAST	basic local alignment search tool
BSA	bovine serum albumin
C2C12	mouse myoblast cell line
CCLE	Cancer Cell Line Encyclopedia
cDNA	complementary DNA
CI, Complex I	NADH/ubiquinone oxidoreductase
CII, Complex II	succinate dehydrogenase
CIII, Complex III	cytochrome <i>c</i> reductase
CIV, Complex IV	cytochrome <i>c</i> oxidase
CV, Complex V	ATP synthase

Cox7c	cytochrome c oxidase subunit VIIc
COXII	cytochrome c oxidase subunit 2
CpG	5'—C—phosphate—G—3'
Crb1	Crumbs Family Member 1
CSC	cancer stem cell
DAPIT	Diabetes Associated Protein in Insulin-sensitive Tissues
DD-PCR	differential display – PCR
DMEM	Dulbecco's modified Eagle's medium
DNA	deoxyribonucleic acid
DNase I	deoxyribonuclease I
dNTP	nucleoside triphosphate
EDTA	ethylenediaminetetraacetic acid
EGTA	aminopolycarboxylic acid
ELISA	enzyme-linked immunosorbent assay
EMBL	European Molecular Biology Laboratory
EMT	epithelial to mesenchymal transition
ESC	embryonic stem cells
EST	expressed sequence tag
F ₁ F ₀ -ATPase	ATP synthase
FADH ₂	reduced flavin adenine dinucleotide
F-ATPase	ATP synthase
FBS	fetal bovine serum
FCCP	carbonyl cyanide-4-(trifluoromethoxy)phenylhydrazone
F ₀	membrane-imbedded complex of ATP synthase
GLUT4	glucose transporter 4
Gpx1	glutathione peroxidase-1
GTP	guanosine triphosphate
GTPase	enzyme hydrolyzing GTP
GABPA	GA binding protein transcription factor, alpha subunit
H ⁺	hydrogen ion
H ₂ O ₂	hydrogen peroxide
HEK293T	human embryonic kidney 293T cells
Hif1a	hypoxia inducible factor 1 <i>alpha</i>
HRP	horseradish peroxidase

HSP60	heat shock protein 60
HUVEC	human umbilical vein endothelial cells
IF1	ATP synthase inhibitory factor 1
IgG	immunoglobulin G
kDa	kilo Dalton
ΔP	mitochondrial membrane potential
LAMP	lysosome-associated membrane glycoprotein
LKB1	loss of liver kinase B1
MIM	mitochondrial inner membrane
miR302/367	cluster of a small non-coding RNA molecule 302 and 367
MIRCO	muscle insulin receptor knockout mice
MitoSox	mitochondrial superoxide indicator
MOM	mitochondrial outer membrane
mPTP	mitochondrial permeability transition pore
mRNA	messenger ribonucleic acid
MS	multiple sclerosis
mtDNA	mitochondrial DNA
c-MYC	proto-oncogene; a cellular homolog of V-Myc Myelocytomatosis Viral Oncogene
NADH	reduced nicotinamide adenine dinucleotide
NAO	10-N-Nonyl acridine orange
NDFUS3	NADH:ubiquinone-oxidoreductase
Ndufs2	NADH Dehydrogenase (Ubiquinone) Fe-S Protein 2
Neb-cGP	flybase ortholog of <i>Usmg5</i> gene
NIH	National Institute of Health
Nme2	nucleoside diphosphate kinase 2
Nnt	nicotinamide nucleotide transhydrogenase
NRF-1	nuclear respiratory factor 1
nt	nucleotide
OPTN	optineurin
ORF	open reading frame
OSCP	oligomycin sensitivity-conferring protein
OXPHOS	oxidative phosphorylation
p	value indicating statistical significance
p2/ras	pointed P2/ras oncogene

p53	phosphoprotein p53
PBS(T)	phosphate-buffered saline (Tween 20 detergent)
PCR	polymerase chain reaction
PDK	pyruvate dehydrogenase kinase
Prx3	peroxiredoxin 3
PFA	paraformaldehyde
PGC-1 α	peroxisome proliferator-activated receptor gamma coactivator 1a
Pi	phosphate ion
PI	propidium iodide
PI3K	phosphatidylinositol-4,5-bisphosphate 3-kinase
PiC	phosphate carrier
pIRES2-EGFP	cloning vector with internal ribosome entry site and enhanced green fluorescence protein
PMS/MTS	commercial reagents for cell proliferation assay
PPAR γ	peroxisome proliferator-activated receptor <i>gamma</i>
PPP1G	protein phosphatase gamma 1
PSC	pluripotent stem cell
PMSF	phenylmethylsulfonyl fluoride
qPCR	quantitative PCR
r	statistical correlation value
RhoA	Ras homolog gene family, member A
RNA	ribonucleic acid
ROS	reactive oxygen species
RT-PCR	reverse transcriptase PCR
SDS-PAGE	sodium dodecyl sulphate - polyacrylamide gel electrophoresis
Ser 129	serin 129
SMA	smooth muscle actin
Mn/Cu/ZnSOD	manganese/copper/zink-dependent sodium dismutase
STZ	streptozotocin
SV40	simian virus 40
TBS(T)	tris-buffered saline (Tween 20 detergent)
TCA	titric acid cycle

TD1	type 1 diabetes
TGF-beta	transforming growth factor beta
Trx2	thioredoxin 2
Thr	threonine
TIC	tumor-initiating cell
TIM	translocase of inner mitochondrial membrane
TMEM70	transmembrane protein 70
TMRM	tetramethylrhodamine, methyl ester
TOM	translocase of outer mitochondrial membrane
TOPO-TA	commercial cloning vector
UCP	uncoupling protein
<i>Usmg5</i>	up-regulated during skeletal muscle growth 5 -gene
V-ATPase	vacuolar ATPase
VDAC	voltage-dependent anion channel
Wnt	signal transducing protein; name "Wnt" combines the genes <i>Wingless</i> and <i>Integration-1</i>
YEATS4	<i>YEATS</i> domain containing 4

1 INTRODUCTION

Type 1 diabetes (TD1) is a common endocrine disease, which exerts its effects through insulin-deficiency. The pancreatic beta cells secreting insulin are destroyed in TD1, introducing an elevated blood glucose level known as hyperglycemia. TD1 requires life-long treatment with insulin injections.

Insulin mediates its cellular responses by binding to and activating the insulin receptor. This facilitates e.g. the cellular uptake of glucose by carrier proteins which bind and transfer glucose molecules across the plasma membrane. Glucose transporter 4 (GLUT4) is the insulin-regulated transporter, most abundant in insulin-sensitive tissues, namely skeletal muscle, cardiac muscle and adipose tissue (Bell et al. 1990). GLUT4 is almost absent in adipose and skeletal muscle tissues from diabetic animals (Garvey, Huecksteadt & Birnbaum 1989, Berger et al. 1989, Kainulainen et al. 1994a, Kainulainen et al. 1994b), in line with hyperglycemia and impaired glucose metabolism. Also various genes involved in coding proteins of the enzymes of the respiratory chain in oxidative phosphorylation in mitochondria are dysregulated in TD1 mice, this indicating metabolic disturbances (Yechoor et al. 2002, Yechoor et al. 2004).

The poorly understood nature of the gene regulation involved in insulin deficiency in diabetes called for a search for novel regulatory proteins at the time this study was initiated. The issue was approached by applying Differential Display PCR (DD-PCR) methodology to study gene expression in TD1 diabetic mouse insulin-sensitive tissues. This methodology made it possible to identify novel genes, of which one warranted characterized in this thesis. In view of the time lapse between the first and second publication, the information regarding the novel protein published by other groups is reported in the review of the literature.

2 REVIEW OF THE LITERATURE

2.1 Type 1 diabetes

Type 1 diabetes (TD1) is an autoimmune disease, which leads to the destruction of the insulin-producing **b**- cells in the islets of Langerhans in the pancreas and is most commonly diagnosed in children and young adults. By the time of diagnosis, patients evince very little endogenous insulin production. Insulin has therefore to be replaced by regular subcutaneous injections, and blood glucose levels frequently monitored to manage the risk of hypoglycemia.

Finland has the world's highest incidence of type 1 diabetes, and the rate has been steadily increasing (Hyttinen et al. 2003). Currently there are reported to be approximately 50 000 patients with TD1 in Finland. (http://www.diabetes.fi/diabetestietoa/tyyppi_1; november 2016).

2.1.1 Streptozotocin-induced diabetes

Streptozotocin (STZ)-induced diabetes in rodents is a widely used animal model mimicking human TD1 (Szkudelski 2001, Lenzen 2008, Rakieten, Rakieten & Nadkarni 1963). Insulin deficiency in rodents can be introduced by a single intraperitoneal injection of streptozotocin, a chemical drug specifically penetrating to and destroying the pancreatic **b**- cells. In rodents, the insulin deficiency initiates for instance hyperglycemia and loss of weight within 5-7 days after injection of the drug and exerts its effects all over the tissues.

In the presence of insulin, the insulin-sensitive tissues metabolize the majority of blood glucose for the energy used by heart, muscles and brain, store glucose as glycogen in the liver and fat in adipose tissue, which also produces heat in the body. These insulin-sensitive tissues are thus of importance in studying the effects of insulin deficiency and in understanding its consequences in metabolic regulation at cellular level. For this purpose the STZ-diabetic rat model is a suitable tool.

2.1.2 Cellular regulation upon insulin deficiency

Insulin mediates its cellular responses by binding to and activating the insulin receptor. This is followed by a series of phosphorylation and signaling cascades regulating the cellular gene expression orchestrating glucose uptake and metabolism (reviewed in Saltiel, Kahn 2001). The STZ-diabetic rat model previously demonstrated impaired translocation of glucose transporter 4 (GLUT4) in insulin-sensitive tissues, which is an example of the consequences of insulin deficiency (Kainulainen et al. 1994b, Kainulainen et al. 1993). Numerous other changes at gene expression level are also reported (Yechoor et al. 2002, Yechoor et al. 2004), including impaired mRNA expression of subunits of respiratory enzymes of oxidative phosphorylation (OXPHOS) in the mitochondria. The effect of TD1 on regulation of the gene expression of mitochondrial ATP synthase, on the other hand, is less well known.

2.2 Mitochondria

Mitochondria are referred to as powerhouses of the cell in being the main source of adenosine triphosphate (ATP), the energy-rich compound which drives fundamental cell functions. These functions include force generation, as seen in muscle contraction and cell division, the biosynthesis, folding and degradation of proteins, and the generation and maintenance of membrane potentials. ATP is generated by the mitochondrial ATP synthase from adenosine diphosphate (ADP) and phosphate ions (Pi). In addition to cellular respiration and ATP synthesis, the mitochondria have numerous other essential functions, including the production of reduced nicotinamide adenine dinucleotide (NADH) and guanosine triphosphate (GTP) in the citric acid cycle, the biosynthesis of amino acids, heme groups and iron-sulfur clusters or the synthesis of phospholipids for membrane biogenesis. They also act in stress responses (Pellegrino, Haynes 2015), calcium signaling (reviewed in Rizzuto et al. 2012), and generally as crossroads in cellular signaling (reviewed in Chandel 2014). Considering this range of input, mitochondria clearly play a fundamental role in human health. Mitochondrial dysfunction is known to cause severe, often maternally inherited diseases (reviewed in Houstek et al. 2006, Servidei 2002). Moreover, the mitochondria are intensively implicated in stemness, apoptosis and ageing (reviewed in Bratic, Larsson 2013, Daum et al. 2013).

2.2.1 Biogenesis, structure and protein transport

Cells identify and dispose of defective mitochondria while stimulating healthy mitochondria to proliferate through mitochondrial biogenesis (reviewed in Piantadosi, Suliman 2012). In the process, highly functional mitochondrial subpopulations are segregated from poorly functional mitochondria, which are targeted for degradation by mitophagy. Mitochondrial biogenesis is normally activated by changes in physiological state which require increases in the rates of ATP utilization, e.g. in thermogenesis, exercise and calorie restriction. Also mitochondrial damage from oxidative stress and pathological inflammation induces biogenesis (Kim et al. 2007, Alvarez-Guardia et al. 2010).

Mitochondrial biogenesis is regulated mainly at the level of transcription via a bi-genomic program. Many nuclear-encoded genes, e.g. electron transport and oxidative phosphorylation proteins, are activated by nuclear respiratory factor-1 (NRF-1) and GA-binding protein A (GABPA)(reviewed in Piantadosi, Suliman 2012). The peroxisome proliferator-activated receptor gamma (PPAR γ) co-activator 1- protein (PGC-1 α) is a central transcriptional co-activator for NRF-1, GABPA, and the PPARs, and is involved in the physiological integration of mitochondrial biogenesis with oxidative metabolism (reviewed in Wu et al. 1999). The PGC family members are known also to activate genes encoding for proteins for mtDNA transcription and replication and mitochondrial protein import (reviewed in Wu et al. 1999).

Mitochondria are found in all higher eukaryote cells except mature red blood cells. They are round or oval-shaped structures with a visible smooth outer membrane (MOM) and inner membrane (MIM) protruding to the matrix forming cristae (Revel, Fawcett & Philpott 1963) (Figure 1). In reality mitochondria form a dynamic network structure with continuous fusion and fission, the network being most dense in the perinuclear area but extending throughout the cytoplasm (Stamer et al. 2002).

The proteins from cytosol enter the mitochondria through the translocases of outer and inner membranes (TOM and TIM complexes (reviewed in Chacinska et al. 2009)). Among various channels in the mitochondria, the voltage-dependent anion channel (VDAC) plays a key role in regulating metabolic and energetic flux across the outer mitochondrial membrane, responding with an open (low) and closed (high) state according to the membrane potential created in the intermembrane space (reviewed in Shoshan-Barmatz, Mizrachi 2012). The VDAC is located in close proximity to ATP/ADP translocase (ANT), phosphate carrier (PiC) and H⁺-ATP

synthase, thereby constituting an entire ATP synthasome (Nuskova et al. 2015, Clemencon 2012).

Uncoupling proteins (UCPs) are a family of inner mitochondrial membrane proteins whose function is to dissipate the proton gradient back to the matrix as heat. This reduces the membrane potential, Δp , and production of reactive oxygen species (ROS). Due to their pivotal role in the intersection between energy efficiency and oxidative stress, UCPs are under investigation for a potential role in cancer and stemness (reviewed in Valle, Oliver & Roca 2010, Zhang et al. 2014, Zhang et al. 2011).

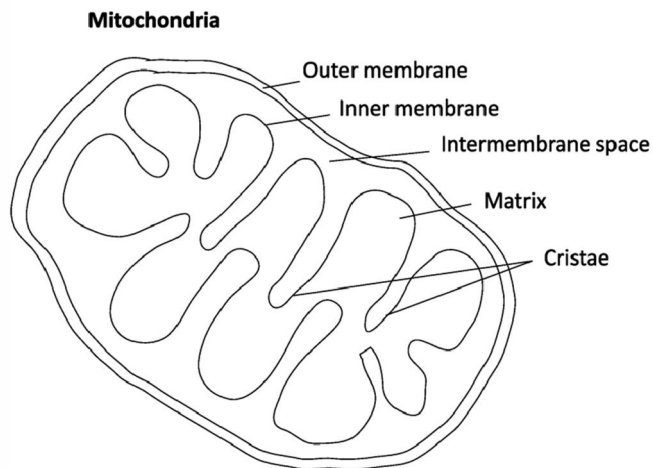


Figure 1. Schematic illustration of a mitochondrion. The mitochondrion has an outer membrane surrounding the whole organelle and an inner membrane encompassing the mitochondrial matrix. The inner membrane is folded into structures called cristae to increase the membrane surface area. Between the membranes is the intermembrane space storing energy in the form of membrane potential, Δp .

2.2.2 Oxidative phosphorylation (OXPHOS)

Oxidative phosphorylation comprises of the electron transport chain (complexes I-IV) pumping protons from the mitochondrial matrix to the intermembrane space and reducing oxygen to form water. The proton motive force obtained drives chemiosmosis in synthesizing ATP from ADP and P_i by complex V, also known as F_1F_0 -ATPase, F-ATPase, H^+ -ATP synthase and ATP synthase. The variety of names reflect the diverse characteristics of ATP synthase and are used in parallel in this thesis, according to the context reported in referred articles.

2.2.2.1 Respiratory chain complexes

The electron transport in the inner mitochondrial membrane shuttles electrons from soluble carrier molecules NADH and reduced flavin adenine dinucleotide (FADH₂) to molecular oxygen by complexes I (NADH/ubiquinone oxidoreductase), III (cytochrome c reductase) and IV (cytochrome c oxidase) (Figure 2). Complex I feeds electrons from the NADH into the respiratory chain and transfers them to a quinol in the membrane. The energy released is utilized for pumping four protons from the matrix into the crista lumen. Complex III takes the electrons from the quinon and transfers them to electron carrier protein cytochrome c, pumping one proton in the process. Finally, complex IV transfers the electrons from cytochrome c to molecular oxygen and contributes to the proton gradient by using up four protons per consumed oxygen molecule to make water. Complex II (succinate dehydrogenase), fed by FADH₂, transfers electrons from succinate directly to quinol and does not contribute to the proton gradient. The activities of respiratory complexes can be studied with complex specific inhibitors in the presence of appropriate substrates.

Mitochondrial respiratory chain complexes

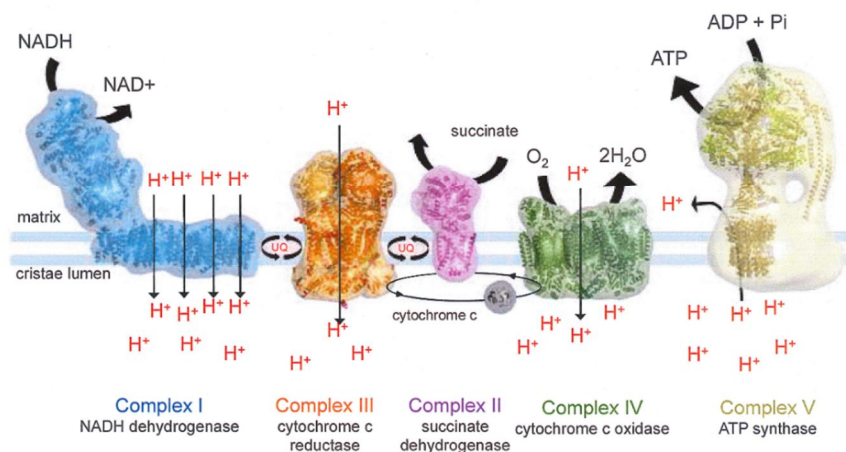


Figure 2. The respiratory chain complexes. Energy for the cell is harnessed by oxidative phosphorylation involving electron transport complexes I (NADH/ubiquinone oxidoreductase, *blue*), II (succinate dehydrogenase, *pink*), III (cytochrome *c* reductase, *orange*), IV (cytochrome *c* oxidase, *green*) and the mitochondrial ATP synthase (also known as complex V, *tan*). Complexes I, III and IV pump protons across the cristae membrane, thereby creating the proton gradient driving ATP synthesis. UQ ubiquinol carrying-electrons. Reprinted under Creative Commons Attribution license 4.0 (<http://creativecommons.org/licenses/by/4.0/>) as published in (Kuhlbrandt 2015).

2.2.2.2 ATP synthase

The energy-transducing membranes of bacteria, chloroplasts and mitochondria contain multiprotein complexes known as ATP synthases. ATP synthases (F-ATPases) are close relatives of the V-ATPases (vacuolar ATPases), which are found in secretory membranes using the energy from ATP hydrolysis to generate ion gradients across these membranes. In the presence of oxygen ATP synthase employs a transmembrane protonmotive force, Δp , as an energy source to drive a mechanical rotary mechanism which leads to the chemical synthesis of ATP.

Only few publications regarding DAPIT and its function existed at the time this thesis was published. This paragraph summarizes the information that was not published in studies I-III. DAPIT is a proteolipid encoded by the *Usmg5* (Up-Regulated During Skeletal Muscle Growth 5 Homolog (Mouse)) gene, which is located in chromosome 10q24 in human (<http://www.genecards.org/cgi-bin/carddisp.pl?gene=USMG5>), Chr 19 in mouse (<https://www.ncbi.nlm.nih.gov/gene/66477>) and Chr 1q54 in rat (<https://www.ncbi.nlm.nih.gov/gene/171069>). Orthologs of DAPIT are found in vertebrates and invertebrates but not in yeast and fungi (Chen et al. 2007). The nucleotide and protein sequence of DAPIT (I), which didn't contain any post-translational modifications in bovine heart mitochondria (Carrol et al. 2006), are shown in the result sections 5.2.2 and 5.2.3. DAPIT is located in the inner membrane of mitochondria N-region orienting to the matrix and C-region to the intermembrane space (Lee et al. 2015). DAPIT is associated with ATP synthase in a stoichiometric manner but it is found in ATP synthase complex only when purified in the presence of phospholipids (Chen et al. 2007, Meyer et al. 2007), which depicts its hydrophobic characteristics. Moreover, DAPIT is prone to dissociate from ATP synthase in the presence of relatively strong detergents, but ATP synthase without DAPIT retains the original ATP hydrolysis activity (Meyer et al. 2007). DAPIT also binds both monomeric and dimeric form of ATP synthasome (Nuskova et al. 2015). Presently, no publications of animal models of DAPIT exist but an *in vitro* knockdown in Hela cells (Ohsakaya et al. 2011) and over-expression model in human embryonal kidney cell, HEK293T (III), are reported.

2.2.2.2.1 Overall structure

The F-ATPase from the mammalian heart mitochondria is a membrane-bound protein assembly of ca 30 polypeptides consisting of 17 different subunits (α 3, β 3, γ , δ , ϵ , a, b, c8,d, e, f, g, A6L, F6, oligomycin sensitivity conferral protein [OSCP], DAPIT, and a 6.8 kDa protein) having a molecular mass of approximately 650 kDa (Meyer et al. 2007, Runswick et al. 2013, reviewed in Walker 2013, Walker et al. 1991). The enzyme can be subdivided into four functional parts (Figure 3): 1) the catalytic part, ($\alpha\beta$)₃, which binds and converts ADP and Pi to ATP; 2) the membrane-embedded part (a, b, c8, e, f, g, ATP8 (or A6L), DAPIT, and the 6.8 kDa protein) through which protons move across the membrane; 3) the central stalk, $\gamma\delta\epsilon$, which transmits the rotation of the membrane-embedded rotor-ring (c8) to the catalytic region; 4) and the peripheral stalk (b, d, F6 and OSCP) resisting the rotational torque of the rotor (reviewed in Walker 2013) to hold the catalytic part attached to the rotary motor, thereby forming an integral stator of the enzyme. The catalytic and central stalk regions form a membrane-extrinsic F₁ domain and the remainder the F_o domain, which generates rotation using the potential energy stored in Δp .

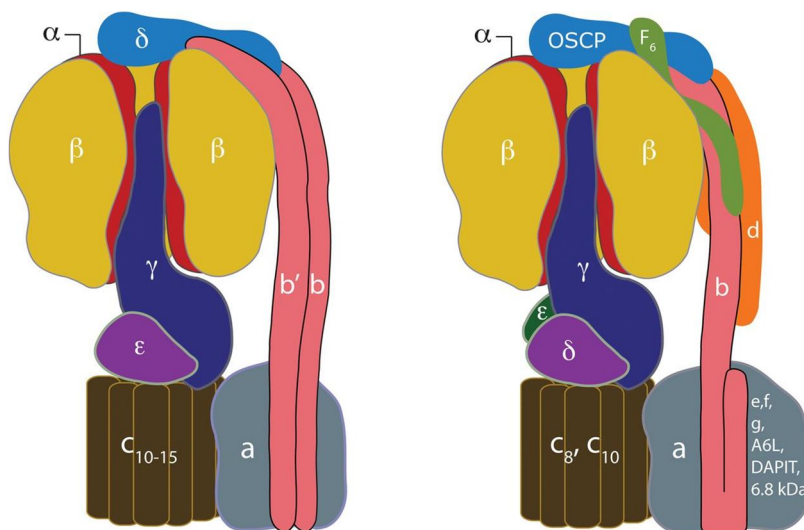


Figure 3. "The bacterial and chloroplast ATP synthases are depicted on the left, and the more complex mitochondrial enzyme is shown on the right. The upper part of each model contains the subunits in the F₁ catalytic domain. One of the three α -subunits (red) has been removed to expose the elongated α -helical structure in the γ -subunit (dark blue), which lies approximately along the central axis of the

spherical $\alpha_3\beta_3$ domain. The γ -subunit (and associated subunits) is in contact with the F_0 membrane domain, which contains the c-ring (brown) and the associated a-subunit (grey). The number of c-subunits in the c-ring differs between species. The rotor of the enzyme comprises the ensemble of the c-ring and the γ -subunit (and associated subunits). The pathway for protons through the F_0 domain lies in the vicinity of the interface between the c-ring and the a-subunit. The peripheral stalk is on the right of each model. In some bacterial enzymes, it consists of the δ -subunit (light blue) and two identical b-subunits (pink). In other bacterial enzymes, and in the chloroplast enzyme, the two b-subunits are replaced by single copies of homologous, but non-identical, subunits b and b'. The N-terminal domain of the δ -subunit binds to the N-terminal region of one of the three α -subunits, and the b- and b'-subunits interact with the a-subunit via their N-terminal transmembrane α -helices. In the mitochondrial enzyme, the peripheral stalk consists of single copies of subunits OSCP, b, d and F_6 . OSCP is the homologue of the bacterial δ -subunit. The sequences of mitochondrial subunits b, d and F_6 are not evidently related to those of the bacterial b and b' subunits. Their structures also differ significantly, although they are both dominated by α -helices, except for the C-terminal domain of OSCP (and presumably the bacterial and chloroplast δ -subunit), which contain β -structures. The membrane domains of the mitochondrial enzyme contain a number of membrane subunits with single transmembrane α -helices not found in bacteria and chloroplasts. These supernumerary subunits have no known roles in the generation of ATP; subunits e, f, g, A6L and DAPIT and the 6.8 kDa proteolipid, which are found in the complex when phospholipids are maintained during the purification of the complex, are shown." (Walker 2013). Transactions by the Biochemical Society (Great Britain) Reproduced with permission of BIOCHEMICAL SOCIETY in the format Thesis/Dissertation via Copyright Clearance Center.

2.2.2.2.2 Supernumerary subunits including DAPIT

The six small proteins, ATP8, e, f, g, DAPIT, and 6.8 kDa proteolipid, are associated with the membrane domain of the bovine enzyme (Lee et al. 2015). Each has a single predicted transmembrane α -helix, and based largely on their staining intensities in gel analyses of the subunit composition of the enzyme, it is assumed that there is one copy of each protein per F-ATPase complex. These proteins are referred to as the "supernumerary" subunits as there are no orthologs in bacterial F-ATPases, and they are not directly involved in the synthesis of ATP. In the yeast enzyme the orthologs of subunits e and g are associated with the formation of dimers of the F-ATPase (Arnold et al. 1998, Paumard et al. 2002), and they probably play the same role in the mammalian enzyme.

Little is known of the function and consequences in impairments of the supernumerary subunits, but a few examples may be cited. Mutations in ATP8 were found to lead to apical hypertrophic cardiomyopathy and neuropathy in man (Jonckheere et al. 2009). This was due to interference in the F-ATPase assembly and its reduced activity. A loss of the amount of ATP synthase in the mitochondria, on the other hand, was encountered upon knock-down of DAPIT in HeLa cells (Ohsakaya et al. 2011).

Only few publications regarding DAPIT and its function occurred in literature at the time this thesis was published. This paragraph summarizes the available data in terms of information not published in studies I-III. DAPIT is a proteolipid encoded by the *Usmg5* (Up-Regulated During Skeletal Muscle Growth 5 Homolog (Mouse)) gene, which is located in chromosome 10q24 in human (<http://www.genecards.org/cgi-bin/carddisp.pl?gene=USMG5>), Chr 19 in mouse (<https://www.ncbi.nlm.nih.gov/gene/66477>) and Chr 1q54 in rat (<https://www.ncbi.nlm.nih.gov/gene/171069>). Orthologs of DAPIT are found in vertebrates and invertebrates but not in yeast and fungi (Chen et al. 2007). In result sections 5.2.2 and 5.2.3 are shown the nucleotide and protein sequence of DAPIT (I), which didn't contain any post-translational modifications in bovine heart mitochondria (Carrol et al. 2006). The orientation of DAPIT in inner membrane of mitochondria is N-region to the matrix side and C-region to the intermembrane space (Lee et al. 2015). DAPIT is associated with ATP synthase in a stoichiometric manner but found in ATP synthase only when purified in the presence of phospholipids (Chen et al. 2007, Meyer et al. 2007), which depicts its hydrophobic characteristics. Moreover, DAPIT is prone to dissociation from ATP synthase in the presence of relatively strong detergents, but ATP synthase without DAPIT still retains the same ATP hydrolysis activity (Meyer et al. 2007). DAPIT is also bound both in monomeric and dimeric form of ATP synthasome (Nuskova et al. 2015). Presently, no publications of animal models of DAPIT exist but an in vitro over-expression model in human embryonal kidney cell, HEK293T (III), is available.

2.2.2.2.3 Inhibitory factor 1 (IF1)

If a cell were to encounter anoxic conditions, the F_0 domain would use the energy stored in ATP and reverse its rotation in order to pump H^+ ions back to the intermembrane space in order to prevent the collapse of Δp . An intrinsically unfolded inhibitor protein, IF1, which inserts itself in the catalytic domain, blocks reverse rotation. This protein thereby inhibits the ATP hydrolytic activity of the intact mitochondrial F_1F_0 -ATPase, but not its ability to synthesize ATP in the presence of a proton motive force (Pullman, Monroy 1963, Runswick et al. 2013). The up-regulated mitochondrial content of IF1 controls the activity of oxidative phosphorylation mediating the shift of cancer cells to enhanced aerobic glycolysis. This happens by triggering mitochondrial hyperpolarization and the subsequent production of superoxide radical (ROS), which further mediates a retrograde prosurvival and proliferative response of cancer cells (Formentini et al. 2012, Sanchez-Cenizo et al. 2010).

2.2.2.2.4 Dimerization, cristae formation and superassemblies

ATP synthases can associate into more complex structures such as dimers and higher oligomers (Seelert, Dencher 2011, Paumard et al. 2002, Davies et al. 2012). The dimers have been shown to self-associate into rows (Davies et al. 2012), resulting in bending of the lipid bilayer of the inner membrane (Kühlbrandt 2015). As ATP synthases are mainly located in the cristae curvatures, this phenomena implements the formation of the cristae shape (Figure 4).

ATP synthase also participates in the formation of ATP synthasome, which is a supramolecular structure suggested to be composed of H⁺-ATP-synthase, ADP/ATP translocase (ANT) and inorganic phosphate carrier (PiC) (Clemencon 2012, Nuskova et al. 2015, Seelert, Dencher 2011). Together they form a single catalytic unit responsible for ATP production.

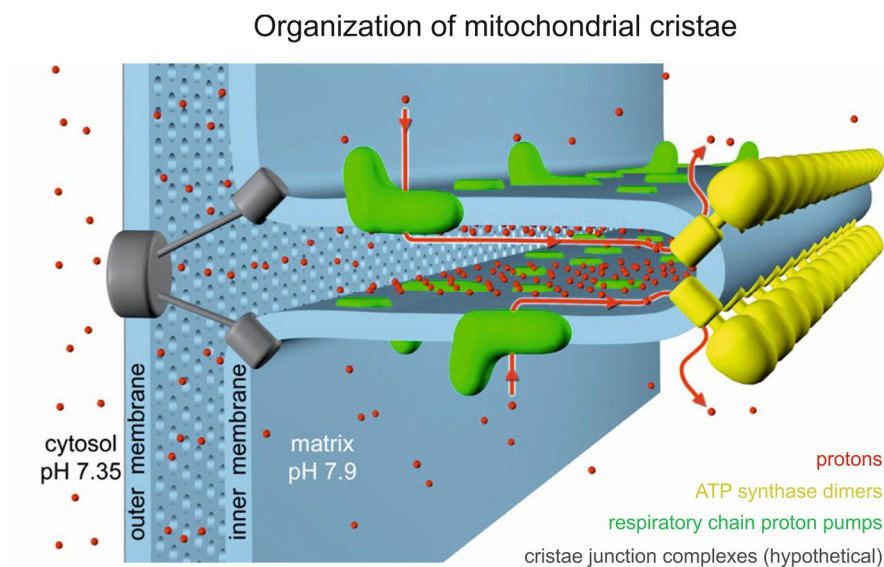


Figure 4. "ATP synthase dimer rows shape the mitochondrial cristae. At the cristae ridges, the ATP synthases (yellow) form a sink for protons (red), while the proton pumps of the electron transport chain (green) are located in the membrane regions on either side of the dimer rows. Guiding the protons from their source to the proton sink at the ATP synthase, the cristae may work as proton conduits which enable efficient ATP production with the shallow pH gradient between cytosol and matrix. Red arrows show the direction of the proton flow." Reprinted under Creative Commons Attribution license 4.0 (<http://creativecommons.org/licenses/by/4.0/>) as published in (Kühlbrandt 2015).

2.2.2.2.5 Membrane permeability

Together with a mitochondrial translocase (ANT), cyclophilin-D, Bax and Bak, the H⁺-ATP synthase comprises a current model of increase in permeability of inner mitochondrial membrane by forming a permeability transition pore (mPTP) (reviewed in Bernardi et al. 2015). Under conditions of oxidative stress this channel, in contrast to catalysing ATP production, is thought to dissipate energy in a Ca²⁺-dependent manner. The opening of mPTP leads to mitochondrial swelling and cell death by apoptosis or necrosis. While the identity of the pore remains to be established, the c-ring of F_o component of ATP synthase, for example, is ruled out (He et al. 2017). If the transition pore is associated with the ATP synthase complex, the most likely components to form the pore are speculated to be any or all of the membrane subunits, b, e, f, and g (He et al. 2017).

2.2.2.2.6 Membrane rearrangement in cellular ageing and stem cell differentiation

Ageing is still a poorly understood biological process affecting all eukaryotic life, for example via deterioration of mitochondria. A cryo-electron-tomogram of mitochondria from the short-lived (~18 days) model organism *Podospora anserina* revealed profound age-dependent changes in the inner membrane architecture (reviewed in Daum et al. 2013). The normal mitochondria in young cells protruded cristae deeply into the matrix, whereas with increasing age, the cristae receded into the inner boundary membrane and the inter-membrane space widened. The matrix broke up into spherical vesicles within the outer membrane. Dispersion of the ATP synthase dimer rows caused them to dissociate into monomers, unable to fulfil the energy demand of the cell, this being followed by vesiculation of the inner membrane and triggering of apoptosis (Li et al. 1997).

Recent studies in germline stem cell differentiation in the *Drosophila* ovary suggest that ATP synthase-dependent crista maturation is a key developmental process required for differentiation independent of oxidative phosphorylation (Teixeira et al. 2015). This was shown by knocking down the supernumerary e and g, which led to immature cristae (Teixeira et al. 2015).

2.2.2.2.7 Ectopic F-ATPase

Ectopic ATP synthase consists of both nuclear- and mtDNA-encoded proteins facing the F₁ domain outwards from the cell (Rai et al. 2013). Its function together with ATP hydrolysis or ATP synthesis is implicated in cell signaling, mediating

various biologic and pathologic functions such as regulation of lipid metabolism and immune recognition of tumors (Champagne et al. 2006, Chi, Pizzo 2006), influenza virus budding (Gorai et al. 2012), Alzheimer's disease (Vacirca et al. 2012) and lung cancer growth (Chang et al. 2012).

2.3 Cell metabolism and differentiation

Cell proliferation requires amino acids, nucleotides and lipids for biosynthesis of proteins, nucleic acids and membranes. These are provided by metabolic intermediates from glycolysis and tricarboxylic acid (TCA) cycle. A major source of the cellular energy and biomass of a new cell is glucose, which is metabolized via glycolysis to pyruvate in cell cytosol. In oxygen-rich conditions the TCA cycle in the mitochondria utilizes pyruvate to generate large amounts of ATP through oxidative phosphorylation. In terms of production efficiency of energy, one mole of glucose generates 36 mol of ATP, whereas glycolysis by it produces 2 mol. In cytosol, pyruvate can also be converted into lactate by lactate dehydrogenase.

The fatty acids and proteins are also essential energy sources for the cell in addition to glucose. Fatty acids enter the mitochondria through the carnitine shuttle, after which they undergo beta-oxidation to produce acetyl coenzyme A capable of entering the TCA cycle. As an example of amino acids, the human body serum is rich in glutamine, which is converted to glutamate and alpha-ketoglutarate used as substrate in the TCA cycle.

2.3.1 Aerobic glycolysis

In 1924, Otto Warburg observed that cancer cells consume much larger quantities of glucose than their normal counterparts. The oxidative phosphorylation in cancer cells was suppressed and the glucose was metabolized predominantly through glycolysis, producing high levels of lactate even in the presence of oxygen (Warburg, Wind & Negelein 1927, Warburg 1956), the lower ATP yield by glycolysis being compensated by higher rates of glycolytic flux. The phenomenon was called aerobic glycolysis, also known as the Warburg effect. This effect is regulated by the PI3K, hypoxia inducible factor (Hif), p53, MYC and AMP-activated protein kinase (AMPK) – liver kinase B1 (LKB1) pathways (reviewed in Cairns, Harris & Mak 2011), (Figure 5).

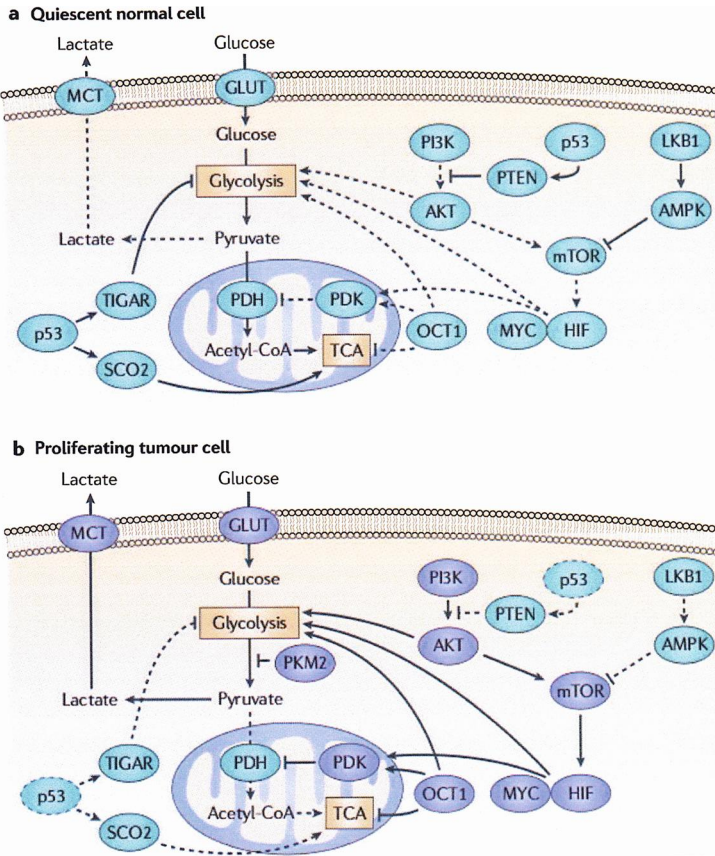


Figure 5. “Relative to normal cells (part a) the shift to aerobic glycolysis in tumor cells (part b) is driven by multiple oncogenic signalling pathways. PI3K activates AKT, which stimulates glycolysis by directly regulating glycolytic enzymes and by activating mTOR. The liver kinase B1 (LKB1) tumor suppressor, through AMP-activated protein kinase (AMPK) activation, opposes the glycolytic phenotype by inhibiting mTOR. mTOR alters metabolism in a variety of ways, but has an effect on the glycolytic phenotype by enhancing hypoxia-inducible factor 1 (HIF1) activity, which engages a hypoxia-adaptive transcriptional program. HIF1 increases the expression of glucose transporters (GLUT), glycolytic enzymes and pyruvate dehydrogenase kinase, isoform 1 (PDK1), which blocks the entry of pyruvate into the tricarboxylic acid (TCA) cycle. MYC cooperates with HIF in activating several genes which encode glycolytic proteins, but also increases mitochondrial metabolism. The tumor suppressor p53 opposes the glycolytic phenotype by suppressing glycolysis through TP53-induced glycolysis and apoptosis regulator (TIGAR), increasing mitochondrial metabolism via SCO2 and supporting expression of PTEN. OCT1 (also known as POU2F1) acts in an opposing manner to activate the transcription of genes which drive glycolysis and suppress oxidative phosphorylation. The switch to the pyruvate kinase M2 (PKM2) isoform affects glycolysis by slowing the pyruvate kinase reaction and diverting substrates into alternative biosynthetic and reduced nicotinamide adenine dinucleotide phosphate (NADPH)-generating pathways. MCT, monocarboxylate transporter; PDH, pyruvate dehydrogenase. The dashed lines indicate loss of p53 function.” Reprinted by permission from Macmillan Publishers Ltd: [Nature Reviews. Cancer (Cairns, Harris & Mak 2011), copyright (2016).

2.3.2 Proliferation and differentiation

The three basic needs of the dividing cell are rapid ATP generation to maintain energy status, increased biosynthesis of macromolecules and tightened maintenance of appropriate cellular redox status (reviewed in Cairns, Harris & Mak 2011). Instead of aerobic respiration, these needs are better satisfied by aerobic glycolysis, which provides an abundance of carbon skeletons to various cell needs and compensates the efficiency of energy production by a flow of glucose metabolized to lactate. This explains why tumors are committed to aerobic glycolysis, the reason currently known as post-Warburg model (reviewed in Cairns, Harris & Mak 2011).

Aerobic glycolysis is associated with both normal cell proliferation and cancer, and it is inhibited upon differentiation to a post-mitotic cell (Agathocleous, Harris 2013). For example, differentiation of embryonic stem cells to cardiomyocytes and fibroblasts, and human mesenchymal stem cells to adipocytes, requires up-regulation of oxidative phosphorylation and down-regulation of glycolysis (Chung et al. 2007, Tormos et al. 2011). In contrast, the reprogramming of fibroblasts to induced pluripotent stem cells activates glycolysis (Panopoulos et al. 2012, Folmes et al. 2011), and stem cells overall maintain their undifferentiated stage by sticking to aerobic glycolysis (reviewed in Teslaa, Teitell 2015, Zhang et al. 2014, Zhang et al. 2011). These examples show that aerobic glycolysis is involved in regulating cell differentiation, as also seen in cancer cells acquiring dedifferentiation through a process called epithelial to mesenchymal transition (see 2.3.4).

2.3.3 Hif1a and ROS

The major transcription factor responsible for gene expression changes under low oxygen levels in a cell is Hif1a, which is rapidly stabilized to the nucleus on exposure to hypoxia. Hif1a undergoes oxygen-dependent hydroxylation by prolyl hydroxylase enzymes under normoxic conditions. This results in its recognition by von Hippel-Lindau tumor suppressor (VHL), an E3 ubiquitin ligase, and subsequent degradation. In addition to hypoxia, Hif1a can be stabilized in normoxia by oncogenic signaling pathways (reviewed in Plas, Thompson 2005, King, Selak & Gottlieb 2006, Selak et al. 2005). When active, Hif1a amplifies the transcription of glucose transporters and glycolytic enzymes, thereby accelerating glycolysis (Semenza 2010). In addition, it activates the pyruvate dehydrogenase kinases (PDKs), inactivating pyruvate dehydrogenase in the mitochondria, resulting in a

reduction of pyruvate in the TCA cycle (Papandreou et al. 2006, reviewed in Kim et al. 2006, Lu et al. 2008).

Reactive oxygen species (ROS) are normal byproduct of metabolic processes in a cell. ROS are heterogeneous in their properties and regulate various down-stream effects in a concentration-dependent manner. At low levels, ROS increase cell survival and proliferation through the post-translational modification of kinases and phosphatases (Giannoni et al. 2005, Cao et al. 2009), whereas at moderate levels they induce the expression of Hif (reviewed in Bell, Emerling & Chandel 2005). At high levels ROS damage macromolecules like DNA triggering senescence and rendering mitochondria permeable, leading to release of cytochrome c and apoptosis (Ramsey, Sharpless 2006, Takahashi et al. 2006, Garrido et al. 2006). The cell counteracts detrimental ROS by producing antioxidant molecules like manganese- and copper/zinc-dependent superoxide dismutase (MnSOD, Cu/ZnSOD), catalases, glutathione peroxidase-1 (Gpx1), peroxiredoxins 3 and 5 (Prx3 and Prx5), the thioredoxin-2 (Trx2) system, and the dietary antioxidant vitamins C, E, A, which prevent irreversible cellular damage (reviewed in Liemburg-Apers et al. 2015).

2.3.4 Epithelial to mesenchymal transition, EMT

Hif1a stabilization is also involved in EMT, which is a process in which epithelial cells lose cell-cell junctions and baso-apical polarity (reviewed in Talbot, Bhattacharya & Kuo 2012, Valenta, Hausmann & Basler 2012, Zeisberg, Neilson 2009). As examples of relevant biomarkers in EMT in vitro N-cadherin replaces E-cadherin and integrins are abundantly expressed on cell surface, expression of α SMA and vimentin are increased in cellular cytoskeleton, and transcription factors β -catenin, snail, twist and slug activated in transcriptional regulation. At the same time these cells acquire plasticity, mobility, invasive capacity, stem-like characteristics (Mani et al. 2008, Batlle et al. 2000, Cano et al. 2000, Yang et al. 2004) and resistance to apoptosis. EMT is active in embryos, fibrosis and wound healing, and in promoting metastasis in cancer. In addition to Hif1a, the Wnt/ β -catenin pathway signalling also controls this cell biology program upon hypoxic stress in cancer (reviewed in Talbot et al., 2012; Valenta et al., 2012), but provides an unlimited proliferative capacity in the case of cancer stem cells (reviewed in Suva, Riggi & Bernstein 2013).

3 AIMS OF THE STUDY

Diabetes is a common endocrine disease, which exerts its effects through insulin deficiency and resistance. The aim of this study was to find and characterize genes expressed differentially in insulin deficiency in order to understand insulin regulation at cellular level.

The specific aims were:

1. To search for novel regulatory genes and proteins involved in the insulin-regulated glucose metabolism. The search was based on DD-PCR methodology, employing insulin deficiency as starting material. The methodology enables simultaneous characterization of sequence tags of both known and novel genes.

Hypothesis: Several differences in gene expression between control and diabetic rat insulin-sensitive tissues will be seen. Novel findings will appear and be further studied.

2. To characterize Diabetes Associated Protein in Insulin-sensitive Tissues (DAPIT):

Hypothesis: The cellular localization and tissue distribution of the protein can be revealed by characterizing a custom-made antibody against DAPIT. The expression level of the protein in insulin-sensitive tissues of type 1-diabetic rodents can be determined.

3. To characterize the cell line over-expressing DAPIT.

Hypothesis:

Since DAPIT is known to be a part of the ATP synthase complex, DAPIT over-expression negatively affects mitochondrial oxygen metabolism and the cells may present phenotypic changes related to abnormal function of the mitochondria.

4 MATERIALS AND METHODS

4.1 Animals, human samples and ethical permission (I, II)

Male Sprague-Dawley rats were injected intraperitoneally with STZ (Sigma-Aldrich, Lyon, France, 80 mg/kg body weight in 0.1 mol/l sodium citrate buffer, pH 4.5) to induce type I diabetes. After seven days the animals were sacrificed and tissues collected. Serum containing glucose >600 mg/dL confirmed the diabetes. Control rats were injected with concomitant diluent which did not induce changes in blood glucose. Ten-week-old male NMRI mice were rendered diabetic by a peritoneal injection of STZ (180mg/kg body weight) (Hulmi et al. 2012) (II). An equal volume of buffer was injected into the control mice. Urine glucose was >200 mg/dl 72 h after the injection of STZ and confirmed the diabetes. The animal experiments followed the "Principles of laboratory animal care" (NIH publication no. 83-25) and the Finnish Law on the protection of animals.

Human tissue samples were collected in resection of carcinomas. Healthy-appearing pieces of kidney clear cell carcinoma from a 68-year-old male and a liver adenocarcinoma sample from a 48-year-old female were used for immunohistochemistry.

Animal experiments were approved by the Animal Experimentation Committees of Tampere and Jyväskylä. The Ethical Committee of Tampere University Hospital approved the use of human tissues.

4.2 Cell lines and cell culture (II, III)

The human embryonic kidney epithelial cells HEK293T (ATCC) were maintained in DMEM (Sigma-Aldrich, Ayrshire, UK or Gibco BRL, Paisley, Scotland, UK), containing 4.5 g/l glucose, 10% fetal calf serum (Sigma), 50 µg/ml uridine, 1 mM sodium pyruvate, 2 mM L-glutamine, 100 U penicillin and 100 µg/ml of streptomycin (Gibco BRL) at 37°C in an incubator with 5% CO₂. Human umbilical vein endothelial cells HUVEC (Lonza Cambrex Bio Science, Walkersville, MD, USA) were cultured in HuMedia-EGMTM (EGM-1)(Clonetics, San Diego, CA,

USA). The murine myoblast cell line C2C12 (a gift from Antero Salminen at the University of Eastern Finland) was maintained in DMEM/F12 (Gibco) containing 4.5 g/l glucose, 10% fetal calf serum (Sigma) and 0,075% sodium bicarbonate (Gibco). All cell cultivation media were supplemented with penicillin and streptomycin antibiotics.

4.3 RNA isolation and detection methods (I, III)

4.3.1 RNA isolation and DD-PCR (I)

Total RNA was isolated from rat control and diabetic muscle (m. gastrocnemius), myocardium and adipose tissue by Trizol reagent (Gibco BRL, Life Technologies, Grand Island, N.Y, U.S.A.) according to the manufacturer's protocol. Pure DNA-free RNA was obtained by DNase I (Roche Molecular Biochemicals) treatment and phenol-chloroform-isoamylalcohol extraction with ethanol precipitation.

DD-PCR was conducted using an RNA map kit (Gen-Hunter, Nashville, TN, U.S.A.) according to the instructions of the manufacturer. Briefly, four reverse transcription reactions were performed for each RNA sample using 0.2 mg DNA-free total RNA in the presence of anchoring 3' oligo(dT) primers (T12NA, T12NC, T12NG or T12NT, where N = G,A,T or C). Thereafter, in a reaction containing PCR buffer (Finnzymes Oy), dNTPs (Finnzymed Oy), 10 μ Ci of α 35S-dATP (Amersham Biosciences) and DyNAtsyme II DNA Polymerase (Finnzymes Oy), the cDNA was amplified in the presence of each of the twenty 5' arbitrary 10-mer oligonucleotides and concomitant anchoring primer. The control and diabetic rat PCR products obtained with the same primer pairs were run on adjacent lanes in non-denaturing 6% polyacrylamide gel electrophoresis and compared in band patterns. The reactions were repeated twice with independently purified control and diabetic total RNA to confirm the reproducibility of the results.

4.3.2 DNA cloning and sequence analysis (I)

The bands demonstrating reproducible differences were recovered from the gel by soaking in water and precipitating with ethanol. The DNA was re-amplified without radioisotope, using appropriate primers as described above, and the fragments cloned in TOPO-TA vector (TOPO-TA cloning kit, Invitrogen, Leek, the

Netherlands) according to manual instruction. The plasmids containing the insert were identified by colony-PCR according to the TOPO-TA manual.

Finally the clones were cycle-sequenced using M13 reverse primer, Terminator Ready Reaction Kit and Big Dye Terminator RR Mix (PE Applied Biosystems, Foster City, CA, U.S.A) according the manufacturer's protocol and employing ABI 310 Genetic Analyzer (PE Applied Biosystems). The sequences obtained were analyzed against public databases (e.g. EMBL, GenBank, Fugu, FlyBase).

4.3.3 Northern hybridization (I)

The plasmid DNA obtained as above was isolated (Wizard Plus SV Minipreps, Promega, Madison, WI, USA), reconstituted (GFX™ PCR DNA and Gel Band Purification Kit, Amersham Pharmacia Biotech, Uppsala, Sweden) and labelled with the Oligolabelling Kit (Pharmacia Biotech, Uppsala, Sweden) with α -[³²P]dCTP. The sequences of probes are listed in Supplement 1.

Standard Northern blotting was performed to verify the differential mRNA expression in control and diabetic rat samples and the expression distribution in a variety of normal rat tissues. Total RNA (20 μ g) or poly(A)RNA (2 μ g) was run on electrophoresis in formaldehyde-denaturing 1.4% agarose gels, transferred onto a Magna Charge nylon membrane (MSI, Westboro, MA, U.S.A) and cross-linked (IBI Ultralinker 400, Eastman, Kodak, France). The labelled probes were hybridized on membranes in standard hybridization buffer. After washings, the membranes were exposed to Biomax™ MS film (Kodak) at -70°C for 16- 90h. Ethidium bromide staining of 18S RNA served as control for RNA integrity and loading.

4.3.4 DNA constructs, transfection and semi-quantitative PCR (III)

The DAPIT coding sequence in the TOPO-TA vector was recloned with the pEGFP sequence of the pIRES2-EGFP vector (Clontech Laboratories, Palo Alto, CA, USA). The primers 5'- acgaattcgattgaagtcattgctggccca -3' and 5'- tcgggatccttatgttgctttcacagctggggt -3' were used in a PCR reaction consisting of cycles at 96°C for 2 min, 4x (96°C for 30 s, 50°C for 1 min, 72°C for 30 s), 25x (96°C for 30 s, 60°C for 1 min, 72°C for 30 s) and 72°C for 10 min. After purification of DAPIT amplicon, it was cloned into the pIRES2-EGFP vector at EcoRI and BamHI (MBI Fermentas GmbH, Leon-Rot, Germany; Clontech Laboratories, Palo Alto, CA, USA) restriction sites and amplified in One Shot™ TOP 10 bacteria

(Invitrogen). The insert was sequenced and its size (~204 bp) confirmed by enzyme digestion. Two micrograms of the construct were used for stable transfection of HEK293T cells.

The Lipofectamine transfection reagent (Invitrogen) was used according to the manufacturer's instructions. Transfection efficiency was estimated by flow cytometry (Accuri C6, BD Biosciences) using GFP (FL1, 533 ± 40 nm) fluorescence. A polyclonal cell line was formed by combining twenty-five antibiotic-selected (GeneticinTM; Calbiochem/Merck KGaA, Darmstadt, Germany) clones. Total RNAs from pIRES2-EGFP and DAPIT-pIRES2-EGFP stably transfected cells were extracted by RNeasy Mini Kit (Qiagen), and 1 μ g total RNA was used for RT-PCR using M-MuLV reverse transcriptase, as suggested by the provider (MBI Fermentas). The cDNAs of control and transgenic cells obtained were multiplied by PCR as indicated in section 4.3.4.

4.4 Protein detection (II, III)

4.4.1 Total and nuclear protein isolation from tissues and cells (II, III)

The rat tissue samples were homogenized (Ultra Turrax T8 disperser; IKA Labortechnik, Staufen, Germany) on ice in standard buffer containing 1% Triton X100, protease inhibitor cocktail (Roche Applied Science, Rotkreuz, Switzerland) and phenylmethylsulfonyl fluoride (PMSF) (Calbiochem/Merck). After half an hour's incubation the samples were centrifuged at 12,000 g for 1 min and the supernatants collected. The total proteins of cells grown on 60-80% confluency were obtained as above but without homogenization.

To obtain nuclear extracts, the sub-confluent cells were collected by centrifugation. The cells were swollen in hypotonic buffer (detailed composition in III) and broken on ice using a Dounce homogenizer. Nuclei were pelleted by centrifugation (228 g, 5 min, +4 °C) and purified by isopycnic centrifugation (1,430 g, 5 min, +4 °C) on a two-step sucrose gradient (detailed in III). The proteins of nuclear fraction were extracted as described above. Bradford assay was applied for determining the protein concentration of all samples.

4.4.2 DAPIT antibodies (II)

For the detection of DAPIT, polyclonal IgG antibodies α D15N and α D15C against the amino- and carboxyterminal peptides (MAGPESDGGQFQFTGI and YFKLRPKKTPAVKAT, respectively) of rat DAPIT were raised in rabbits (Davids Biotechnologie, Regensburg, Germany). The immunizations of the animals were once intra-dermally, followed by four intra-muscular repeats. The sera were collected for affinity purification of IgG, and the concentrations of affinity-purified IgG fractions were determined by ELISA, being 0.38 mg/mL for α D15N and 0.16 mg/mL for α D15C.

4.4.3 Western blot (II, III)

In Western blot analyses the Bio-RAD Mini-Protein Tetra Cell system (Bio-Rad Laboratories, Espoo, Finland) were used. Twenty μ g of total protein and 50 μ g of nuclear protein were loaded on 12% denaturing SDS-polyacrylamide electrophoresis gels. The proteins were transferred onto a nitrocellulose membrane (Hybond TM-C Extra; Amersham Biosciences Ltd., Little Chalfont, UK) and blocked with 5% milk for non-specific binding sites of antibodies. The primary antibodies (Table 1) were incubated for two hours to overnight, followed by incubation with horseradish peroxidase (HRP)-conjugated anti-mouse, -rabbit or –goat secondary antibodies (1:2000, DAKO A/S, Copenhagen, Denmark). The enhanced chemiluminescence (Amersham Biosciences) signal was exposed on autoradiography film (Kodak, New Haven, CT, USA), which was scanned for densitometry analysis with image analysis software (Kodak).

Table 1. List of primary antibodies and dilutions used in Western blot.

Antibody	Dilution	Host	Manufacturer
ATP5a	1:4000	Mouse monoclonal	Abcam, #MS502
β -catenin	1:400	Mouse monoclonal	Transduction Laboratories, BD Biosciences, #610153
Connexin 43	1:1000	Rabbit polyclonal	Sigma, #C6219
α D15C (anti-DAPIT)	1:160	Rabbit polygonal	Custom made (II)
E-cadherin	1:1000	Rabbit polyclonal	Santa Cruz, #sc-7870
γ -tubulin	1:4000	Mouse monoclonal	Sigma, #T5326
GFP	1:10000	Mouse monoclonal	Zymed, #33-2600
Hif1 α	1:1000	Mouse monoclonal	Abcam, #10625, ab8366
Histone H1	1:500	Mouse monoclonal	Santa Cruz, #sc-8030
HSP60	1:600	Mouse monoclonal	Sigma, #4149
Integrin α 2	1:200	Mouse monoclonal	Santa Cruz, #sc-13546
N-cadherin	1:1000	Mouse monoclonal	Sigma, #C2542
RhoA	1:200	Mouse monoclonal	Santa Cruz, #sc-418
Sirt3	1:400	Goat polyclonal	Abcam, #118334
Smooth muscle actin	1:200	Mouse monoclonal	Sigma, #A5228
VDAC/Porin	1:1000	Mouse monoclonal	Nordic BioSite, #MSA03
Vimentin	1:200	Goat polyclonal	Millipore #AB1620
Zo-1	1:300	Mouse monoclonal	Invitrogen, #339100

4.4.4 Immunohistochemistry and -fluorescence of cells and tissues (II, III)

HEK293T, HUVEC and C2C12 cells were fixed with 4% paraformaldehyde in standard buffer for 15 min at room temperature, washed with TBS pH 8.0 buffer and permeabilized for 10 min with 0,1 % Triton X-100 (II, III). Thirty minutes' incubation in 5% fat-free milk was used to block the unspecific binding sites of antibodies. Primary antibodies were incubated at 0.5-1 μ g/ml dilution for 1-2 hours at room temperature. Cells were washed with TBS buffer supplemented with 0,1% Tween 20 (Sigma), followed by incubation with secondary antibody conjugated with a fluorophor for 1 hour. Either single or double staining was performed, the double staining constructed one signal upon another. The samples were examined by confocal microscopy (Perkin Elmer-Cetus/Wallac UltraWiev LCI system; Wellesly, MA, USA) or a fluorescence microscope (Olympus BX60, Olympus Corp., Tokyo,

Japan). Details of microscope cameras, software and data-processing are reported in studies II and III.

Four- μ m-thick sections of paraffin-embedded tissues from the rat skeletal muscle, myocardium, adipose tissue, kidney, liver, brain and small bowel, and human liver and kidney were used for immunohistochemical staining applying the standard immunoperoxidase method. Briefly, deparaffinized sections were boiled for 15 min in 0.01 M citrate buffer (pH 6.0) to retrieve the antigen. The signal was constructed with primary antibody α D15C (anti-DAPIT) (dilution 1:150-1:200) incubated overnight at 4°C, followed by incubation with the secondary antibody (biotinylated anti-rabbit IgG, Vector Laboratories, 1:100) for 30 min at room temperature. Endogenous peroxidase activity was removed using 0.3% H₂O₂ for 30 min, followed by ABC-reaction with the Vectabond TM reagent (Vector Laboratories) for 30 min at room temperature. Antigen-antibody complexes were visualized using diaminobenzidine (DAB, DakoCytomation Inc., Carpinteria, CA, USA) as chromogen. Finally, the sections were counterstained with Mayer's hematoxylin (Merck KGaA, Darmstadt, Germany), washed with tap water, dehydrated and mounted with Pertex mounting medium. Sections incubated with the peptide-blocked antibody or without the primary antibody served as negative controls.

4.5 Mitochondrial function (III)

4.5.1 DNA copy number (III)

For mtDNA copy-number analysis, total DNA was prepared as reported in (Fukuoh et al., 2014). The isolated DNA from 0.4×10^6 cells were re-suspended in TE buffer (pH 8.0), purified and quantified by Nanodrop. The relative mtDNA copy number was measured by real-time qPCR using primers for mitochondrial COXII subunit and nuclear APP (primer sequences in III) in a StepOnePlus instrument (Applied Biosystems) using Fast SYBR Green Master Mix (Applied Biosystems) under conditions recommended by the manufacturer, with 20 sec of enzyme activation at 95°C, followed by 40 cycles of 95°C for 3 sec and 60°C for 30 sec.

4.5.2 Activity of TCA cycle and respiratory chain (III)

The activity of citrate synthase in the cells was measured using the (Sigma-Aldrich CS0720) kit according to manufacturer's instructions with an automated KoneLab device (Thermo Scientific, Vantaa, Finland).

A Clark-type electrode (Oxygraph, Hansatech Instruments Ltd, Norfolk, UK) was applied for measuring oxygen consumption in intact cells. A total of 1×10^7 cells were suspended in 500 μ l cell culture medium at 37°C and the maximum respiration obtained by FCCP (uncoupler, Sigma) titration (5–9 μ M). Oxygen consumption was inhibited with 150 nM rotenone (complex I inhibitor), 30 ng/ml antimycin A (complex III inhibitor), 100 μ M Cyanide (Complex IV inhibitor) or 100–200 nM Oligomycin (Complex V inhibitor) (Sigma).

The 1×10^7 cells were permeabilized with 80 μ g/ml digitonin and oxygen consumption recorded in respiratory buffer A (225 mM sucrose, 75 mM mannitol, 10 mM Tris-buffer pH 7.4, 10 mM KCl, 10 mM KH_2PO_4 , 5 mM MgCl_2 , 1mg/ml BSA (Sigma)) at 37°C. The substrates (Sigma) used were 10 mM ADP, 5 mM pyruvate + 5 mM malate for complex I, 10 mM succinate for complex II, and 50 μ M TMPD and 1 mM ascorbate for complex IV. All measurements were independently corrected by subtracting the residual oxygen consumption present after full inhibition of the respiratory chain.

4.5.3 Mass, membrane potential and superoxide level assays (III)

Flow cytometry was used to determine mitochondrial mass, membrane potential and superoxide level in intact cells. The cationic dyes penetrating specifically to mitochondria in living cells were used. The concentrations and incubation times of the dyes were essentially titrated for previous application using HEK293T cells transfected with respiratory bypass enzymes (Cannino et al. 2012), and these parameters were followed in study III.

Equal numbers of subconfluent control and DAPIT over-expressing cells were treated with 200 nM 10-nonyl acridine orange (NAO; Invitrogen,) for 30 min at 37°C to measure mitochondrial mass, 200nM tetramethyl rhodamine methyl ester (TMRM; Invitrogen,), for 30 min at 37°C to measure membrane potential or 2.5 μ M MitoSox (Invitrogen,), for 45 min at 37°C for measuring superoxide level. Replacing staining medium with 1xPBS stopped the reaction and the cells were maintained at 37°C (NAO and TMRM) or on ice (MitoSox) until measured. Negative controls for

mitochondrial membrane potential were obtained by adding 10 μ M FCCP before flow cytometry analysis.

BD Accuri C6 flow cytometry (BD Biosciences) was used in counting fluorescence from 40,000 cells excluding debris and dead cells. The staining was measured using 488 nm (bandpass) excitation and emission of FL2 (585 ± 40 nm) for NAO and TMRM, FL3 (620 ± 15 nm) for Mitosox and FL1 (533 ± 40 nm) for GFP. Fluorescence bleeding was compensated independently for each series of experiments. All measurements provided as “relative to mitochondrial (mt) content” were normalized by NAO quantification, while measurements provided as “per cell” were normalized to the cell count.

4.5.4 Isolation of mitochondria and complex V activity (III)

The cells from four 17.5 cm or 8–10 10 cm in diameter culture plates were collected by centrifugation at room temperature. All the following steps were performed at 4°C degrees. For crude extraction of mitochondria, the cells were bloated in 5.5 ml of ice-cold hypotonic buffer (10mM NaCl, 1.5mM MgCl₂, 10mM Tris-HCl pH 7.5 (Sigma) supplemented with protease inhibitor cocktail (Roche, Mannheim, Germany)) for 8–13 min and ruptured with eight strokes using a Dounce homogenizer. To sustain the mitochondria, 4 ml of 2.5X MS buffer (700 mM sucrose, 2.5 mM EDTA, 12.5 mM Tris-HCl pH 7.5, protease inhibitors) was added. To remove nuclei and cell debris, the samples were centrifuged at 1,300 g for 10 min. Centrifugation at 17,000 g for 15 min was used to pellet the mitochondria, which were further diluted to 0.5–1 ml of 1X MS buffer (0.28 mM sucrose, 5 mM Tris-HCl, 1 mM EDTA pH 7.5, protease inhibitors).

For sucrose gradient purification of mitochondria, fifteen ml of 1.5 M and 1.0 M sucrose in buffer (10mM Tris-HCl pH 7.4, 1 mM EGTA, 0,1% BSA, protease inhibitors) were layered in ultracentrifuge tubes. The crude extract of mitochondria was layered on top of sucrose and centrifuged at high speed (60 000 g) for 20 min at 4°C with a Beckman Optima XL-1 ultracentrifuge (Beckman Coulter Life Sciences) device. The resulting fraction of mitochondria in the interphase of sucrose layers was collected, measured in volume and slowly diluted on ice for 4X with 0.2M mannitol in Tris-EGTA-BSA buffer. Finally, the mitochondria were pelleted at 17,000 g for 15 min at 4°C, diluted to 40–50 μ l of 1X MS buffer and stored at -80°C.

The oligomycin-sensitive activity of complex V was spectrophotometrically measured as essentially described in (Benit et al. 2006, Rustin et al. 1994). The

measurements utilized lactic dehydrogenase and pyruvate kinase as coupling enzymes.

4.6 Cell functional measurements (III)

4.6.1 Growth, mortality and synchronization (III)

Cell growth and mortality were determined by following cell proliferation for five days, counting the living and dead cells in a Burker hemocytometer after trypan blue labelling (0.4%; Sigma). Fifteen thousand cells were seeded on a 24-well culture plate (Nunclon, Thermo Scientific) in 500 μ l of culture medium a day prior to the test.

In order to follow the cell division more accurately, the control and DAPIT-overexpressing cells were synchronized by a double thymidine block method (DIAMONDS Deliverable 1-D1.1.3, ResearchGate.net). At 30% confluence on a 24-well culture plate, the cells were supplemented with 1 ml of cell culture medium containing 2 mM thymidine (Sigma) for 18 hours. Cell division was released by adding fresh cell culture medium for nine hours followed by another thymidine step for 17 hours. This prepared the cells to progress synchronously through the G2- and mitotic phases. Upon release from thymidine, the cells were cultured in normal medium for various times ranging from 4 to 24 hours, and cell cycle progress followed. At the time point under measurement, the cells were pelleted and stained with 250 μ l of PI staining solution (25 μ g/ml propidium iodide, 100 μ g/ml RNase A, 0.1% sodium citrate, 0.1% Triton X-100 (Sigma)) for 20 min on ice and examined using flow cytometry (channel FL3). The number of cells (arbitrary units) was blotted against the DNA content at each time point and the test repeated for four times.

4.6.2 Migration and adhesion (III)

The migration of control and DAPIT-over expressing cells was studied by scratch wound assay on a 12-well culture plate (Nunclon) grown confluent. After 1 hour treatment with 20 μ g/ml Mitomycin C (Sigma), a tip was used to scratch a wound on the plate, fresh medium added and the cells incubated overnight at 37°C. After fixation with 4% PFA (Sigma) for 15 min, the cells were stained with crystal violet (0.5 mM, Sigma) for 5 min in 70% ethanol. The cells migrating in the scratched area were counted using a phase contrast microscope (Axiovert 200 M, Zeiss).

Cell attachment was studied using PMS/MTS reagents (Promega, Madison, WI, USA) as instructed by the manufacturer. Cell detachment, in turn, was determined using the same protocol as in migration assays on a 48-well culture plate (Nunclon) without wounding. The areas where the cells had detached from the bottom of the wells were quantified using ImageJ (imagej.nih.gov/ij) software.

4.6.3 Glucose and lactate assays (III)

Glucose and lactate levels were analyzed using the enzymatic-amperometric method and chip-sensor technology (Biosen C-line Sport, EKF Diagnostic, Magdeburg, Germany). Glucose consumption and lactate production were measured in cell culture media from the proliferation test and results normalized with the corresponding cell number.

4.6.4 Oncomine and CCLE data-analysis (III)

The Oncomine Cancer Genomics Data Analysis tool (Rhodes et al. 2004) and the Cancer Cell Line Encyclopedia, CCLE (Barretina et al. 2012) were used to mine the copy number profiles of *Usmg5* in a large subset of cancer cell lines (Barretina et al. 2012, Beroukhim et al. 2010, Beroukhim et al. 2007, Rothenberg et al. 2010, Nikolsky et al. 2008, Chin et al. 2007, Hu et al. 2009, Lu et al. 2010, Olejniczak et al. 2007, Sos et al. 2009). In the dataset, the values of log₂ copy number units ($\geq 0,34$) were analyzed. The number of DNA copies ($= 2^{(2^{\text{y-axis value}})}$) was calculated as advised in the Oncomine instructions.

5 RESULTS

5.1 DD-PCR in diabetic rat insulin-sensitive tissues (I)

Several alterations in gene expression were identified associated with STZ-induced insulin depletion. In total 160 differential display reactions were run utilizing the total RNA of normal and type 1 diabetic Sprague Dawley rat skeletal muscle and adipose tissue. From approximately 2800 visualized transcripts in skeletal muscle (Figure 6A), 49 were repeatedly differentially displayed. Thirty-nine of these were down-regulated and ten up-regulated in the diabetic tissue. Fifteen of these differentially displayed cDNAs were reliably cloned and sequenced. Ten transcripts were detected by Northern blotting. Five of these transcripts were confirmed to be down-regulated in diabetic skeletal muscle and five (aldolase A, Nnt and Atp6V0d1, OPTN and YEATS4) showed opposite expression compared to DD-PCR. In the DD-PCR method several transcripts of the same size may overlap (OPTN and YEATS4 originating from the same clone) and the clones are seen as one transcript in electrophoresis (Liang, Pardee 1995). This phenomenon may introduce variation between DD-PCR and Northern blot results. The remaining five cloned and sequenced cDNAs could not be detected by Northern blotting.

In the rat adipose tissue (Figure 6B), approximately 3200 transcripts were obtained, of which 35 were differentially displayed. Eleven of these were down-regulated and 24 up-regulated in the diabetic tissue. Fifteen cDNAs were reliably cloned and sequenced. Five transcripts were detected by Northern blotting and three of these were confirmed to be up-regulated, one down-regulated and one showed opposite expression (PPP1G) compared to DD-PCR. Ten of the cDNAs could not be detected by Northern blotting.

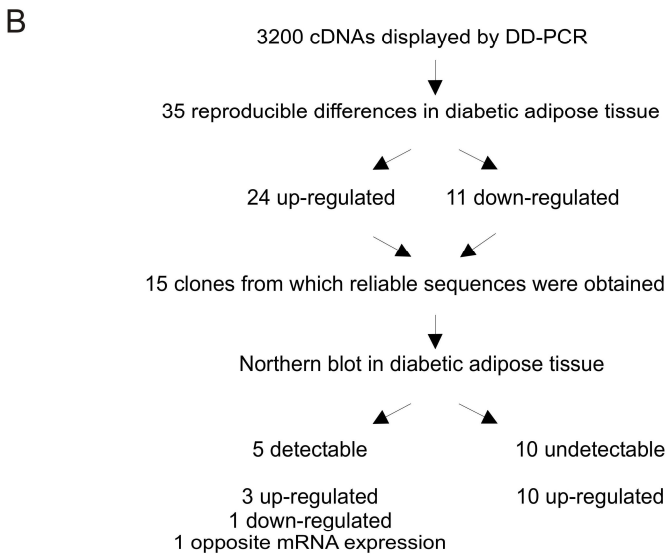
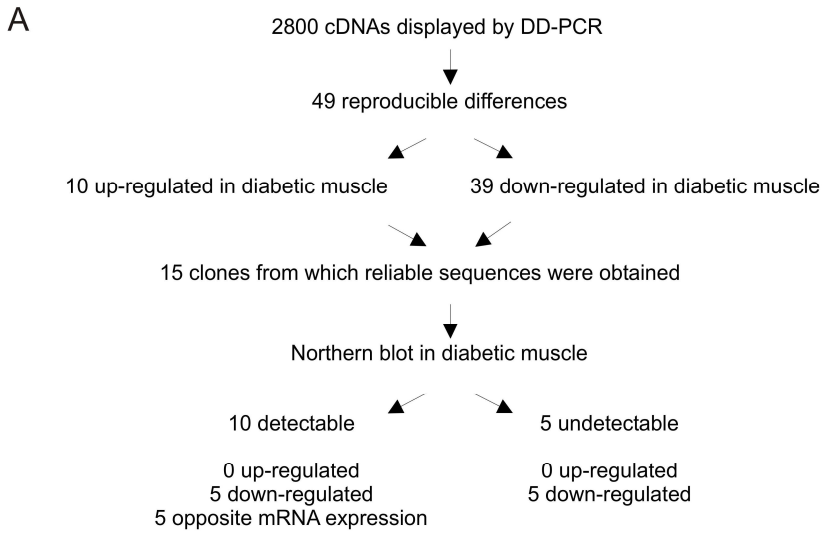


Figure 6. Schematic diagram of mRNA DD-PCR of A) skeletal muscle and B) adipose tissue.

The Northern blot expression of the transcripts other than DAPIT detected by DD-PCR is shown in Table 2. The transcripts are identified with the DD-PCR clone, valid accession number, mRNA size and relative changes in expression between diabetic and control tissue. The values are calculated from quantitated blot intensities, which were normalized with that of ribosomal 18S RNA. The transcripts are annotated to categories involving protein dephosphorylation, glycolysis, oxidative phosphorylation, gene expression, lysosomal H⁺-transport and other functions.

Large scale changes in gene expression involved in the substrate and energy metabolism in the skeletal muscle of STZ-diabetic mice were reported previously (Yechoor et al. 2002, Yechoor et al. 2004). The DD-PCR originated mRNAs related to glycolysis and oxidative phosphorylation shown in Table 2 are in line with the findings of Yechoor et al. (Yechoor et al. 2002, Yechoor et al. 2004). However, the known genes or expressed sequence tags (ESTs) reported by Yechoor et al. did not contain DAPIT/*Usmg5*. Therefore, DD-PCR was of relevance in discovering DAPIT as a novel cDNA, which contained a conserved open reading frame of an entire protein. Its mRNA level was validated to be differentially expressed in the insulin-sensitive tissues of STZ-diabetic animals, and the putative protein was deposited to public database, and chosen for further studies.

5.2 Molecular characterization of DAPIT (I)

5.2.1 Northern blot analysis of DAPIT mRNA (I)

Clone 20Cc2 containing 322 base pairs was found by DD-PCR in STZ-diabetic skeletal muscle and used as a probe for Northern blotting (Figure 7A on page 53 and Supplement 1 on page 109). One band of 0,4 kb was confirmed to be down-regulated in skeletal muscle and myocardium but not in control brain (Figure 7B). Examination of the Northern blot panel of 13 rat normal tissues revealed the strongest expression in two insulin-sensitive tissues, skeletal and cardiac muscle (Figure 7C). The expression was moderate in brain, thymus, stomach and testis and lowest in lung, liver, kidney, adrenal gland, spleen, small intestine and adipose tissue.

Table 2. mRNAs expressed in control and diabetic insulin-sensitive tissues.

Accession number	Functional ontology	Gene	mRNA size (kb) reported/found	Relative change in diabetes					
				Muscle		Fat		Heart	
				C	D	C	D	C	D
NM 022498	Protein dephosphorylation	PPP1G	2.193/ 2.2						
				1.13		-1.19		2.81	
NM008705	Transphosphorylation of nucleotidedephosphates	Nme2	0.603 / 0.6						
				-1.45		-1.43		-117	
NM001271536	Glycolysis	Aldolase A	1.442/ 1.5						
								-1.12	
NM001011927	Electron-proton transport	Atp6V0d1	1.808 / 1.8						
				1.53		1.44		1.03	
NM001013157	NAD-metabolism	Nnt	4.149/ 4.0 2.5 2.0						
								-1.67	
								-1.47	
								-1.16	
NM001011905	Oxidative phosphorylation	Ndufs2	1.612/ 1.6						
				-1.10		1.88		-4.3	
NM001134705	Oxidative phosphorylation	Cox7c	0.444/ 0.4						
				-1.59		1.55		-56	
NM023093	Oxidative phosphorylation	Atp5a1	1.871/4.5						
								-1.23	
AJ271158	Oxidative phosphorylation	DAPIT	0.4						
				-1.35				-1.10	
NM001127927	Transcription factor activity	YEATS4	1189/ 1.4						
				1.33		1.07		-154	
XM006254264	Rab GTPase binding	OPTN	3853/ 3.5						
				1.80					
AF1667170	Photoreceptor morphogenesis	Crb1	2.046/ 2.0						
								1.13	

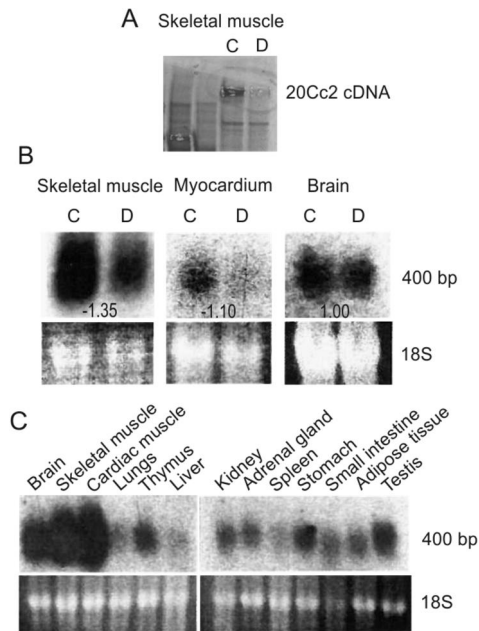


Figure 7. Clone 20Cc2 (DAPIT mRNA) in insulin-sensitive tissues of STZ-induced diabetes and other rat tissues. *C* and *D* stand for control and diabetic animals, respectively. A) cDNA in control and diabetic skeletal muscle by DD-PCR. B) Effect of STZ-induced diabetes on mRNA expression in control and diabetic skeletal muscle, myocardium and brain. C) Expression in normal rat tissues. Ethidium bromide-stained bands for the 18S ribosomal RNA shown as internal control. This figure (without A and quantification in B) was originally published as Fig.1 in *Acta Diabetologica* 2001;38(2):83-6 by Päivärinne H and Kainulainen H (© Springer-Verlag 2001), and reprinted with permission of Springer for purpose of dissertation.

5.2.2 mRNA and protein sequence of DAPIT and its homologues (I)

The cDNA clone 20Cc2 contained a conserved open reading frame (ORF) of 174 nt for a putative protein of 58 amino acids (Figure 8a). Similarity searches using BLAST in EMBL and GenBank databases revealed various rat, mouse, rabbit, porcine and bovine ESTs. Also *Xenopus* EST and over 50 human ESTs were encountered. Most of these ESTs, derived from various tissue and cell lines, contained an ORF of 156-177 bases and 64-96% identity with 20Cc2 ORF. The sequence similarity among the species was considerably lower outside ORF.

The predicted 58 amino acid protein was designated DAPIT (Diabetes-Associated Protein in Insulin-sensitive Tissues, EMBL accession no. CAB71156;

GenBank: AJ271158.1 [http://www.ncbi.nlm.nih.gov/nucore/AJ271158]). The ORF of 20Cc2 resembling mammalian, *Xenopus* and *Fugu* ESTs encode proteins highly similar to DAPIT (58-98% identity)(Figure 8b). DAPIT also had 38% identity to a flesh fly peptide Neb-cGP and 40 % identity to *Drosophila melanogaster*. Thirteen amino acids were fully conserved in all predicted proteins.

a

```

gtgatcggacgaagaagattgaagtcattggctggcccagaaagtgatggccaattccagt 60
                M A G P E S D G Q F Q F 12

tcactggtattaaaaatatttcaactcttataccctcacaggtagaatgaattgtgtcc 120
  T G I K K Y F N S Y T L T G R M N C V L 32

tggccacatatggaggcattgctttgttgctctatactttaagttaaggcctaaaaaa 180
  A T Y G G I A L L V L Y F K L R P K K T 52

ccccagctgtgaaagcaacataaatggattttgaaatgtctggccttatctgttaagtc 240
  P A V K A T Stop 58

cacgcctgaagaagctgatgtgaactcatcatgtaataactcaatttgtaataaattat 300
gaacctggaaaaaaaaaaaaaaaaa 322

```

b

R. norvegicus	M A G P E S D G Q F Q F T G I K K Y F N S Y T L T G R M N C 30
M. musculus	M A G A E S D G Q F Q F T G I K K Y F N S Y T L T G R M N C 30
O. cuniculus	M A G P E T D A Q F Q F T G I K K Y F N S Y T L T G R M N C 30
S. scrofa	M A G P E T D A Q F Q F T G I K K Y F N S Y T L T G R M N C 30
B. taurus	M A G P E A D A Q F H F T G I K K Y F N S Y T L T G R M N C 30
E. caballus	M - - - - P Q F Q F T G I K K Y F N S Y T L T G R M N C 24
H. sapiens	M A G P E S D A Q Y Q F T G I K K Y F N S Y T L T G R M N C 30
X. laevis	M G G H Y S G T H H Q F T G I Q K Y F N A Y T I T G R R N C 30
F. rubripes	M G G H D A G T Q H Q F T G I A K Y F N A Y T I T G R R N C 30
D. melanogaster	M A G E G E - - - K L T G L S K I F N G T T M S G R A N V 26
Neb-cGP	A G A E A E - - - K L S G L S K Y F N G T T M A G R A N V 26

R. norvegicus	V L A T Y G G I A L L V L Y F K L R P K K - T P A V K A T 58
M. musculus	V L A T Y G G I A L L V L Y F K L R P K K - T P A V K A T 58
O. cuniculus	V L A T Y G G I A L L V L Y F K L R S K K - T P A V K A T 58
S. scrofa	V L A T Y G G I A L L V L Y F K L R S K K - T P A V K A T 58
B. taurus	V L A T Y G S I A L I V L Y F K L R S K K - T P A V K A T 58
E. caballus	V L A T Y G S I A L L V L Y F K L R S K K - T P A V K A T 52
H. sapiens	V L A T Y G S I A L I V L Y F K L R S K K - T P A V K A T 58
X. laevis	V L A T Y A G I A T L I L F F K L K P K K Q T P A I T D K 59
F. rubripes	V L A T Y A S I L G V V L F F K L K P K K K - - A I T E K 57
D. melanogaster	A K A T Y A V M G L L I A Y Q V L K P K K K 48
Neb-cGP	A K A T Y A V I G L I I A Y N V M K P K K K 48

Figure 8. Sequences of DAPIT and its homologues. a) Nucleotide and deduced amino acid sequences of DAPIT (clone 20Cc2). The amino acid sequence is shown in single-letter code. PolyA signal is

underlined. The predicted location of the putative transmembrane region is presented in the black box and the dilysine motif in the gray box. b) Alignment of rat DAPIT (EMBL accession number CAB71156), the predicted amino acid sequences from mouse, rabbit, porcine, bovine, equine, human, *Xenopus* and pufferfish ESTs (exemplary GenBank accession numbers AA105851, C83342, AW619544, AW353693, AW260934, AI417855, AW642342 and identification number FRd031apcG18 in the Fugu database (http://fugu.hgmp.mrc.ac.uk/fugu/fugu_cdna), respectively), predicted gene product of *Drosophila* (GenBank no. AAF46590) and cAMP-generating peptide (Neb-cGP) isolated from the flesh fly *Neobellieria bullata* (GenBank no. AAB36093). Amino acids differing from the DAPIT sequence are boxed. This figure was originally published as Fig.2 in *Acta Diabetologica* 2001;38(2):83-6 by Päivärinne H and Kainulainen H (© Springer-Verlag 2001), and reprinted with permission of Springer for purpose of dissertation.

5.2.3 Structural analysis of DAPIT (I)

The hydrophobic sequence in DAPIT amino acids 27-46 suggested a possible transmembrane region (Figure 8a). Several analysis programs confirmed this by predicting a transmembrane helix varying from residues 23-33 to 45-47 and supporting a feature of single pass. A cytoplasmic orientation of DAPIT was also suggested. The di-lysine motif in the C-terminal end of DAPIT and the positive charge of this cytosolic tail suggested targeting to endoplasmic reticulum. Also two of the six threonine residues (Thr-25 and Thr-52) were predicted to be phosphorylated. All the analysis programs used are listed in study I. The N-terminal end flanking the transmembrane region contained no known motifs.

5.3 Localization and tissue expression of DAPIT (II)

5.3.1 Specificity of DAPIT antibodies (II)

Custom-made polyclonal rabbit antibodies against the amino- and carboxyterminus of DAPIT (aD15N and aD15C, respectively) were used. In transient transfection studies in HEK293T cells, the concomitant antibody recognized both DAPIT fused to N- and to C-terminus of EGFP. Incubation with antigen-blocked antibody abolished all DAPIT staining in immunofluorescence of HUVEC cells (Figure 1, left in upper and Figure 3, left in middle panel in II). In isolated proteins from HEK293T and HUVEC cells, approximately 6.7kDa band disappeared in SDS-PAGE upon peptide blocking of aD15C (Figure 2A in II), whereas the aD15N failed to have an effect in blotting and the band size of native protein recognized in other applications

could not be confirmed. In Western blot of control and STZ-diabetic insulin-sensitive tissues, the C-terminal antibody recognized a correct-size protein (Figure 10K), and in skeletal muscle also a protein of ca. 50kDa was seen. All bands disappeared upon peptide blocking of the antibody. Also DAPIT staining in immunohistochemical studies was negative after peptide blocking of the α D15C (Figure 9 A). Staining with α D15N (Figure 9B) in immunohistochemistry was similar to that of α D15C (Figure 10D), thereby confirming the specificity of the antibody against DAPIT in this application. As the C-terminal antibody was validated in all three applications, it was selected for use in subsequent studies.

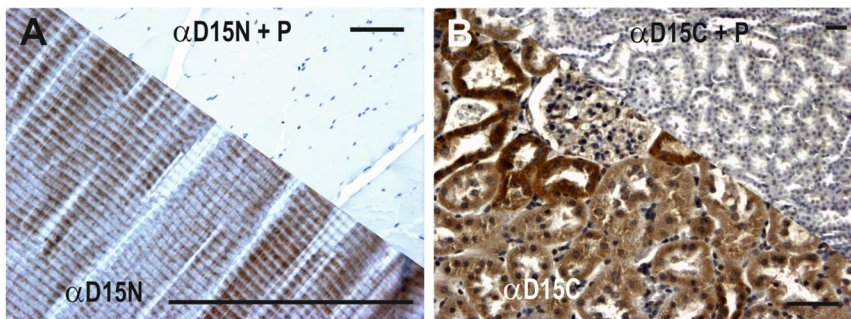


Figure 9. Specificity of the anti-DAPIT antibodies by immunohistochemistry. A) Longitudinal section of rat cardiac muscle and B) kidney proximal tubules were stained with corresponding antibody. In right upper corner is shown the staining with peptide-blocked antibody. Scale bars 50 μ m and magnification; 20x, 100x (A), 10x, 20x (B).

5.3.2 Cellular localization of DAPIT by immunofluorescence (II)

After the discovery of the DAPIT protein, this was published as a subunit of the F_o portion of ATP synthase (Chen et al. 2007, Meyer et al. 2007), which share a structure similar to vacuolar ATPase. Thus, DAPIT localization in mitochondria and lysosomes was confirmed by immunofluorescence in human and rodent cell lines HEK293T, HUVEC and C₂C₁₂. The C₂C₁₂ cells showed mainly mitochondrial (Figure 10 A) and HEK293T cells also some lysosomal (Figure 10B) location of DAPIT. The HUVEC cells expressed an abundance of lysosomes containing DAPIT (Figure 3 in II), indicating that its lysosomal expression may be a cell type-dependent phenomenon.

5.3.3 Tissue expression of DAPIT by immunohistochemistry and Western blot (II)

The expression of DAPIT was investigated in several healthy rat and human tissues by immunohistochemistry (Figure 10 on page 59) with antibody against carboxy-terminal end of the protein. The expression of DAPIT varied in intensity within a tissue and from one tissue to another, showing mainly cytoplasmic staining but also occasional staining in some nuclei. The expression in cytoplasm varied, exhibiting both smeary and finely granular staining patterns. In general, the strongest DAPIT expression was observed in insulin-sensitive and epithelial cells as well as in neurons. Cardiocytes and the myofibers showed strong expression of DAPIT complying with the sarcomeric structure (Figure 10 C,D). Staining intensities of skeletal muscle cells showed considerable differences. Double staining with type IIa-specific myosin antibody demonstrated that DAPIT was more abundant in highly oxidative (type IIa) than in less oxidative or glycolytic muscle fibers (Figure 10E) and was located preferentially under the sarcolemma. Adipocytes of white and brown adipose tissue (Figure 10F) showed distinct cytoplasmic staining, which was considerably stronger in brown fat. In hepatocytes, granular cytoplasmic staining was observed (Figure 10G). This staining and granularity tended to be more intensive in the cells surrounding blood vessels and bile ducts. Pyramidal cells of the hippocampus (Figure 10H) and Purkinje cells of the cerebellum were strongly stained in rat brain. The epithelial cells of proximal tubuli in the kidney were intensively stained (Figure 10I) showing, however, considerable difference in staining intensity from cell to cell. Epithelial cells of the rat small intestine were stained from the base of the crypt to the villus tips showing also some nuclear staining (Figure 10J). The staining with the antibody against the amino-terminal end of DAPIT were similar to those of the carboxy-terminal antibody.

The qualitative level of protein expression of DAPIT in insulin-sensitive tissues from control and diabetic rats showed up-regulation in the diabetic myocardium, m. gastrocnemius and epididymal adipose tissue, but down-regulation in the liver in the early stage of diabetes (Figure 10K). Western blot also showed two tissue specific bands of ca. 50 kDa in skeletal muscle but not in other tissues.

In contrast to rats, the expression of DAPIT did not change in comparing healthy and diabetic calf muscle complexes (gastrocnemius, soleus, plantaris) of mice with diabetes for 1-5 weeks (Figure 2C in II). However, DAPIT correlated well with the mitochondrial proteins cytochrome c ($r = 0.450$, $p = 0.014$) and ATP synthase subunit alpha ($r = 0.689$, $p \geq 0.001$) in mouse skeletal muscle.

5.4 Metabolism and cell behavior of DAPIT over-expressing HEK293T cells (III)

5.4.1 Terminology and normalization of mitochondrial parameters (III)

To simplify the terminology, the cells transfected with the empty pIRES-EGFP vector are called “control cells” and those with a transgene as “DAPIT cells”. The mRNA and protein level, and mitochondrial mass in HEK293T cells were measured to assure the cell culture model. As mitochondrial mass is sensitive to H⁺-ATP synthase impairments (Fukuoh et al., 2014; for refs. see Piantadosi & Suliman, 2012; Scarpulla, Vega, & Kelly, 2012), the reported parameters were normalized on mitochondrial mass.

In DAPIT cells, DAPIT was localized to the mitochondria (Figure 11A on page 60), showing very few DAPIT-positive lysosomes. This suggested a pure mitochondrial manifestation.

5.4.2 Decreased mitogenesis (III)

Mitogenesis in DAPIT cells was decreased: The mitochondrial mass in DAPIT cells was significantly lower than in control and HEK293T cells (Figure 11B), while it was intermediate in HEK293T cells. This result was in line with decreased translocation of PGC1 α to the nuclei and the mtDNA content in DAPIT cells (Figure 1F,G in III).

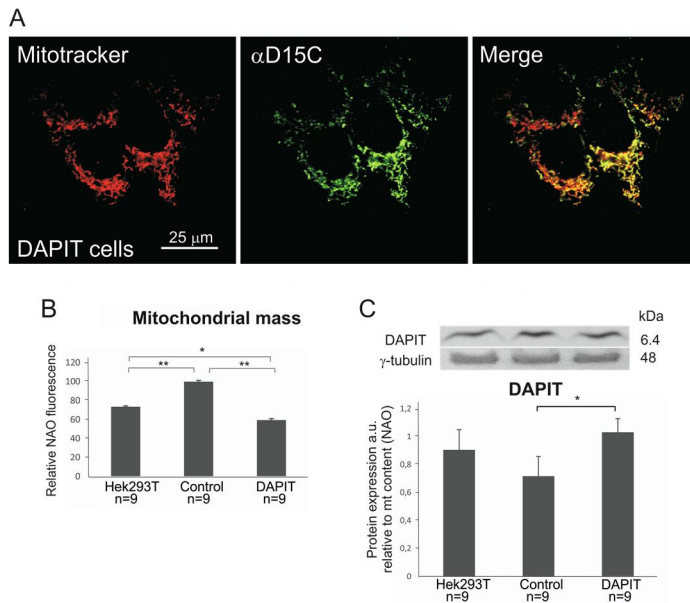


Figure 11. DAPIT over-expression reduced the mitochondrial mass in DAPIT over-expressing cells. (A) Representative confocal microscopy images of cells stained by Mitotracker and anti-DAPIT antibody, α D15C. (B) Mitochondrial mass was measured by flow cytometry of NAO-stained cells. (C) Protein level of DAPIT estimated by Western blot. The error bars are S.D. and asterisks indicate: * $p < 0.05$, ** $p < 0.01$. Adapted under Creative Commons Attribution License from Figure 1 in original publication III.

5.4.3 DAPIT over-expression (III)

The transgenic construct was functional, presenting a higher level of *Usmg5* messenger RNA compared to the HEK293T and control cells. At protein level (Figure 11C), DAPIT expression was slightly decreased in control cells (vehicle) as compared to HEK293T cells. A mild but not significant increase was observed between HEK293T and DAPIT cells, but significantly higher expression was seen in DAPIT than in control cells ($p < 0.05$). The translation of green fluorescent protein from internal ribosome entry was lower in DAPIT cells compared to translation from the 5'RNA CAP (Figure 1D in III), a phenomenon previously reported typical for IRES-containing bicistronic vectors (Stein et al., 1998).

5.4.4 Metabolic activity of mitochondria (III)

The effect of DAPIT over-expression on mitochondrial protein transport, TCA cycle activity, respiratory chain activity in intact cells and oxygen consumption driven by complexes I, II and IV in permeabilized cells was estimated. The results are reported both at cellular level (Supplement 2 on page 111) and in relation to mitochondrial content (Figure 12).

At mitochondrial level, the expression of VDAC1, the activity of citrate synthase and CI subunit NDUF53 were significantly increased upon DAPIT over-expression ($p = 0.001$, 0.005 and 0.004 , respectively) (Figure 12A-C). The oxygen consumption from complexes I, II and IV in digitonin-permeabilized cells and respiration of intact cells was also increased ($p = 0.044$, 0.000 , 0.002 , 0.000 , respectively) (Figure 2D in III), showing no rise in CV content, as sustained by unaltered expression of F₁ complex subunit ATP5a (Figure 12D). The increase in respiratory chain function was further supported by unchanged expression of Sirt3 (Figure 2G in III), a modulator of the activity of metabolic enzymes. DAPIT cells exhibited elevated basal and maximal respiration ($p = 0.003$ and 0.004 , respectively) (Figure 12E), increased oligomycin-sensitive respiration (Figure 12F) and decreased activity of ATP synthase ($p = 0.05$) (Figure 12G). Accordingly, the membrane potential ($p = 0.001$) (Figure 12 H) and superoxide ($p = 0.001$) (Figure 12I) levels were increased. When assessed at cell level, respiration (Supplement 2I on page 111) and TCA cycle activity (Supplement 2C) remained unchanged between cell lines, but VDAC1 expression (Supplement 2B), CV activity (Supplement 2J), membrane potential (Supplement 2K) and superoxide (Supplement 2L) showed the same changes as when normalized to mitochondrial mass. Taken together, these results suggest enhanced capacity of the respiratory chain due to DAPIT over-expression. The significant increase in HSP60 ($p = 0.009$) at protein level indicated an appropriate maintenance of the mitochondrial proteins in cells over-expressing DAPIT.

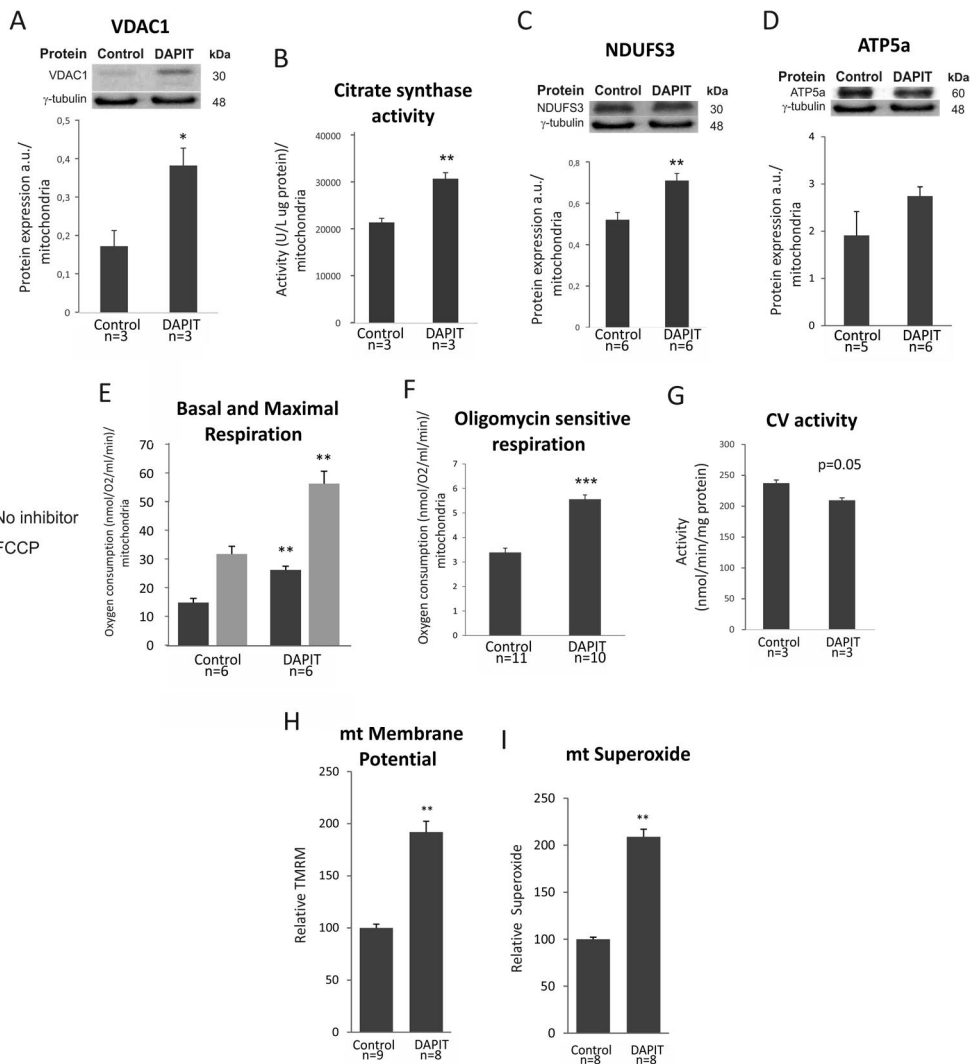


Figure 12. Mitochondrial activity in DAPIT over-expression (relative to mitochondrial mass (NAO)). (A) Protein level of VDAC1 by Western blot of cellular lysates. (B) Citrate synthase activity was measured by spectrophotometric analysis in protein extracts from control and DAPIT cells. (C) Protein level of NDUFS3. (D) Protein level of ATP5a. (E) Basal and maximal respiration by oxygen consumption of living cells. (F) Inhibitor-sensitive oxygen consumption of complex V in intact cells. (G) Spectrophotometric analysis applied to measure CV activity in backward direction using lactic dehydrogenase and pyruvate kinase as coupling enzymes. Mitochondrial (H) membrane potential and (I) superoxide levels measured by flow cytometry of TMRM and Mitosox-stained cells. The error bars are S.D. and asterisks indicate: * $p < 0.05$, ** $p < 0.01$ and *** $p < 0.001$. Adapted under Creative Commons Attribution License from Figure 2 in original publication III.

5.4.5 Nuclear proteins (III)

An increase in nuclear translocation of the Hif1a and b-catenin transcription factors (Figure 13 A,B) facilitated relocation of E-cadherin from cell junctions to the cytosol in DAPIT cells (Figure 13C), the parameters known to be involved in cellular dedifferentiation.

5.4.6 Cell morphology and junction and adhesion proteins (III)

The over-expression of DAPIT induced changes in cell morphology. The regular cuboidal epithelial-like control cells transformed to cells with irregular size and shape and decreased intercellular separation (Figure 13C). These cells also evinced a polygonal, sheet-like appearance but unaffected cell projections.

Protein levels of E-cadherin decreased significantly (Figure 13D). N-cadherin (Figure 13E), Connexin 43, ZO-1, Vimentin, Integrin $\alpha 2$, SMA (albeit non-significant) and their modulator RhoA GTPase (Figure 4C-I in III) were all increased. Such patterns of expression resemble EMT, which is observed in embryogenesis, wound healing and cancer.

5.4.7 Cell growth, mortality, migration and adhesion (III)

DAPIT cells showed slower growth (Figure 14A on page 65) but unaltered mortality during the active growing phase (days 1–3) (Figure 5B in III). Thymidine-synchronization revealed DAPIT cells entering the G1 phase approximately four hours later than control cells (Figure 5C in III), the delay starting at time point 8h (Figure 14B). This retardation resulted in a significant change in the amount of cells in the S phase at 12 h and in G2 at 4 h onwards, and confirmed the slower growth of DAPIT cells.

The migration capacity of DAPIT cells was decreased ($p < 0,01$) (Figure 14C). Capacity to attach was not changed (Figure 5E in III), but that of detachment (Figure 14D) was significantly enhanced ($p < 0,01$). This indicated adhesion characteristics typical of EMT.

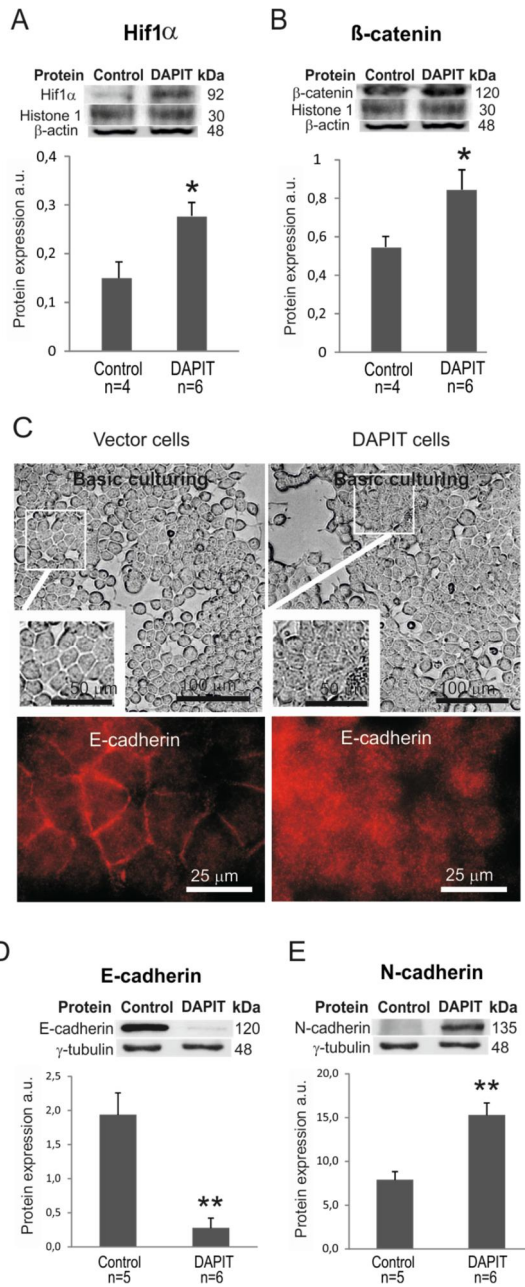


Figure 13. DAPIT over-expression regulates nuclear translocation of Hif1 α and β -catenin, leading to morphological changes. Nuclear protein level of (A) Hif1 α and (B) β -catenin by Western blot. (C) Microscope view of living control and DAPIT cells (upper panel, 20x magnification) and immunofluorescence of E-cadherin (lower panel, 100x magnification). Protein level by Western blot of (D) E-cadherin and (E) N-cadherin. The error bars are S.D. and asterisks indicate * $p < 0.05$ and ** $p < 0.01$. Adapted under Creative Commons Attribution License from Figure 3 and 4 in original publication III.

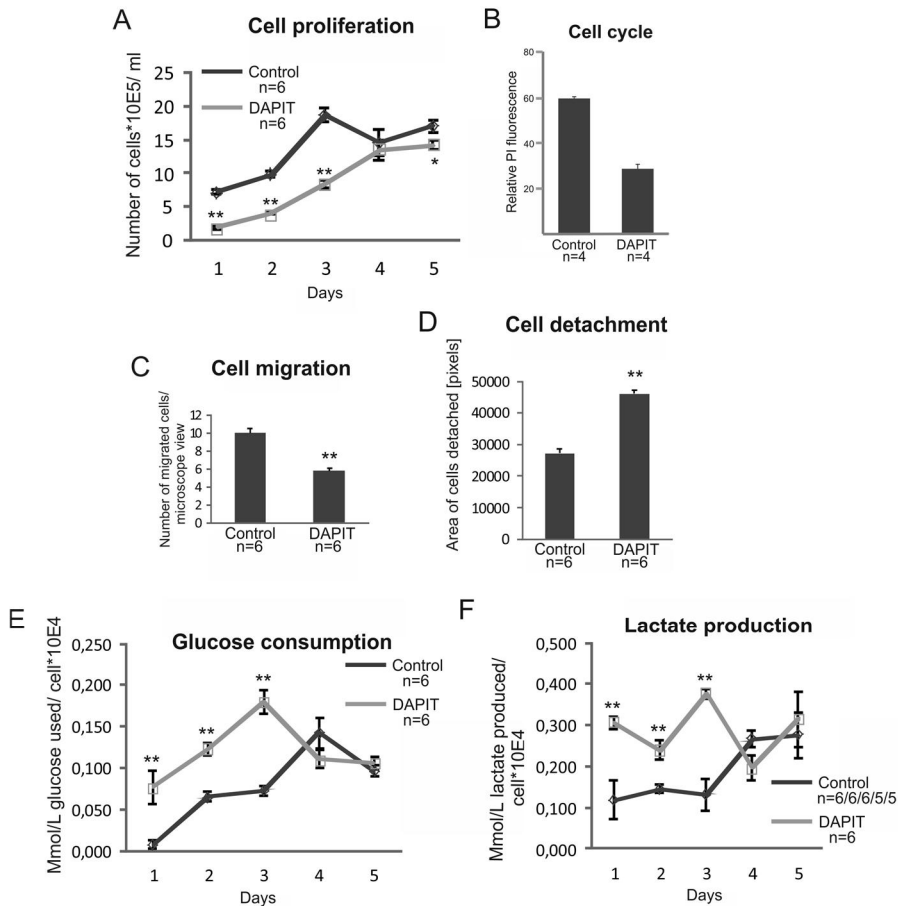


Figure 14. Characteristics of cell behavior and metabolism of DAPIT over-expressing cells. (A) Cell proliferation by cell counting. (B) Flow cytometric analysis of cell cycle progression in G1 8h after double thymidine synchronization of the cells. (C) Cell migration by scratch wound assay. (D) Cell detachment according to migration test. (E) Glucose consumption and (F) lactate production measured in parallel from the culture medium of the cell proliferation test. The error bars are S.D. and asterisks indicate: * $p < 0.05$, ** $p < 0.01$ and *** $p < 0.001$. Adapted under Creative Commons Attribution License from Figure 5 in original publication III.

5.4.8 Glucose consumption and lactate production (III)

Glucose consumption and lactate production in DAPIT cells were measured in parallel. DAPIT cells consumed significantly more glucose (Figure 14E) and

produced more lactate (Figure 14F) during exponential growth at days 1–3. A plateau in cell growth was reached at day 4, which was associated with a decrease in glucose consumption and lactate production, a metabolic switch attributable to cell quiescence.

5.4.9 *Usmg5* copy number in cancer cell lines (III)

A duplication (3–4 copies) of *Usmg5* copy number in a large panel of cell lines was found in the Oncomine Cancer Genomics database and CCLE. Uniform increases in copy number in various lung (NCI-H1775, NCI-H1993, NCI-H1563, NCI-H1755, VMRC-LCD, SBC-5, NCI-H1703), gastric (HCT116, Hs746T, MKN74, SNU-668), ovarian (OVTOKO, MCAS), liver (SNU-398) and pancreatic (PSN1, PANC-1) cancer cell lines were indicated in several data sets (Correction Oct 15;10(10):e0141036 in III). The copy number was also confirmed in breast (SUM-52PE), endometrial (AN3CA), esophagus (OE33), hematopoietic (MPLM6), kidney (SNU-1272) and lymphoid (Ki-JK) cell lines, being encountered once in the others. This cell line information strongly suggests DAPIT over-expression in cancers.

6 DISCUSSION AND FUTURE PERSPECTIVES

6.1 DD- PCR (I)

In the late 1990s DD-PCR was a contemporary methodology used to hunt for rare and/or new genes in a given research setting (Liang, Pardee 1992, Liang, Pardee 1995). The expected advantages were a fast method producing a band pattern in two days, increased sensitivity compared to previous methods, good detection of low-abundance genes, both induced and repressed and the possibility to compare two or more samples, and only a small amount of starting material was needed (Lievens, Goormachtig & Holsters 2001a, Lievens, Goormachtig & Holsters 2001). Despite its major contribution in molecular biology toolbox, the DD-PCR methodology had limitations and many variations to the protocol were published. The method has encountered criticism e.g. due to artefacts caused by short primers and low annealing temperature and the manual excision of bands giving false positives by overlapping gene expression patterns from neighboring bands.

In this study, total RNA of control and STZ-diabetic animals was exposed twice on DD-PCR to verify the expressed band pattern. Northern blot with a single band was applied to confirm the gene expression, thereby attributing the excised candidate band to the correct clone. This methodology has been successfully applied in several diabetes-related studies (Huang et al. 1999, Nishio et al. 1995, Vicent et al. 1998).

Although DD-PCR is not comparable in sensitivity to the currently used microarrays, several differentially expressed genes in diabetic skeletal muscle and adipose tissue were detected in this study (Table 1). Functionally these genes are involved in glucose transport, glycolysis, electron-proton transport and ATP production, reflecting the predicted impairment of glucose homeostasis and energy metabolism in the insulin-sensitive tissues of the insulin-deficient diabetic rat. Further, the observed novel genes (YEATS4, OPTN and Crb1) may open new paths to study previously unknown responses of insulin-sensitive tissues to diabetic conditions.

The DD-PCR methodology was of relevance in extracting, discovering and naming DAPIT in its diabetic content. This protein, its cellular and histological

expression and the effects of up-regulation are characterized more precisely in this thesis.

6.2 Structural analysis and cellular localization of DAPIT (I, II)

DAPIT is ubiquitously expressed in rat and human tissues and cells (<http://www.genecards.org/cgi-bin/carddisp.pl?gene=USMG5>) and the sequence conserved in the animal kingdom (I). It is noteworthy that 13 amino acids are fully conserved in all predicted proteins, indicating that they may be of significant structural and /or functional importance. Recently a DAPIT transmembrane helix was published to span from amino acid 29 to amino acid 47 (Lee et al. 2015), which is in line with the hydrophobic sequence encountered in the study I.

Despite the two predicted phosphorylation sites in the DAPIT sequence (I), no post-translational modifications were detected in proteomic studies of mitochondrial membrane proteins enrolling DAPIT (Carroll, Fearnley & Walker 2006). The ortholog of DAPIT is found in vertebrates and invertebrates but not in yeast or fungi (Chen et al. 2007). DAPIT was recognized as a product of the *Usmg5* gene, whose mRNA level is increased during skeletal muscle growth in rats (<http://www.ncbi.nlm.nih.gov/gene/84833>) and decreased by treatment with STZ, a drug inducing diabetes (I). DAPIT is a proteolipid associated with ATP synthase in a stoichiometric manner and requires the presence of phospholipids to remain bound to the synthase complex (Chen et al. 2007). In the presence of detergents, DAPIT is prone to dissociate from ATP synthase, which, however, retains its hydrolysis activity without DAPIT (Meyer et al. 2007).

Studies in the covalent cross-linking of the supernumerary subunits g, f, e, 6,8 PL and DAPIT oriented their N-region to the matrix side and the C-region to the intermembrane space (Lee et al. 2015)(Figure 15). In this orientation, DAPIT was the outermost protein cross-linked from its K55 in the C side to K49 in the C side of 6,8 kDa proteolipid, which further cross-linked to subunits e and f, the f alone bridging to g (Lee et al. 2015). Interestingly, all these subunits plus other F_o ATP8 OSCP, F6, b,d but not the 6.8 kDa proteolipid, c and a were expressed in both monomeric and dimeric extractions of ATP synthasome (Nuskova et al. 2015). The importance of supernumeraries including DAPIT, not in enzymatic production of ATP, but in the regulation of the dimerization of ATP synthase, is currently under intensive study (reviewed in Walker, 2013).

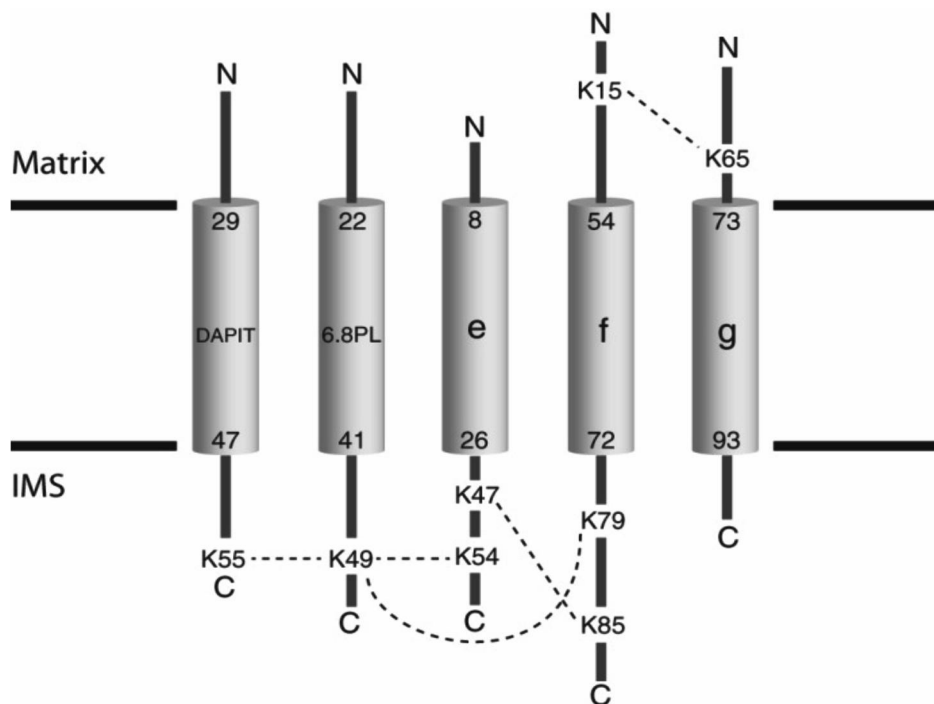


Figure 15. "Intersubunit cross-links detected in the nuclear encoded supernumerary subunits of the bovine F-ATPase. The *cylinders* represent the transmembrane α -helices predicted to be present in each of subunits e, f, g, DAPIT, and 6.8PL. The positions of the α -helices in the sequences of the subunits are indicated by the *numbers at the top and bottom of each cylinder*. The *dashed lines* represent the intersubunit cross-links, introduced by reaction of the bifunctional cross-linking agents with the numbered lysine residues in the N- and C-terminal regions of each subunit. *IMS*, intermembrane space". Reprinted under Creative Commons Attribution license 3.0 (<http://creativecommons.org/licenses/by/3.0/>) as published in (Kühlbrandt 2015).

The mitochondrial localization of DAPIT was validated with fluoromarkers such as Mitotracker, a cationic dye penetrating living mitochondria, and anti-DAPIT antibody. More precise localization in the F_0 subunit of ATP synthase was previously reported by two separate studies (Chen et al. 2007, Meyer et al. 2007).

Lysosomes are acidified by V-ATPase, which has a structural and functional relation to F-ATPase (Hirata et al. 2003, Imamura et al. 2003, Jefferies, Cipriano & Forgac 2008, Hinton, Bond & Forgac 2009). Both lysosome-specific cationic dye and antibody against V-ATPase were used to specify the vacuolar location of DAPIT. The abundant lysosomal localization of DAPIT in HUVEC and the less intensive in HEK293T cells suggests it either being a subunit of V-ATPase or a protein preserving the composition of the holoenzyme (Chen et al., 2007; J. Lee et

al., 2015; Meyer et al., 2007). The lysosomal abundance of DAPIT may also be a cell type-dependent phenomenon. The aminoterminal antibody against DAPIT recognized vacuolar protein in HUVEC, the carboxyterminal in both HUVEC and HEK293T cells. This would imply that the structure of V-ATPase may vary in different cell types.

Native DAPIT located both in lysosomes and mitochondria in HEK293T cells (II), whereas in DAPIT cells the protein location was mainly mitochondrial (III). Any plausible explanation for this discrepancy is not known, except the discrete origin of transcripts encoding DAPIT, either under regulation of *Usmg5* gene or both the *Usmg5* gene and IRES vector.

Majority of the information available for V-ATPase arises from the species *Saccharomyces cerevisiae*, which does not contain DAPIT ortholog (Chen et al. 2007, Rewel et al. 2016). Therefore, the structural studies at present do not confirm the possible involvement of DAPIT in composition of V-ATPase, which remains to be studied.

Even though study II showed lysosomal localization of DAPIT, considering the physiological function of lysosomes in destroying cellular cargo, it is worth noting that DAPIT in lysosomes may be a result of mitophagy (Wei, Liu & Chen 2015). However, the protein sequence of DAPIT has no processed mitochondrial import signal other than the removal of the translational initiator methionine residue (Chen et al., 2007), thus rendering it a protein also useful in cellular drafts outside the mitochondria.

6.3 Specificity of DAPIT antibodies (II)

The specificity of custom made-antibodies against DAPIT was shown in various cell lines and tissues by peptide blocking of the antibody. In immunofluorescence, the aminoterminal antibody recognized cellular structures selectively showing vacuolar structures in HUVEC cells, nothing in denatured immunoblot, and its activity in immunohistochemistry was similar to that of the carboxyterminal antibody. In all further studies the carboxyterminal antibody was used. This antibody turned out to be reliable in all applications, recognizing both mitochondrial and vacuolar localization of DAPIT and the correct size of the protein in immunoblots. In these, the carboxyterminal antibody also recognized approximately 50 kDa protein in rat but not mouse skeletal muscle. At present, protein databases do not recognize any proteins of greater size than DAPIT with the antigenic sequence used to raise the

specific antibody. It remains to be shown whether a still unknown longer isoform of DAPIT or an unknown skeletal muscle-specific protein exists. Therefore it cannot be ruled out that the carboxyterminal antibody also detects another protein in skeletal muscle in immunohistochemistry.

6.4 Tissue expression of DAPIT by Western blot and immunohistochemistry (II)

Significant correlations of DAPIT with cytochrome c and ATP synthase subunit alpha supported the observed close association of DAPIT with the mitochondria.

DAPIT expression in insulin-sensitive tissues of rat and mouse requires further studies. Previously it was shown that DAPIT mRNA was down-regulated in the myocardium and skeletal muscle in early type 1 diabetes (I). Interestingly, similar results in the STZ-diabetic rat myocardium (GDS3153) are reported in Gene Expression Omnibus database, GEO, and in mouse skeletal muscle subjected to endurance training (GDS1541)(Kivela et al. 2006, Lehti et al. 2007, Lehti et al. 2006). At protein level DAPIT was up-regulated in the insulin-sensitive tissues of the diabetic rat, except the liver. The differential expression of mRNA and protein in rat skeletal muscle and myocardium suggests a post-transcriptional regulation of DAPIT, the typical mode of regulation of protein expression in metabolism and mitochondria (reviewed in Pinti, Hathaway & Hollander 2016, Sanchez-Arago et al. 2013a). Recently, genome-encoded transcription was shown to be regulated by miRNAs in regards to ischemic heart failure with oxidative stress response (reviewed in Pinti, Hathaway & Hollander 2016). The same response is involved in insulin-deficiency (reviewed in Maiese 2015) supporting the post-transcriptional regulation of DAPIT by miRNAs. Essentially, no change in protein expression of DAPIT was seen in the mouse calf muscle complex after 1-5 weeks of STZ-induced diabetes (II). These conflicting data are very likely due to heterogeneity of the samples, since the composition of muscles differs in type of fibers, which are known to contain varying amounts of mitochondria (reviewed in Mishra et al. 2015, Pette, Staron 2000).

Histologically DAPIT expression was shown in several healthy rat and human tissues. In all tissues studied DAPIT showed smeary and granular-type expression, which was most intensive in tissues known to contain cells with copious mitochondria, including cardiomyocytes, skeletal muscle cells, hepatocytes and epithelial cells related to active transport of nutrients and ions.

6.5 Metabolism and cell behavior of DAPIT over-expressing cells (III)

Five multi-subunit enzymes known as complexes I, II, III, IV and V comprise the OXPHOS system. The electron transfer through complexes I-IV is coupled to proton translocation across the inner membrane. This results in a transmembrane electrochemical potential which is converted into chemical energy in the form of ATP by H⁺-ATP synthase (CV).

DAPIT is a structural component of H⁺-ATP synthase membrane domain F_o and its deletion results in the loss of H⁺-ATP synthase (Chen et al. 2007; Lee et al. 2015; Meyer et al. 2007; Ohsakaya et al. 2011). DAPIT is post-transcriptionally regulated upon insulin deficiency and over-expressed in various other diseases, discussed more precisely in section 6.6.3 This suggests that, in addition to its structural role, DAPIT may also be a regulatory component of H⁺-ATP synthase. In consequence, DAPIT up-regulation could lead to both structural changes and alterations in respiratory chain regulation.

To study the effects of its over-expression, DAPIT was stably transfected into HEK293T cells. A strategy permitting both the transgene and an EGFP reporter to be translated from a single bicistronic mRNA without formation of a fusion protein was used. The cell line was studied in mitochondria, nuclei, cell junction, morphology, behavior- and metabolism-related parameters.

6.5.1 Overall effects on mitochondria (III)

Cells can adapt to mitochondrial dysfunctions and energy depletion by regulating mitochondrial biogenesis (reviewed in Piantadosi, Suliman 2012, Scarpulla, Vega & Kelly 2012). In this study a significant decrease in nuclear content of PGC1 α and mtDNA due to inactivation of mitogenesis in DAPIT cells was observed.

When calculated in terms of mitochondrial mass, H⁺-ATP synthase content did not change according to unchanged expression of ATP5 α , but its activity decreased, rendering DAPIT cells glycolytic, as estimated by increased glucose consumption and lactate production (III). DAPIT over-expression increased the basal respiration and inhibitor-sensitive oxygen consumption of complexes I, II and IV, together with elevated maximal respiration. It may be concluded that DAPIT over-expression modulates respiration enhancing the respiratory chain capacity. In agreement with such a conception, membrane potential, citrate synthase activity and VDAC1

expression were increased, which reflects an increase in the availability and use of respiratory chain substrates. As DAPIT cells were glycolytic, they may have altered their catabolic balance in order to fuel the respiration. Accordingly, along with increased respiration, an accumulation of superoxide production was observed in DAPIT cell mitochondria. Interestingly, a previous study showed that the intracellular balance of respiratory substrates contributes to the cellular decision between differentiation and stemness (Carey et al. 2015).

6.5.2 ATP synthase activity (III)

The mitochondria provide most of the human energy in the form of ATP through oxidative phosphorylation. ATP synthesis maintains cellular homeostasis but is sensitive to oxidative damage and other cellular injuries (reviewed in Piantadosi & Suliman, 2012). Also alterations in ATP synthase biogenesis increase ROS production while reducing energy production (Geromel et al. 2001). Mitochondrial integrity can be disrupted by the damaging effect of ROS. Depending on cellular energy status this may contribute to apoptosis, necrosis or aerobic glycolysis, promoting cancer formation and/or cell dedifferentiation. During exponential growth, DAPIT cells did not differ in cell mortality compared to control cells, thereby supporting cell senescence.

The activity of H⁺-ATP-synthase was decreased in DAPIT cells in spite of increased mitochondrial respiration and good coupling. Some aspects and mechanisms contributing to this kind of “pseudoactive” oxidative phosphorylation are reported or could be speculated. The most obvious reason could be that the number of H⁺-ATP-synthase complexes in the mitochondrial inner membrane is diminished. Although the expression of an enzymatic portion subunit ATP5a remained unchanged (III), a method like blue native gel electrophoresis describing the actual composition of subunits present in the functional complex would give an exact answer.

In addition to ATP synthesis, H⁺-ATP-synthase can also work in the opposite direction by hydrolyzing ATP and translocating protons from the matrix to the inter-membrane space (reviewed in Walker 2013, Zhang et al. 2011). Basically, this helps mitochondria to maintain membrane potential and sustain cell viability if this is threatened (Zhang et al., 2011). DAPIT cells expressed enhanced TCA activity, respiration and hyperpolarized mitochondria but decreased ATP synthesis. The decrease in the enzymatic activity of ATP synthase is well documented in human

tumors, where the IF1 of H⁺-ATP-synthase mediates the metabolic shift of cancer cells to aerobic glycolysis with mitochondrial hyperpolarization and subsequent production of superoxide radicals (Formentini et al. 2012, Sanchez-Cenizo et al. 2010). These characteristics were also seen in DAPIT cells. A recent study showed that regulated degradation of IF1 controlled energy metabolism during osteogenic differentiation of human mesenchymal stem cells by hindering their self-renewal and favoring differentiation (Sanchez-Arago et al. 2013b). This mito-cellular mechanism by which the activity of H⁺-ATP-synthase is physiologically regulated in stemness, differentiation and cancer, may also be involved in cells over-expressing DAPIT.

H⁺-ATP-synthases form dimers and higher oligomers, which are crucial for the formation of mitochondrial cristae (Seelert, Dencher 2011, Chaban, Boekema & Dudkina 2014). The number of DAPIT per synthase dimer is not firmly established, but as a supernumerary subunit it presumably is involved in anchoring the synthase monomers in correct position and angle in the inner membrane. It may be speculated that the presence of extra DAPIT molecules may incur defective dimerization and oligomerization, thus inducing inefficient H⁺-ATP-synthase activity. This effect may also hinder the assembly and function of the ATP synthasome supercomplexes, where DAPIT is one of components (Nuskova et al. 2015).

In addition to regulation of membrane potential and cristae formation, ATP-synthase oligomerization also forms energy-dissipating permeability transition pore, mPTP, under conditions of oxidative stress (reviewed in Bernardi et al. 2015). The mPTP opening is known to be modulated by a sudden decrease in membrane potential and an increase in matrix pH, but is functional only in the presence of synthase dimers and oligomers. Since the mPTP opening is well demonstrated in ischemic heart, brain, kidney and liver, with severe loss of mitochondrial membrane potential (reviewed in Bernardi et al. 2015), DAPIT over-expression is unlikely to be involved in the formation of mPTP.

All these speculations indicate that the actual mechanism of reduced ATP synthase activity in DAPIT cells requires further studies. Altogether, the results presented show that DAPIT over-expression accelerates mitochondrial respiration and attenuates H⁺-ATP synthase activity.

6.5.3 Aerobic glycolysis and epithelial to mesenchymal transition (III)

Aerobic cellular metabolism is shifted to glycolysis upon Hif1 induction (reviewed in Cairns, Harris & Mak 2011, Sena, Chandel 2012, Wallace 2012, Yang, Soga &

Pollard 2013). Hif1a activation usually requires hypoxia but can also be activated in normoxia in response to ROS production and/or accumulation of TCA intermediates (Sullivan et al. 2013, Wheaton, Chandel 2011). Accordingly, elevated ROS production in DAPIT cells translocated Hif1a to the nucleus, leading to a significant enhancement of glucose consumption and lactate production. These changes are typical features of aerobic glycolysis, also known as the Warburg effect, which is observed in many cancers and stem cells.

The disappearance of E-cadherin from the cell membrane and its replacement with N-cadherin are among the hallmarks of EMT in cancer (Mani et al. 2008, Batlle et al. 2000, Cano et al. 2000, Yang et al. 2004). Several key transcription factors regulating E-cadherin expression and/or the fate of other epithelial molecules are direct or indirect transcriptional targets of the canonical Wnt pathway (reviewed in Valenta, Hausmann & Basler 2012). Accordingly, in DAPIT cells the nuclear expression of b-catenin was seen, indicating activation of Wnt signaling and the shift of E-cadherin to N-cadherin. The involvement of DAPIT over-expression in altered mitochondrial function in cancer and stemness is supported by these molecular findings.

6.5.4 Morphology, migration and proliferation (III)

EMT-like changes in DAPIT cells manifested as morphological transformation of regular cuboidal epithelial-like cells into irregularly sized and shaped cells. These cells were tightly packed, showing a polygonal and sheet-like appearance with short projections which are features of mesenchymal-like cells. However, DAPIT cells evinced an unexpected decrease in migration, which is in contrast to mesenchymal cancer cells but implicated in stemness (Lu et al. 2016, Chia et al. 2010). The cell adhesion was unaltered but dissociation from the surface more frequent in DAPIT cells, again in line with characteristics in stemness.

DAPIT cells presented normal viability while growing more slowly than the control cells. Thymidine synchronization showed that DAPIT cells remained a longer time in G1. Interestingly, slow-cycling stem cells are present in various cancers and are suggested to escape chemotherapy, which is targeted to rapidly dividing cells (reviewed in Buczacki, Davies & Winton 2011, Hua et al. 2012). Previously it was shown that the activation of Hif1a (which occurred in DAPIT cells) in embryonic stem cells and colon cancer cells under hypoxia-inhibited transcriptional activity of b-catenin results in G1 arrest (Carmeliet et al. 1998, Kaidi, Williams &

Paraskeva 2007). Taken together, the physiological properties of cells over-expressing DAPIT resemble an EMT-like phenotype with mitochondrial impairment, which leads to glycolytic metabolism, decreased cell proliferation and migration, and an increase in cell dissociation from the surface. All these features are manifested in varying conditions of cancer and stem cells.

6.6 Defects and diseases of mitochondrial ATP synthase

6.6.1 Nuclear genetic defects

Disorders of ATP synthase are involved in the most severe metabolic diseases manifesting as early-onset mitochondrial encephalopathies (reviewed in Hejzlarova et al. 2014). In the study in question, mutations in four nuclear genes (ATP5A1, ATP5E, ATPAF2 and TMEM70) were associated with a deficiency of ATP synthase. The first two genes encode for F₁ subunits α and ϵ , and the following the ancillary biogenetic factors which are not part of the enzyme structure. All these mutations share a similar biochemical phenotype with a pronounced decrease in the content of ATP synthase, thereby limiting mitochondrial ATP production in vivo.

Despite low activity, ATP synthase was well coupled to respiration in DAPIT cells (III). It has been reported in TMEM70 and ATP5E mutated fibroblasts that low capacity of ATP synthase leads to elevated levels of membrane potential when the synthase is intensively coupled to respiration (reviewed in Hejzlarova et al., 2014). This stimulates an electron leak within the respiratory chain thus increasing the formation of ROS. Thus ATP synthase deficiency/impairment is connected both to altered energy production and to enhanced oxidative stress, characteristics also implicated in DAPIT cells.

6.6.2 DAPIT down-regulation

The examples of *Usmg5* down-regulation in diseases in the GEO database include defects in cardiac and skeletal muscle function (myocardial infarction GDS3655 (Lachtermacher et al. 2010), STZ-diabetic heart GDS3153, muscle aging GDS288 (Welle et al. 2003)), cancer ((synovial sarcoma GDS2698 (Haldar et al. 2007), multiple myeloma GDS3578 (Dutta-Simmons et al. 2009) and Notch1-driven

leukemogenesis GDS4303 (Ntziachristos et al. 2012)), reproduction (teratozoospermia GDS2697 (Platts et al. 2007)) and immunology (hypoxia effect on B lymphocyte cell line, GDS1807 (Kim et al. 2006)). Also an *Usmg5* association with asthma (Ferreira et al. 2016), migraine (Rodriguez-Acevedo et al. 2015) and White matter hyperintensities (WMH) doubling the risk of stroke and dementia (Lopez et al. 2015, Debette, Markus 2010) has previously been reported. In all of these impairments possible down-regulation of DAPIT at protein level means compromising ATP production due to a reduction in the amount of ATP synthase complexes (Ohsakaya et al. 2011). However, considering the possible post-transcriptional regulation of the decreased mRNA level leading to increased protein expression of DAPIT in diabetic heart and skeletal muscle as seen in study II, a compromise of ATP production would be expected by the decrease in activity of ATP synthase reported in study III.

6.6.3 DAPIT over-expression

The variety of diseases or causative symptoms would imply that DAPIT expression is under diverse regulation including genetic, hormonal, energy supply, post-transcriptional and epigenetic regulation, which is typical for metabolism adapting to and regulating cellular homeostasis. This emphasizes both the vulnerability and the power of ATP synthase, with DAPIT over-expression regulating its activity apart from its enzymatic activity in response to health and disease.

6.6.3.1 Cancer cell lines, tumors and stemness

As DAPIT over-expression in HEK293T cells was induced by stable transfection of a transgene, this possibly integrated several copies of the transgene into the cell genome. As cancers are known to be heterogeneous, with active amplification of genes normally expressed in diploid, the obvious locus to search for up-regulation for *Usmg5* gene was within this disease. Interestingly, searching in the Oncomine cancer genomics database (Rhodes et al. 2004) and the Cancer Cell Line Encyclopedia, CCLE (Beroukhir et al. 2007), revealed a duplication in *Usmg5* copy number in various cancer cell lines. Several lung, gastric, ovarian, liver and pancreatic cancer cell lines supported fidelity in duplication. The copy number was also confirmed in some breast, endometrial, esophageal, hematopoietic, kidney and lymphoid cell lines. Even though a link between DAPIT and the tumorigenic

capacity has not been sufficiently demonstrated, this result strengthens the conception of a correlative involvement of DAPIT in cancer and suggests a possible oncogenic function for it.

In addition to increased gene copy number in various cancer cell lines, the over-expression of *Usmg5* mRNA as reported in the GEO database was found in high-grade prostate cancer (GDS5072;(Satake et al. 2010)) and in colon, breast and ovarian cancers evincing chemoresistance (GDS1792; (Lee et al. 2005), GDS3330; (Selga et al. 2008), GDS4061; (Al Saleh, Al Mulla & Luqmani 2011), GDS3754; (Li et al. 2009), GDS2755;(Chang et al. 2007)). This could indirectly indicate actively respiring, depolarized mitochondria in these malignancies.

Furthermore, *Usmg5* was ranked among the top-20 significant genes differentially expressed between primary samples from patients who developed metastasis in human osteosarcoma and those who did not (Namlos et al. 2012). The cancers with up-regulation of *Usmg5* did not metastasize (4 patients out of 11), whereas those with down-regulated *Usmg5* had metastases. This suggests that up-regulation of *Usmg5* is involved in pathways preventing metastasis in osteosarcoma. This parallels the behavior (diminished proliferation and migration) of DAPIT cells.

EMT has been reported to generate cells with properties of stem cells (Mani et al. 2008, Batlle et al. 2000, Cano et al. 2000, Yang et al. 2004). Stimulation of human mammary epithelial cells by TGF-beta has been seen to induce EMT, which was accompanied by the formation of breast cancer stem cells (CSC) (Mani et al. 2008, Czerwinska, Kaminska 2015). In addition to epigenetic regulation and post-transcriptional modifications, the mechanisms regulating the self-renewal of stem cells and CSCs include the WNT/beta-catenin pathway (reviewed in Czerwinska, Kaminska 2015, Jang et al. 2015). CSC have a slow rate of cell turnover, which facilitates escape from chemotherapeutic agents targeted to rapidly proliferating cells (reviewed in Gottesman, Fojo & Bates 2002, Gangemi et al. 2009). These well-documented phenomena were characterized in DAPIT over-expressing cells, which, in contrast to metastatic cells, migrated and proliferated more slowly than normal HEK293T cells (Figure 16).

Effects of DAPIT over-expression in HEK293T cells

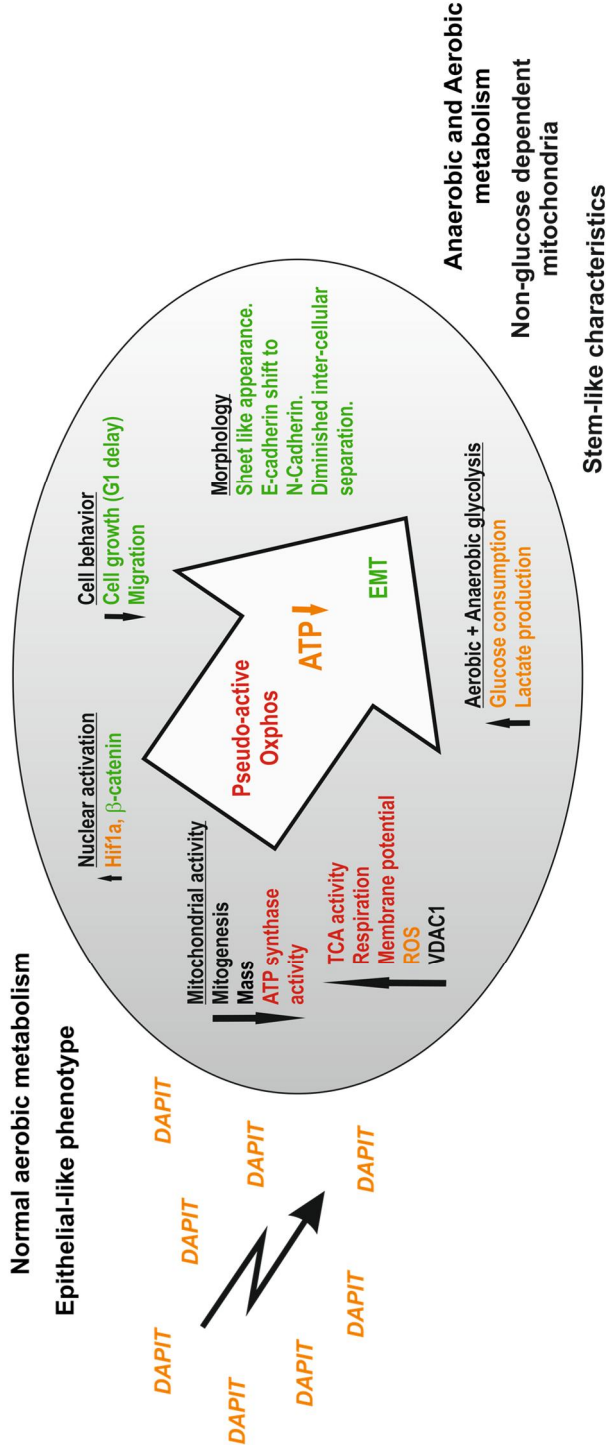


Figure 16. Schematic presentation of effects of DAPIT over-expression in HEK293T cells. Despite good coupling, the inactivity of ATP synthase in cells over-expressing DAPIT up-regulated respiration and increased membrane potential, leading to the formation of ROS (pseudo-active Oxphos). As a consequent nuclear activation, the cell favored glycolytic metabolism in the presence of oxygen, seen as increases in glucose consumption and lactate production. This metabolic shift interfered with the cell cycle, migration and epithelial characteristics, leading to the transition of cell phenotype from epithelial-like to stem-cell-like cells. The color codes denote changes in the pseudo-active Oxphos (red), aerobic glycolysis (orange) and EMT (green) cell activities.

Embryonal and pluripotent stem cells, ESC and PSC respectively, have been reported to contain less mitochondrial content and a lower mtDNA copy number when compared to somatic cells (Prigione et al. 2010, Facucho-Oliveira et al. 2007). Also mitochondria of PSC and CSC were shown to be capable of consuming oxygen at a similar rate to differentiated cells (Zhang et al. 2011, reviewed in Jang et al. 2015) and to maintain a higher membrane potential than their differentiated derivatives (reviewed in Teslaa, Teitell 2015, Chung et al. 2007, Armstrong et al. 2010, Prigione et al. 2010). CSCs, on the other hand, show a higher mitochondrial membrane potential than other stem cell populations and involve ROS regulation in their signaling pathways (Zhang et al. 2015), in contrast to ESC and PSC, which polarize themselves through UCP2 (J. Zhang et al., 2011; L. Zhang et al., 2014). CSCs resemble ESC and PSC and involve decreased mitogenesis, depolarized mitochondria and ROS regulation, as also seen in DAPIT cells. Various stem cells, such as DAPIT cells, are also known to rely on glycolysis for their energy production (reviewed in Xu et al. 2013, Teslaa, Teitell 2015, Jang et al. 2015).

As CSCs are an asymmetrically dividing subpopulation of cells within a tumor which can self-renew, differentiate and drive tumor growth (reviewed in Marjanovic, Weinberg & Chaffer 2013), the duplication of the *Usmg5* gene suggests that DAPIT might possibly introduce CSC-like characteristics by maintaining aerobic glycolysis and strong, depolarized mitochondria. An interesting observation is that the colon cancer cell line HCT116 has been reported to contain mainly CSC (Yeung et al. 2010). Furthermore, in that cell line the over-expression of mir-34 introduced a 4-fold increase in *Usmg5* expression (GDS2755).

Interestingly, mitochondrial ATP synthase acts as an essential differentiation factor, independent of oxidative phosphorylation, to promote the developmentally regulated maturation of mitochondrial cristae in the *Drosophila* ovary, and knockdown of subunit e or g has destabilized ATP synthase dimers (Teixeira et al. 2015). Considering the notion that vertebrate supernumerary subunits of ATP synthase are also involved in the same phenomenon, it can be speculated that DAPIT over-expression could interfere with the maturation of cristae, and thereby promote dedifferentiation up to the level of a CSC in the presence of an oncogenic stimulus. Worthy of note is that the GEO database reports up-regulated expression of *Usmg5* in pluripotent cancer stem cells reprogrammed from prostate cancer-associated stromal cells, an EphB2^{low}-population of intestinal stem cells, Non-small cell lung cancer H460-derived stem cells, in the sphere vs. monolayer of neuroblastoma SKNAS-induced and CD133⁺ glioblastoma-derived stem cells (Vencio et al. 2012, Merlos-Suarez et al. 2011, Lopez-Ayllon et al. 2014, Ikegaki et al.

2013, Beier et al. 2007). All this information goes to confirm the involvement of DAPIT over-expression in metabolic disturbances in a variety of cancers and cancer stem cells.

6.6.3.2 Type 1 diabetes, Parkinson's disease and multiple sclerosis (MS)

Post-transcriptional up-regulation of DAPIT protein was found in early type 1 diabetes of STZ-mice (I,II). In contrast to our finding after seven days of inducing diabetes (I), *Usmg5* gene upregulation has been found in the myocardium of STZ-diabetic rats after four weeks (GDS3151; (van Lunteren, Moyer 2007)). The mRNA up-regulation has also been seen in a mouse model of diabetic embryopathy (GDS4590; (Pavlinkova, Salbaum & Kappen 2009)). These observations indicate that both mRNA and protein expression of DAPIT are under intensive regulation in insulin deficiency and changes in either direction compromise the energy supply (III and Ohsakaya et al., 2011).

The conception that DAPIT over-expression shows differential manifestation according to cell and tissue type is further supported by neurological impairments, where an increased level of either *Usmg5* or DAPIT was reported in Schwann cells in diabetic neuropathy (Zhang et al. 2010), the brain synaptosomes of a murine model of Parkinson's disease showing high affinity to Ser129-phosphorylated alpha-synuclein (McFarland et al. 2008), and in brain lesions of autoimmune inflammation causing demyelination in the human pathogenesis of multiple sclerosis (MS), (GDS4218; (Han et al. 2012)).

6.6.3.3 Weight-gaining, cardiac hypertrophy and arsenic metabolism

Usmg5 was upregulated in mouse and cell culture models of adipose tissue from high weight gainers after a high saturated fat diet (GDS2319 (Koza et al. 2006)) and in cardiac hypertrophy with p21ras over-expression and fibronectin stimuli (GDS696). These characteristics correspond to epigenetically driven cellular senescence, where mitochondrial dysfunction is a general feature occurring independently of the senescence stimuli (e.g. telomere dysfunction, oncogene activation and genotoxic stress) (reviewed in Correia-Melo, Passos 2015). Moreover, a dissociation of ATP synthase dimers and loss of inner-membrane cristae in the mitochondria are reported age-dependently in yeast (reviewed in Daum et al. 2013). This impairs the ability of mitochondria to supply the cell with sufficient ATP to maintain essential functions.

One further epigenetic finding of DAPIT over-expression is the correlation of increased expression of *Usmg5* with a reduction in arsenic methyltransferase (AS3MT) in haplotype-associated altered CpG methylation of AS3MT (Engstrom et al. 2013). Interestingly, arsenic has been observed to induce sustained impairment of skeletal muscle and muscle progenitor cell ultrastructure and bioenergetics (Ambrosio et al. 2014), which were manifested as defects in muscle stem cell proliferation and myogenic differentiation (Steffens, Hong & Bain 2011, Yen et al. 2010), myofiber hypertrophy and swollen mitochondria with disrupted cristae. Accordingly, the arsenic-exposed fibers evinced increased oxygen consumption and mitochondrial activity. Many of these features are similar to those of DAPIT cells.

6.7 Strengths, limitations and future prospects

DAPIT over-expression in HEK293T cells reprogrammed the metabolism and epithelial characteristics of the cells to a mesenchymal-like. The morphology of DAPIT cells was irregular and polygonal, with sheet-like appearance. The similar morphology of embryonic stem-like cells derived from HEK293T cells through Lentiviral miR302/367 expression was previously reported to differentiate into germ-like cells (Wang et al. 2014). As the behavioral and mitochondrial characteristics of DAPIT over-expressing cells did not resemble the metastatic cancer cell but instead CSC, further efforts should be made to clarify the cell transcriptome with respect to metabolic and other cellular regulations. Also mitochondrial dynamics and ultrastructure, and when feasible the pluripotency, characterization of the sphere germ layers, in vitro differentiation and compatible CD markers in cell surface should be tested.

HEK293T cells have been immortalized with adenovirus 5 genes. The cell genome also carries SV40 large T antigen to bind SV40 enhancers of expression vectors to increase transgenic protein production. However, the oncogenic large T antigen is known to interfere e.g. with tumor suppressor p53 which regulates gene expression in cancers (reviewed in Ahuja, Saenz-Robles & Pipas 2005). Despite the reported contribution of T antigen in cellular regulation, the transformation-related phenomena in DAPIT cells is derived by over-expression of the *Usmg5* gene interrupting the H⁺-ATP synthase function, the T antigen possibly accelerating the transforming capacity by suppressing the anti-tumorous trait. In this study it was not possible to resolve whether DAPIT and SV40 large T antigen (T) have synergistic effects or whether they function independently in DAPIT over-expressing cells. The

T antigen also significantly promotes the efficiency and pace of generation of induced pluripotent stem cells from human adult and fetal fibroblasts when co-transfected with reprogramming genes and cultured with feeder cells (Mali et al., 2008).

The mitochondrial and nuclear characteristics of DAPIT over-expressing cells clarify our understanding of the consequences of miss-regulated ATP synthase - with and/or without a viral contribution - and could thus be applied to various impairments and diseases involving over-expression of DAPIT. Despite the EMT seen in this study, the morphological/cell phenotypic implications obviously change according to cell and tissue type over-expressing DAPIT. The DAPIT cell line is potentially a helpful tool when designing drugs for diseases where DAPIT overexpression is implicated, as for example chemoresistant CSC.

Cell culture models are valuable and necessary tools in characterizing molecular mechanisms, but the results obtained are limited to the study conditions used. The validation of parameters in DAPIT over-expression at tissue level with more complex inter-cellular communication would thus provide more comprehensive information. For pathological manifestations, the approaches with the xenograft mice injected with DAPIT overexpressing cells and a genetic *Usmg5* knock-in would be of prime interest. Likewise the current mouse models of CSC are of interest in possible marker development.

7 SUMMARY

A variety of diseases involve metabolic defects due to impaired oxidative phosphorylation in the mitochondria. Diabetes mellitus is one of those disorders as yet inadequately understood as to its metabolic pathophysiology. From this approach we discovered novel protein DAPIT, which is well conserved from insects to vertebrates underlining its functional importance. Histological analysis of DAPIT in rat and human tissues revealed elevated expression in cells with high aerobic metabolism and in epithelial cells involved in the active transport of nutrients and ions. Differential expression in the insulin-sensitive tissues of diabetic rats revealed down-regulation of DAPIT mRNA but up-regulation of the protein, suggesting that it is post-transcriptionally regulated in early type-1 diabetes.

DAPIT turned out to be a membrane imbedded-subunit of mitochondrial ATP synthase, which forms dimer rows in the mitochondrial inner membrane, leading to its bending and formation of cristae. The dimerization of ATP synthase is another regulatory level of the efficiency of energy production apart from synthase enzymatic activity in producing ATP. DAPIT is also implicated in the formation of ATP synthasome, coordinating the energy flux in a cell, and the deletion of DAPIT reduces cell viability via loss of the ATP synthase complex.

The cell model over-expressing DAPIT accelerates mitochondrial respiration by inactivating ATP synthase activity. This increases the mitochondrial membrane potential, leading to excessive formation of ROS which results in metabolic and cell behavioral regulations by transcription factors Hif1a and b-catenin. The cells rely on glycolysis in their energy production, meaning that the mitochondria presumably use fatty- and amino acids for fueling the TCA cycle and respiration. Thus cellular metabolism is both aerobic and anaerobic (Warburg effect), with decreased mitochondrial biogenesis. In culture conditions, these cells were prone to detach from the surface of the culture dish and underwent EMT and cell cycle delay at G1, thereby possibly promoting oncogenic effects and CSC-like metabolism and behavior.

As reliance on glycolysis is a peculiar cellular phenomenon in metabolic disturbances, we searched for conditions where DAPIT over-expression could be involved. This was done by investigating databases (GEO, Oncomine, CCLE) and

the literature. Increased protein expression of DAPIT was found in a mouse model of Parkinson's disease and over-expression of DAPIT mRNA or increased gene copy number was found in various cancers, cardiac hypertrophy, the adipose tissue of high weight gainers after a high saturated fat diet, and multiple sclerosis, correlating with a reduction in arsenic methyltransferase AS3MT, causing impairment of arsenic metabolism and epithelial-like HEK293T cell dedifferentiation into stem-like cells. These findings suggest that DAPIT over-expression could be a more common phenomenon in regulating dimerization of ATP-synthase and mitochondrial inactivity in diseases where metabolic disturbances play a significant role, among them diabetes, cancer, degenerative, autoimmune, toxin and epigenetically regulated conditions. This study series brought out a need for transcriptomic, mitochondrial and stem cell studies, and mouse models to gain a pathophysiologic understanding of the consequences of impaired oxidative phosphorylation upon DAPIT over-expression.

8 ACKNOWLEDGEMENTS

This study was carried out at the Tampere Center for Child Health Research, School of Medicine and the Institute of Biomedical Technology (IBT) at the University of Tampere. I wish to thank Professors Markku Mäki, Matti Korppi, Per Ashorn and Howy Jacobs for providing me with excellent research facilities during the years. For one year this project was also temporarily carried out in the University of Eastern Finland in the lab of Research Director Antero Salminen, whose help is accordingly acknowledged.

I had the privilege to have been a student in the Tampere Graduate Program in Biomedicine and Biotechnology (TGPBB), whose support is acknowledged in financial support, scientific education and travel grant. The Competitive Research Funding of the Pirkanmaa Hospital District (EVO), Finnish Cultural Foundation, Pirkanmaa Regional fund, Finnish Diabetes Research Foundation, Academy of Finland and Finnish Cultural Foundation Central Fund, are also thanked for financial support during my work on this thesis.

First of all I want to express my deepest gratitude to my supervisors Professor Heikki Kainulainen, PhD, Docent and Professor Markku Mäki, MD, PhD for the opportunity to work on an interesting research topic in an inspiring work community. Dear Heikki, I have been privileged to work under your pleasant supervision and with your commitment to this project, which finally ended up in the very heart of the metabolism. You provided time, expertise and colleagues for the DAPIT-project and shared the wondering interest while new piece of information in the literature were to be published. Your inexhaustible and close engagement with constant encouragement in research during the years, despite the distance to your core research group in the University of Jyväskylä, kept me going throughout this project. Dear Markku, I wish to thank you for your support and guidance during my thesis project, and for many years as a member of the thesis committee. Your enthusiasm also for metabolism and your positive and inspiring words, attitude and actions simply raised challenges to be resolved!

I am thankful to Professor Tapio Visakorpi, MD, PhD and Docent Katri Lindfors, PhD for your expertise and kind participation in my thesis committee, in and outside official meetings. Professor Katri Kaukinen, MD, PhD and the Coeliac

Disease Research Center is also deeply appreciated for all the comfort and flexibility during the writing period.

I want to express my gratitude to my co-authors Docent Juha Hulmi, PhD and Paavo Rahkila, MSc, Docent Eric Dufour, PhD, Post Doc Giuseppe Cannino, PhD and Professor Pierre Rustin, PhD. Without your spontaneous effort this study would never have been finished. Especially I want to thank you Eric for the unstinted time you gave in measuring my samples, sharing your expertise and hands-on teaching me in techniques, not forgetting your notable contribution to the review of the III manuscript. Eric, and Giuseppe also with your helpful guiding expertise, you were "The Senior Scientist and Post Doc" whom I had been longing for many years to foresee the importance of DAPIT. It was my pleasure to collaborate with all of you.

The external reviewers of this thesis study Adjunct Professor Pekka Taimen, MD, PhD and Head of Department Tomáš Mráček, RNPhD deserve special thanks for valuable comments and discussion, which significantly improved the quality of this dissertation. Many thanks also to Mr Robert MacGilleon, M.A., who kindly revised the English language of this thesis.

My warmest thanks to all past and present colleagues at the Coeliac Disease Study Group, the Hemato-oncology Research Group, FinnPedMed, Histology, Molecular Neurology in Kuopio, Howylab in Mitochondrial Genetics and Biology in the early 2000s and the Department of Biology of Physical Activity in Jyväskylä. In an intensive research atmosphere I have enjoyed the cosines created by you Tiina Rauhavirta, PhD, Suvi Kalliokoski, PhD, Laura Airaksinen, MSc, Minna Hietikko, MSc, Outi Koskinen, MD, PhD, Cristina Nadalutti, PhD, Kaija Laurila, MSc, Mrs Anne Heimonen, Mrs Soili Peltomäki, Mr Jorma Kulmala, Matti Kannisto, MSc, Mrs Marja-Leena Koskinen, Mrs Mervi Matero, Mikko Oittinen, MSc, Joel George, MSc and Keijo Viiri, PhD, Docent Olli Lohi, MD, PhD, Kaisa Teittinen, PhD, Susanna Teppo, MSc, Toni Grönroos, MSc, Saara Laukkanen, MSc, Laura Oksa, MSc, Pirkko Lepola, MSc, Juha Taavela, MD, PhD, Anne Lahdenperä, PhD, Anja Rovio, PhD, Mrs Merja Jokela and all former colleagues. All of you are warmly thanked for your help and for sharing either cheerful moments or results when working together.

I wish to thank all of my dear friends Minna, Kati, Rauni, Sanna, Riitta and others in the LadySet, and Tytti, Hanna and Meri for the great times and discussions we have had together. Having friends and life outside the lab and family duties is refreshing and reformative, at simplest a necessity.

I am also grateful to my dear aunt Tuija and her husband Keijo for all the hospitality and care during summer and winter holidays when being a child.

I would like to express my heartfelt thanks to my parents Marjut and the late Ilkka Päivärinne, and grandmother Siiri for trust and support over the years at home and grown-up. Äiti, kiitos kaikesta avusta ja tuesta, jota olet ehtymättä antanut niin opiskelu kuin tutkimusvuosien ajan minulle ja perheellemme.

Finally I wish to express my blessings and gratitude to my husband Peter and our wonderful children Ilkka and Isaruth for their constant love, patience and support, not least financial, during this project.

Tampere, December 2016
Heidi Kontra

9 REFERENCES

- Agathocleous, M. & Harris, W.A. 2013, "Metabolism in physiological cell proliferation and differentiation", *Trends in cell biology*, vol. 23, no. 10, pp. 484-492.
- Ahuja, D., Saenz-Robles, M.T. & Pipas, J.M. 2005, "SV40 large T antigen targets multiple cellular pathways to elicit cellular transformation", *Oncogene*, vol. 24, no. 52, pp. 7729-7745.
- Al Saleh, S., Al Mulla, F. & Luqmani, Y.A. 2011, "Estrogen receptor silencing induces epithelial to mesenchymal transition in human breast cancer cells", *PLoS one*, vol. 6, no. 6, pp. e20610.
- Alvarez-Guardia, D., Palomer, X., Coll, T., Davidson, M.M., Chan, T.O., Feldman, A.M., Laguna, J.C. & Vazquez-Carrera, M. 2010, "The p65 subunit of NF-kappaB binds to PGC-1alpha, linking inflammation and metabolic disturbances in cardiac cells", *Cardiovascular research*, vol. 87, no. 3, pp. 449-458.
- Ambrosio, F., Brown, E., Stolz, D., Ferrari, R., Goodpaster, B., Deasy, B., Distefano, G., Roperti, A., Cheikhi, A., Garciafigueroa, Y. & Barchowsky, A. 2014, "Arsenic induces sustained impairment of skeletal muscle and muscle progenitor cell ultrastructure and bioenergetics", *Free radical biology & medicine*, vol. 74, pp. 64-73.
- Armstrong, L., Tilgner, K., Saretzki, G., Atkinson, S.P., Stojkovic, M., Moreno, R., Przyborski, S. & Lako, M. 2010, "Human induced pluripotent stem cell lines show stress defense mechanisms and mitochondrial regulation similar to those of human embryonic stem cells", *Stem cells (Dayton, Ohio)*, vol. 28, no. 4, pp. 661-673.
- Arnold, I., Pfeiffer, K., Neupert, W., Stuart, R.A. & Schagger, H. 1998, "Yeast mitochondrial F1F0-ATP synthase exists as a dimer: identification of three dimer-specific subunits", *The EMBO journal*, vol. 17, no. 24, pp. 7170-7178.
- Barretina, J., Caponigro, G., Stransky, N., Venkatesan, K., Margolin, A.A., Kim, S., Wilson, C.J., Lehar, J., Kryukov, G.V., Sonkin, D., Reddy, A., Liu, M., Murray, L., Berger, M.F., Monahan, J.E., Morais, P., Meltzer, J., Korejwa, A., Jane-Valbuena, J., Mapa, F.A., Thibault, J., Bric-Furlong, E., Raman, P., Shipway, A., Engels, I.H., Cheng, J., Yu, G.K., Yu, J., Aspesi, P., Jr, de Silva, M., Jagtap, K., Jones, M.D., Wang, L., Hatton, C., Palesscandolo, E., Gupta, S., Mahan, S., Sougnez, C., Onofrio, R.C., Liefeld, T., MacConaill, L., Winckler, W., Reich, M., Li, N., Mesirov, J.P., Gabriel, S.B., Getz, G., Ardlie, K., Chan, V., Myer, V.E., Weber, B.L., Porter, J., Warmuth, M., Finan, P., Harris, J.L., Meyerson, M., Golub, T.R., Morrissey, M.P., Sellers, W.R., Schlegel, R. & Garraway, L.A. 2012, "The Cancer

Cell Line Encyclopedia enables predictive modelling of anticancer drug sensitivity", *Nature*, vol. 483, no. 7391, pp. 603-607.

- Batlle, E., Sancho, E., Franci, C., Dominguez, D., Monfar, M., Baulida, J. & Garcia De Herreros, A. 2000, "The transcription factor snail is a repressor of E-cadherin gene expression in epithelial tumour cells", *Nature cell biology*, vol. 2, no. 2, pp. 84-89.
- Beier, D., Hau, P., Proescholdt, M., Lohmeier, A., Wischhusen, J., Oefner, P.J., Aigner, L., Brawanski, A., Bogdahn, U. & Beier, C.P. 2007, "CD133(+) and CD133(-) glioblastoma-derived cancer stem cells show differential growth characteristics and molecular profiles", *Cancer research*, vol. 67, no. 9, pp. 4010-4015.
- Bell, E.L., Emerling, B.M. & Chandel, N.S. 2005, "Mitochondrial regulation of oxygen sensing", *Mitochondrion*, vol. 5, no. 5, pp. 322-332. Review.
- Bell, G.I., Kayano, T., Buse, J.B., Burant, C.F., Takeda, J., Lin, D., Fukumoto, H. & Seino, S. 1990, "Molecular biology of mammalian glucose transporters", *Diabetes care*, vol. 13, no. 3, pp. 198-208.
- Benit, P., Goncalves, S., Philippe Dassa, E., Briere, J.J., Martin, G. & Rustin, P. 2006, "Three spectrophotometric assays for the measurement of the five respiratory chain complexes in minuscule biological samples", *Clinica chimica acta; international journal of clinical chemistry*, vol. 374, no. 1-2, pp. 81-86.
- Berger, J., Biswas, C., Vicario, P.P., Strout, H.V., Saperstein, R. & Pilch, P.F. 1989, "Decreased expression of the insulin-responsive glucose transporter in diabetes and fasting", *Nature*, vol. 340, no. 6228, pp. 70-72.
- Bernardi, P., Rasola, A., Forte, M. & Lippe, G. 2015, "The Mitochondrial Permeability Transition Pore: Channel Formation by F-ATP Synthase, Integration in Signal Transduction, and Role in Pathophysiology", *Physiological Reviews*, vol. 95, no. 4, pp. 1111-1155. Review.
- Beroukhi, R., Getz, G., Nghiemphu, L., Barretina, J., Hsueh, T., Linhart, D., Vivanco, I., Lee, J.C., Huang, J.H., Alexander, S., Du, J., Kau, T., Thomas, R.K., Shah, K., Soto, H., Perner, S., Prensner, J., DeBiasi, R.M., Demichelis, F., Hatton, C., Rubin, M.A., Garraway, L.A., Nelson, S.F., Liao, L., Mischel, P.S., Cloughesy, T.F., Meyerson, M., Golub, T.A., Lander, E.S., Mellinghoff, I.K. & Sellers, W.R. 2007, "Assessing the significance of chromosomal aberrations in cancer: methodology and application to glioma", *Proceedings of the National Academy of Sciences of the United States of America*, vol. 104, no. 50, pp. 20007-20012.
- Beroukhi, R., Mermel, C.H., Porter, D., Wei, G., Raychaudhuri, S., Donovan, J., Barretina, J., Boehm, J.S., Dobson, J., Urashima, M., Mc Henry, K.T., Pinchback, R.M., Ligon, A.H., Cho, Y.J., Haery, L., Greulich, H., Reich, M., Winckler, W., Lawrence, M.S., Weir, B.A., Tanaka, K.E., Chiang, D.Y., Bass, A.J., Loo, A., Hoffman, C., Prensner, J., Liefeld, T., Gao, Q., Yecies, D., Signoretti, S., Maher, E., Kaye, F.J., Sasaki, H., Tepper, J.E., Fletcher, J.A., Taberner, J., Baselga, J., Tsao, M.S., Demichelis, F., Rubin, M.A., Janne, P.A., Daly, M.J., Nucera, C., Levine, R.L., Ebert, B.L., Gabriel, S., Rustgi, A.K., Antonescu, C.R., Ladanyi, M.,

- Letai, A., Garraway, L.A., Loda, M., Beer, D.G., True, L.D., Okamoto, A., Pomeroy, S.L., Singer, S., Golub, T.R., Lander, E.S., Getz, G., Sellers, W.R. & Meyerson, M. 2010, "The landscape of somatic copy-number alteration across human cancers", *Nature*, vol. 463, no. 7283, pp. 899-905.
- Bratic, A. & Larsson, N.G. 2013, "The role of mitochondria in aging", *The Journal of clinical investigation*, vol. 123, no. 3, pp. 951-957. Review.
- Buczacki, S., Davies, R.J. & Winton, D.J. 2011, "Stem cells, quiescence and rectal carcinoma: an unexplored relationship and potential therapeutic target", *British journal of cancer*, vol. 105, no. 9, pp. 1253-1259. Review.
- Cannino G., El-Khoury R., Pirinen M., Hutz B., Rustin P., Jacobs H.T. and Dufour E. 2012, "Glucose Modulates Respiratory Complex I Activity in Response to Acute Mitochondrial Dysfunction", *J Biol Chem*. Nov 9; 287(46): 38729–38740.
- Cairns, R.A., Harris, I.S. & Mak, T.W. 2011, "Regulation of cancer cell metabolism", *Nature reviews.Cancer*, vol. 11, no. 2, pp. 85-95. Review.
- Cano, A., Perez-Moreno, M.A., Rodrigo, I., Locascio, A., Blanco, M.J., del Barrio, M.G., Portillo, F. & Nieto, M.A. 2000, "The transcription factor snail controls epithelial-mesenchymal transitions by repressing E-cadherin expression", *Nature cell biology*, vol. 2, no. 2, pp. 76-83.
- Cao, J., Schulte, J., Knight, A., Leslie, N.R., Zagazdzon, A., Bronson, R., Manevich, Y., Beeson, C. & Neumann, C.A. 2009, "Prdx1 inhibits tumorigenesis via regulating PTEN/AKT activity", *The EMBO journal*, vol. 28, no. 10, pp. 1505-1517.
- Carey, B.W., Finley, L.W., Cross, J.R., Allis, C.D. & Thompson, C.B. 2015, "Intracellular alpha-ketoglutarate maintains the pluripotency of embryonic stem cells", *Nature*, vol. 518, no. 7539, pp. 413-416.
- Carmeliet, P., Dor, Y., Herbert, J.M., Fukumura, D., Brusselmans, K., Dewerchin, M., Neeman, M., Bono, F., Abramovitch, R., Maxwell, P., Koch, C.J., Ratcliffe, P., Moons, L., Jain, R.K., Collen, D. & Keshert, E. 1998, "Role of HIF-1alpha in hypoxia-mediated apoptosis, cell proliferation and tumour angiogenesis", *Nature*, vol. 394, no. 6692, pp. 485-490.
- Carroll, J., Fearnley, I.M. & Walker, J.E. 2006, "Definition of the mitochondrial proteome by measurement of molecular masses of membrane proteins", *Proceedings of the National Academy of Sciences of the United States of America*, vol. 103, no. 44, pp. 16170-16175.
- Chaban, Y., Boekema, E.J. & Dudkina, N.V. 2014, "Structures of mitochondrial oxidative phosphorylation supercomplexes and mechanisms for their stabilisation", *Biochimica et biophysica acta*, vol. 1837, no. 4, pp. 418-426. Review.
- Chacinska, A., Koehler, C.M., Milenkovic, D., Lithgow, T. & Pfanner, N. 2009, "Importing Mitochondrial Proteins: Machineries and Mechanisms", *Cell*, vol. 138, no. 4, pp. 628-644. Review.

- Champagne, E., Martinez, L.O., Collet, X. & Barbaras, R. 2006, "Ecto-F1Fo ATP synthase/F1 ATPase: metabolic and immunological functions", *Current opinion in lipidology*, vol. 17, no. 3, pp. 279-284.
- Chandel, N.S. 2014, "Mitochondria as signaling organelles", *BMC Biology*, vol. 12, pp. 34-7007-12-34. Review.
- Chang, H.Y., Huang, H.C., Huang, T.C., Yang, P.C., Wang, Y.C. & Juan, H.F. 2012, "Ectopic ATP synthase blockade suppresses lung adenocarcinoma growth by activating the unfolded protein response", *Cancer research*, vol. 72, no. 18, pp. 4696-4706.
- Chang, T.C., Wentzel, E.A., Kent, O.A., Ramachandran, K., Mullendore, M., Lee, K.H., Feldmann, G., Yamakuchi, M., Ferlito, M., Lowenstein, C.J., Arking, D.E., Beer, M.A., Maitra, A. & Mendell, J.T. 2007, "Transactivation of miR-34a by p53 broadly influences gene expression and promotes apoptosis", *Molecular cell*, vol. 26, no. 5, pp. 745-752.
- Chen, C.T., Hsu, S.H. & Wei, Y.H. 2012, "Mitochondrial bioenergetic function and metabolic plasticity in stem cell differentiation and cellular reprogramming", *Biochimica et biophysica acta*, vol. 1820, no. 5, pp. 571-576.
- Chen, R., Runswick, M.J., Carroll, J., Fearnley, I.M. & Walker, J.E. 2007, "Association of two proteolipids of unknown function with ATP synthase from bovine heart mitochondria", *FEBS letters*, vol. 581, no. 17, pp. 3145-3148.
- Chi, S.L. & Pizzo, S.V. 2006, "Cell surface F1Fo ATP synthase: a new paradigm?", *Annals of Medicine*, vol. 38, no. 6, pp. 429-438.
- Chia, N.Y., Chan, Y.S., Feng, B., Lu, X., Orlov, Y.L., Moreau, D., Kumar, P., Yang, L., Jiang, J., Lau, M.S., Huss, M., Soh, B.S., Kraus, P., Li, P., Lufkin, T., Lim, B., Clarke, N.D., Bard, F. & Ng, H.H. 2010, "A genome-wide RNAi screen reveals determinants of human embryonic stem cell identity", *Nature*, vol. 468, no. 7321, pp. 316-320.
- Chin, S.F., Teschendorff, A.E., Marioni, J.C., Wang, Y., Barbosa-Morais, N.L., Thorne, N.P., Costa, J.L., Pinder, S.E., van de Wiel, M.A., Green, A.R., Ellis, I.O., Porter, P.L., Tavaré, S., Brenton, J.D., Ylstra, B. & Caldas, C. 2007, "High-resolution aCGH and expression profiling identifies a novel genomic subtype of ER negative breast cancer", *Genome biology*, vol. 8, no. 10, pp. R215.
- Chung, S., Dzeja, P.P., Faustino, R.S., Perez-Terzic, C., Behfar, A. & Terzic, A. 2007, "Mitochondrial oxidative metabolism is required for the cardiac differentiation of stem cells", *Nature clinical practice. Cardiovascular medicine*, vol. 4 Suppl 1, pp. S60-7.
- Clemençon, B. 2012, "Yeast mitochondrial interactosome model: metabolon membrane proteins complex involved in the channeling of ADP/ATP", *International journal of molecular sciences*, vol. 13, no. 2, pp. 1858-1885.
- Correia-Melo, C. & Passos, J.F. 2015, "Mitochondria: Are they causal players in cellular senescence?", *Biochimica et biophysica acta*, vol. 1847, no. 11, pp. 1373-1379. Review.

- Czerwinska, P. & Kaminska, B. 2015, "Regulation of breast cancer stem cell features", *Contemporary oncology (Poznan, Poland)*, vol. 19, no. 1A, pp. A7-A15. Review.
- Daum, B., Walter, A., Horst, A., Osiewacz, H.D. & Kuhlbrandt, W. 2013, "Age-dependent dissociation of ATP synthase dimers and loss of inner-membrane cristae in mitochondria", *Proceedings of the National Academy of Sciences of the United States of America*, vol. 110, no. 38, pp. 15301-15306. Review.
- Davies, K.M., Anselmi, C., Wittig, I., Faraldo-Gomez, J.D. & Kuhlbrandt, W. 2012, "Structure of the yeast F1Fo-ATP synthase dimer and its role in shaping the mitochondrial cristae", *Proceedings of the National Academy of Sciences of the United States of America*, vol. 109, no. 34, pp. 13602-13607.
- Debette, S. & Markus, H.S. 2010, "The clinical importance of white matter hyperintensities on brain magnetic resonance imaging: systematic review and meta-analysis", *BMJ (Clinical research ed.)*, vol. 341, pp. c3666.
- Dutta-Simmons, J., Zhang, Y., Gorgun, G., Gatt, M., Mani, M., Hideshima, T., Takada, K., Carlson, N.E., Carrasco, D.E., Tai, Y.T., Raje, N., Letai, A.G., Anderson, K.C. & Carrasco, D.R. 2009, "Aurora kinase A is a target of Wnt/beta-catenin involved in multiple myeloma disease progression", *Blood*, vol. 114, no. 13, pp. 2699-2708.
- Engstrom, K.S., Hossain, M.B., Lauss, M., Ahmed, S., Raqib, R., Vahter, M. & Broberg, K. 2013, "Efficient arsenic metabolism--the AS3MT haplotype is associated with DNA methylation and expression of multiple genes around AS3MT", *PLoS one*, vol. 8, no. 1, pp. e53732.
- Facucho-Oliveira, J.M., Alderson, J., Spikings, E.C., Egginton, S. & St John, J.C. 2007, "Mitochondrial DNA replication during differentiation of murine embryonic stem cells", *Journal of cell science*, vol. 120, no. Pt 22, pp. 4025-4034.
- Ferreira, M.A., Jansen, R., Willemsen, G., Penninx, B., Bain, L.M., Vicente, C.T., Revez, J.A., Matheson, M.C., Hui, J., Tung, J.Y., Baltic, S., Le Souef, P., Montgomery, G.W., Martin, N.G., Robertson, C.F., James, A., Thompson, P.J., Boomsma, D.I., Hopper, J.L., Hinds, D.A., Werder, R.B., Phipps, S. & Australian Asthma Genetics Consortium Collaborators 2016, "Gene-based analysis of regulatory variants identifies 4 putative novel asthma risk genes related to nucleotide synthesis and signaling", *The Journal of allergy and clinical immunology*, vol. 139, no. 4, pp.1148-1157.
- Folmes, C.D., Nelson, T.J., Martinez-Fernandez, A., Arrell, D.K., Lindor, J.Z., Dzeja, P.P., Ikeda, Y., Perez-Terzic, C. & Terzic, A. 2011, "Somatic oxidative bioenergetics transitions into pluripotency-dependent glycolysis to facilitate nuclear reprogramming", *Cell metabolism*, vol. 14, no. 2, pp. 264-271.
- Formentini, L., Sanchez-Arago, M., Sanchez-Cenizo, L. & Cuezva, J.M. 2012, "The mitochondrial ATPase inhibitory factor 1 triggers a ROS-mediated retrograde prosurvival and proliferative response", *Molecular cell*, vol. 45, no. 6, pp. 731-742.

- Fukuoh, A., Cannino, G., Gerards, M., Buckley, S., Kazancioglu, S., Scialo, F., Lihavainen, E., Ribeiro, A., Dufour, E. & Jacobs, H.T. 2014, "Screen for mitochondrial DNA copy number maintenance genes reveals essential role for ATP synthase", *Molecular systems biology*, vol. 10, no. 6, pp. 734.
- Gangemi, R., Paleari, L., Orengo, A.M., Cesario, A., Chessa, L., Ferrini, S. & Russo, P. 2009, "Cancer stem cells: a new paradigm for understanding tumor growth and progression and drug resistance", *Current medicinal chemistry*, vol. 16, no. 14, pp. 1688-1703.
- Garrido, C., Galluzzi, L., Brunet, M., Puig, P.E., Didelot, C. & Kroemer, G. 2006, "Mechanisms of cytochrome c release from mitochondria", *Cell death and differentiation*, vol. 13, no. 9, pp. 1423-1433.
- Garvey, W.T., Huecksteadt, T.P. & Birnbaum, M.J. 1989, "Pretranslational suppression of an insulin-responsive glucose transporter in rats with diabetes mellitus", *Science (New York, N.Y.)*, vol. 245, no. 4913, pp. 60-63.
- Geromel, V., Kadhom, N., Cebalos-Picot, I., Ouari, O., Polidori, A., Munnich, A., Rotig, A. & Rustin, P. 2001, "Superoxide-induced massive apoptosis in cultured skin fibroblasts harboring the neurogenic ataxia retinitis pigmentosa (NARP) mutation in the ATPase-6 gene of the mitochondrial DNA", *Human molecular genetics*, vol. 10, no. 11, pp. 1221-1228.
- Giannoni, E., Buricchi, F., Raugei, G., Ramponi, G. & Chiarugi, P. 2005, "Intracellular reactive oxygen species activate Src tyrosine kinase during cell adhesion and anchorage-dependent cell growth", *Molecular and cellular biology*, vol. 25, no. 15, pp. 6391-6403.
- Gorai, T., Goto, H., Noda, T., Watanabe, T., Kozuka-Hata, H., Oyama, M., Takano, R., Neumann, G., Watanabe, S. & Kawaoka, Y. 2012, "F1Fo-ATPase, F-type proton-translocating ATPase, at the plasma membrane is critical for efficient influenza virus budding", *Proceedings of the National Academy of Sciences of the United States of America*, vol. 109, no. 12, pp. 4615-4620.
- Gottesman, M.M., Fojo, T. & Bates, S.E. 2002, "Multidrug resistance in cancer: role of ATP-dependent transporters", *Nature reviews.Cancer*, vol. 2, no. 1, pp. 48-58. Review.
- Haldar, M., Hancock, J.D., Coffin, C.M., Lessnick, S.L. & Capecchi, M.R. 2007, "A conditional mouse model of synovial sarcoma: insights into a myogenic origin", *Cancer cell*, vol. 11, no. 4, pp. 375-388.
- Han, M.H., Lundgren, D.H., Jaiswal, S., Chao, M., Graham, K.L., Garris, C.S., Axtell, R.C., Ho, P.P., Lock, C.B., Woodard, J.I., Brownell, S.E., Zoudilova, M., Hunt, J.F., Baranzini, S.E., Butcher, E.C., Raine, C.S., Sobel, R.A., Han, D.K., Weissman, I. & Steinman, L. 2012, "Janus-like opposing roles of CD47 in autoimmune brain inflammation in humans and mice", *The Journal of experimental medicine*, vol. 209, no. 7, pp. 1325-1334.

- He J, Ford H.C., Carroll J., Ding S., Fearnley I.M., Walker J.E. 2017 "Persistence of the mitochondrial permeability transition in the absence of subunit c of human ATP synthase", *Proc Natl Acad Sci U S A*. Mar 13.
- Hejzlarova, K., Mracek, T., Vrbacky, M., Kaplanova, V., Karbanova, V., Nuskova, H., Pecina, P. & Houstek, J. 2014, "Nuclear genetic defects of mitochondrial ATP synthase", *Physiological Research / Academia Scientiarum Bohemoslovaca*, vol. 63 Suppl 1, pp. S57-71. Review.
- Hinton, A., Bond, S. & Forgac, M. 2009, "V-ATPase functions in normal and disease processes", *Pflugers Archiv : European journal of physiology*, vol. 457, no. 3, pp. 589-598.
- Hirata, T., Iwamoto-Kihara, A., Sun-Wada, G.H., Okajima, T., Wada, Y. & Futai, M. 2003, "Subunit rotation of vacuolar-type proton pumping ATPase: relative rotation of the G and C subunits", *The Journal of biological chemistry*, vol. 278, no. 26, pp. 23714-23719.
- Houstek, J., Pickova, A., Vojtiskova, A., Mracek, T., Pecina, P. & Jesina, P. 2006, "Mitochondrial diseases and genetic defects of ATP synthase", *Biochimica et biophysica acta*, vol. 1757, no. 9-10, pp. 1400-1405. Review.
- Hu, X., Stern, H.M., Ge, L., O'Brien, C., Haydu, L., Honchell, C.D., Haverty, P.M., Peters, B.A., Wu, T.D., Amler, L.C., Chant, J., Stokoe, D., Lackner, M.R. & Cavet, G. 2009, "Genetic alterations and oncogenic pathways associated with breast cancer subtypes", *Molecular cancer research : MCR*, vol. 7, no. 4, pp. 511-522.
- Hua, S., Xiaotao, X., Renhua, G., Yongmei, Y., Lianke, L., Wen, G. & Yongqian, S. 2012, "Reduced miR-31 and let-7 maintain the balance between differentiation and quiescence in lung cancer stem-like side population cells", *Biomedicine & pharmacotherapy = Biomedecine & pharmacotherapie*, vol. 66, no. 2, pp. 89-97.
- Huang, X., Eriksson, K.F., Vaag, A., Lehtovirta, M., Hansson, M., Laurila, E., Kanninen, T., Olesen, B.T., Kurucz, I., Koranyi, L. & Groop, L. 1999, "Insulin-regulated mitochondrial gene expression is associated with glucose flux in human skeletal muscle", *Diabetes*, vol. 48, no. 8, pp. 1508-1514.
- Hulmi, J.J., Silvennoinen, M., Lehti, M., Kivela, R. & Kainulainen, H. 2012, "Altered REDD1, myostatin and Akt/mTOR/FoxO/MAPK Signaling in Streptozotocin-induced Diabetic Muscle Atrophy", *American journal of physiology. Endocrinology and metabolism*, vol 302, E307-15.
- Hyttinen, V., Kaprio, J., Kinnunen, L., Koskenvuo, M. & Tuomilehto, J. 2003, "Genetic liability of type 1 diabetes and the onset age among 22,650 young Finnish twin pairs: a nationwide follow-up study", *Diabetes*, vol. 52, no. 4, pp. 1052-1055.
- Ikegaki, N., Shimada, H., Fox, A.M., Regan, P.L., Jacobs, J.R., Hicks, S.L., Rappaport, E.F. & Tang, X.X. 2013, "Transient treatment with epigenetic modifiers yields stable neuroblastoma stem cells resembling aggressive large-cell neuroblastomas",

Proceedings of the National Academy of Sciences of the United States of America, vol. 110, no. 15, pp. 6097-6102.

- Imamura, H., Nakano, M., Noji, H., Muneyuki, E., Ohkuma, S., Yoshida, M. & Yokoyama, K. 2003, "Evidence for rotation of V1-ATPase", *Proceedings of the National Academy of Sciences of the United States of America*, vol. 100, no. 5, pp. 2312-2315.
- Jang, H., Yang, J., Lee, E. & Cheong, J.H. 2015, "Metabolism in embryonic and cancer stemness", *Archives of Pharmacal Research*, vol. 38, no. 3, pp. 381-388. Review.
- Jefferies, K.C., Cipriano, D.J. & Forgac, M. 2008, "Function, structure and regulation of the vacuolar (H⁺)-ATPases", *Archives of Biochemistry and Biophysics*, vol. 476, no. 1, pp. 33-42.
- Jonckheere, A.I., Hogeveen, M., Nijtmans, L., van den Brand, M., Janssen, A., Diepstra, H., van den Brandt, F., van den Heuvel, B., Hol, F., Hofste, T., Kapusta, L., Dillmann, U., Shamdeen, M., Smeitink, J., Smeitink, J. & Rodenburg, R. 2009, "A novel mitochondrial ATP8 gene mutation in a patient with apical hypertrophic cardiomyopathy and neuropathy", *BMJ case reports*, vol. 2009, pp. 10.1136/bcr.07.2008.0504. Epub 2009 Jan 23.
- Kaidi, A., Williams, A.C. & Paraskeva, C. 2007, "Interaction between beta-catenin and HIF-1 promotes cellular adaptation to hypoxia", *Nature cell biology*, vol. 9, no. 2, pp. 210-217.
- Kainulainen, H., Breiner, M., Schurmann, A., Marttinen, A., Virjo, A. & Joost, H.G. 1994a, "In vivo glucose uptake and glucose transporter proteins GLUT1 and GLUT4 in heart and various types of skeletal muscle from streptozotocin-diabetic rats", *Biochimica et biophysica acta*, vol. 1225, no. 3, pp. 275-282.
- Kainulainen, H., Komulainen, J., Joost, H.G. & Vihko, V. 1994b, "Dissociation of the effects of training on oxidative metabolism, glucose utilisation and GLUT4 levels in skeletal muscle of streptozotocin-diabetic rats", *Pflugers Archiv : European journal of physiology*, vol. 427, no. 5-6, pp. 444-449.
- Kainulainen, H., Schurmann, A., Vilja, P. & Joost, H.G. 1993, "In-vivo glucose uptake and glucose transporter proteins GLUT1 and GLUT3 in brain tissue from streptozotocin-diabetic rats", *Acta Physiologica Scandinavica*, vol. 149, no. 2, pp. 221-225.
- Kim, H.J., Park, K.G., Yoo, E.K., Kim, Y.H., Kim, Y.N., Kim, H.S., Kim, H.T., Park, J.Y., Lee, K.U., Jang, W.G., Kim, J.G., Kim, B.W. & Lee, I.K. 2007, "Effects of PGC-1alpha on TNF-alpha-induced MCP-1 and VCAM-1 expression and NF-kappaB activation in human aortic smooth muscle and endothelial cells", *Antioxidants & redox signaling*, vol. 9, no. 3, pp. 301-307.
- Kim, J.W., Tchernyshyov, I., Semenza, G.L. & Dang, C.V. 2006, "HIF-1-mediated expression of pyruvate dehydrogenase kinase: a metabolic switch required for cellular adaptation to hypoxia", *Cell metabolism*, vol. 3, no. 3, pp. 177-185.

- King, A., Selak, M.A. & Gottlieb, E. 2006, "Succinate dehydrogenase and fumarate hydratase: linking mitochondrial dysfunction and cancer", *Oncogene*, vol. 25, no. 34, pp. 4675-4682. Review.
- Kivela, R., Silvennoinen, M., Touvra, A.M., Lehti, T.M., Kainulainen, H. & Vihko, V. 2006, "Effects of experimental type 1 diabetes and exercise training on angiogenic gene expression and capillarization in skeletal muscle", *FASEB journal : official publication of the Federation of American Societies for Experimental Biology*, vol. 20, no. 9, pp. 1570-1572.
- Koza, R.A., Nikonova, L., Hogan, J., Rim, J.S., Mendoza, T., Faulk, C., Skaf, J. & Kozak, L.P. 2006, "Changes in gene expression foreshadow diet-induced obesity in genetically identical mice", *PLoS genetics*, vol. 2, no. 5, pp. e81.
- Kuhlbrandt, W. 2015, "Structure and function of mitochondrial membrane protein complexes", *BMC biology*, vol. 13, pp. 89-015-0201-x. Review.
- Lachtermacher, S., Esporcatte, B.L., Montalvao, F., Costa, P.C., Rodrigues, D.C., Belem, L., Rabischoffsky, A., Faria Neto, H.C., Vasconcellos, R., Iacobas, S., Iacobas, D.A., Dohmann, H.F., Spray, D.C., Goldenberg, R.C. & Campos-de-Carvalho, A.C. 2010, "Cardiac gene expression and systemic cytokine profile are complementary in a murine model of post-ischemic heart failure", *Brazilian journal of medical and biological research = Revista brasileira de pesquisas medicas e biologicas*, vol. 43, no. 4, pp. 377-389.
- Lee, C.H., Bang, S.H., Lee, S.K., Song, K.Y. & Lee, I.C. 2005, "Gene expression profiling reveals sequential changes in gastric tubular adenoma and carcinoma in situ", *World journal of gastroenterology : WJG*, vol. 11, no. 13, pp. 1937-1945.
- Lee, J., Ding, S., Walpole, T.B., Holding, A.N., Montgomery, M.G., Fearnley, I.M. & Walker, J.E. 2015, "Organisation of Subunits in the Membrane Domain of the Bovine F-ATPase Revealed by Covalent Cross-linking", *The Journal of biological chemistry*, .
- Lehti, T.M., Silvennoinen, M., Kivela, R., Kainulainen, H. & Komulainen, J. 2007, "Effects of streptozotocin-induced diabetes and physical training on gene expression of titin-based stretch-sensing complexes in mouse striated muscle", *American journal of physiology. Endocrinology and metabolism*, vol. 292, no. 2, pp. E533-42.
- Lehti, T.M., Silvennoinen, M., Kivela, R., Kainulainen, H. & Komulainen, J. 2006, "Effects of streptozotocin-induced diabetes and physical training on gene expression of extracellular matrix proteins in mouse skeletal muscle", *American journal of physiology. Endocrinology and metabolism*, vol. 290, no. 5, pp. E900-7.
- Lenzen, S. 2008, "The mechanisms of alloxan- and streptozotocin-induced diabetes", *Diabetologia*, vol. 51, no. 2, pp. 216-226.
- Li, M., Balch, C., Montgomery, J.S., Jeong, M., Chung, J.H., Yan, P., Huang, T.H., Kim, S. & Nephew, K.P. 2009, "Integrated analysis of DNA methylation and

- gene expression reveals specific signaling pathways associated with platinum resistance in ovarian cancer", *BMC Medical Genomics*, vol. 2, pp. 34-8794-2-34.
- Li, P., Nijhawan, D., Budihardjo, I., Srinivasula, S.M., Ahmad, M., Alnemri, E.S. & Wang, X. 1997, "Cytochrome c and dATP-dependent formation of Apaf-1/caspase-9 complex initiates an apoptotic protease cascade", *Cell*, vol. 91, no. 4, pp. 479-489.
- Liang, P. & Pardee, A.B. 1995, "Recent advances in differential display", *Current opinion in immunology*, vol. 7, no. 2, pp. 274-280.
- Liang, P. & Pardee, A.B. 1992, "Differential display of eukaryotic messenger RNA by means of the polymerase chain reaction", *Science*, vol. 257, no. 5072, pp. 967-971.
- Liemburg-Apers, D.C., Willems, P.H., Koopman, W.J. & Grefte, S. 2015, "Interactions between mitochondrial reactive oxygen species and cellular glucose metabolism", *Archives of Toxicology*, vol. 89, no. 8, pp. 1209-1226. Review.
- Lievens, S., Goormachtig, S. & Holsters, M. 2001a, "A critical evaluation of differential display as a tool to identify genes involved in legume nodulation: looking back and looking forward", *Nucleic acids research*, vol. 29, no. 17, pp. 3459-3468.
- Lopez, L.M., Hill, W.D., Harris, S.E., Valdes Hernandez, M., Munoz Maniega, S., Bastin, M.E., Bailey, E., Smith, C., McBride, M., McClure, J., Graham, D., Dominiczak, A., Yang, Q., Fornage, M., Ikram, M.A., Debette, S., Launer, L., Bis, J.C., Schmidt, R., Seshadri, S., Porteous, D.J., Starr, J., Deary, I.J. & Wardlaw, J.M. 2015, "Genes from a translational analysis support a multifactorial nature of white matter hyperintensities", *Stroke; a journal of cerebral circulation*, vol. 46, no. 2, pp. 341-347.
- Lopez-Ayllon, B.D., Moncho-Amor, V., Abarrategi, A., Ibanez de Caceres, I., Castro-Carpeno, J., Belda-Iniesta, C., Perona, R. & Sastre, L. 2014, "Cancer stem cells and cisplatin-resistant cells isolated from non-small-lung cancer cell lines constitute related cell populations", *Cancer medicine*, vol. 3, no. 5, pp. 1099-1111.
- Lu, C.W., Lin, S.C., Chen, K.F., Lai, Y.Y. & Tsai, S.J. 2008, "Induction of pyruvate dehydrogenase kinase-3 by hypoxia-inducible factor-1 promotes metabolic switch and drug resistance", *The Journal of biological chemistry*, vol. 283, no. 42, pp. 28106-28114.
- Lu, X., Zhang, K., Van Sant, C., Coon, J. & Semizarov, D. 2010, "An algorithm for classifying tumors based on genomic aberrations and selecting representative tumor models", *BMC medical genomics*, vol. 3, pp. 23-8794-3-23.
- Lu, Y., Wan, Z., Zhang, X., Zhong, X., Rui, L. & Li, Z. 2016, "PRDM14 inhibits 293T cell proliferation by influencing the G1/S phase transition", *Gene*, Dec 31;595(2):180-186.
- Maiese, K. 2015, "New Insights for Oxidative Stress and Diabetes Mellitus", *Oxid Med Cell Longev.*, 2015:875961. Review.

- Mani, S.A., Guo, W., Liao, M.J., Eaton, E.N., Ayyanan, A., Zhou, A.Y., Brooks, M., Reinhard, F., Zhang, C.C., Shipitsin, M., Campbell, L.L., Polyak, K., Brisken, C., Yang, J. & Weinberg, R.A. 2008, "The epithelial-mesenchymal transition generates cells with properties of stem cells", *Cell*, vol. 133, no. 4, pp. 704-715.
- Marjanovic, N.D., Weinberg, R.A. & Chaffer, C.L. 2013, "Cell plasticity and heterogeneity in cancer", *Clinical chemistry*, vol. 59, no. 1, pp. 168-179. Review.
- McFarland, M.A., Ellis, C.E., Markey, S.P. & Nussbaum, R.L. 2008, "Proteomics analysis identifies phosphorylation-dependent alpha-synuclein protein interactions", *Molecular & cellular proteomics : MCP*, vol. 7, no. 11, pp. 2123-2137.
- Merlos-Suarez, A., Barriga, F.M., Jung, P., Iglesias, M., Cespedes, M.V., Rossell, D., Sevillano, M., Hernando-Momblona, X., da Silva-Diz, V., Munoz, P., Clevers, H., Sancho, E., Mangues, R. & Batlle, E. 2011, "The intestinal stem cell signature identifies colorectal cancer stem cells and predicts disease relapse", *Cell stem cell*, vol. 8, no. 5, pp. 511-524.
- Meyer, B., Wittig, I., Trifilieff, E., Karas, M. & Schagger, H. 2007, "Identification of two proteins associated with mammalian ATP synthase", *Molecular & cellular proteomics : MCP*, vol. 6, no. 10, pp. 1690-1699.
- Mishra, P., Varuzhanyan, G., Pham, A.H. & Chan, D.C. 2015, "Mitochondrial Dynamics is a Distinguishing Feature of Skeletal Muscle Fiber Types and Regulates Organellar Compartmentalization", *Cell metabolism*, vol. 22, no. 6, pp. 1033-1044. Review.
- Namlos, H.M., Kresse, S.H., Muller, C.R., Henriksen, J., Holdhus, R., Saeter, G., Bruland, O.S., Bjerkehagen, B., Steen, V.M. & Myklebost, O. 2012, "Global gene expression profiling of human osteosarcomas reveals metastasis-associated chemokine pattern", *Sarcoma*, vol. 2012, pp. 639038.
- Nikolsky, Y., Sviridov, E., Yao, J., Dosymbekov, D., Ustyansky, V., Kaznacheev, V., Dezso, Z., Mulvey, L., Macconail, L.E., Winckler, W., Serebryiskaya, T., Nikolskaya, T. & Polyak, K. 2008, "Genome-wide functional synergy between amplified and mutated genes in human breast cancer", *Cancer research*, vol. 68, no. 22, pp. 9532-9540.
- Nishio, Y., Warren, C.E., Buczek-Thomas, J.A., Rulfs, J., Koya, D., Aiello, L.P., Feener, E.P., Miller, T.B., Jr, Dennis, J.W. & King, G.L. 1995, "Identification and characterization of a gene regulating enzymatic glycosylation which is induced by diabetes and hyperglycemia specifically in rat cardiac tissue", *The Journal of clinical investigation*, vol. 96, no. 4, pp. 1759-1767.
- Ntziachristos, P., Tsirigos, A., Van Vlierberghe, P., Nedjic, J., Trimarchi, T., Flaherty, M.S., Ferres-Marco, D., da Ros, V., Tang, Z., Siegle, J., Asp, P., Hadler, M., Rigo, I., De Keersmaecker, K., Patel, J., Huynh, T., Utro, F., Poglio, S., Samon, J.B., Paietta, E., Racevskis, J., Rowe, J.M., Rabadan, R., Levine, R.L., Brown, S., Pflumio, F., Dominguez, M., Ferrando, A. & Aifantis, I. 2012, "Genetic inactivation of the polycomb repressive complex 2 in T cell acute lymphoblastic leukemia", *Nature medicine*, vol. 18, no. 2, pp. 298-301.

- Nuskova, H., Mracek, T., Mikulova, T., Vrbacky, M., Kovarova, N., Kovalcikova, J., Pecina, P. & Houstek, J. 2015, "Mitochondrial ATP synthasome: Expression and structural interaction of its components", *Biochemical and biophysical research communications*, vol. 464, no. 3, pp. 787-793.
- Ohsakaya, S., Fujikawa, M., Hisabori, T. & Yoshida, M. 2011, "Knockdown of DAPIT (diabetes-associated protein in insulin-sensitive tissue) results in loss of ATP synthase in mitochondria", *The Journal of biological chemistry*, vol. 286, no. 23, pp. 20292-20296.
- Olejniczak, E.T., Van Sant, C., Anderson, M.G., Wang, G., Tahir, S.K., Sauter, G., Lesniewski, R. & Semizarov, D. 2007, "Integrative genomic analysis of small-cell lung carcinoma reveals correlates of sensitivity to bcl-2 antagonists and uncovers novel chromosomal gains", *Molecular cancer research : MCR*, vol. 5, no. 4, pp. 331-339.
- Panopoulos, A.D., Yanes, O., Ruiz, S., Kida, Y.S., Diep, D., Tautenhahn, R., Herrerias, A., Batchelder, E.M., Plongthongkum, N., Lutz, M., Berggren, W.T., Zhang, K., Evans, R.M., Siuzdak, G. & Izpisua Belmonte, J.C. 2012, "The metabolome of induced pluripotent stem cells reveals metabolic changes occurring in somatic cell reprogramming", *Cell research*, vol. 22, no. 1, pp. 168-177.
- Papandreou, I., Cairns, R.A., Fontana, L., Lim, A.L. & Denko, N.C. 2006, "HIF-1 mediates adaptation to hypoxia by actively downregulating mitochondrial oxygen consumption", *Cell metabolism*, vol. 3, no. 3, pp. 187-197.
- Paumard, P., Vaillier, J., Couлары, B., Schaeffer, J., Soubannier, V., Mueller, D.M., Brethes, D., di Rago, J.P. & Velours, J. 2002, "The ATP synthase is involved in generating mitochondrial cristae morphology", *The EMBO journal*, vol. 21, no. 3, pp. 221-230.
- Pavlinkova, G., Salbaum, J.M. & Kappen, C. 2009, "Maternal diabetes alters transcriptional programs in the developing embryo", *BMC genomics*, vol. 10, pp. 274-2164-10-274.
- Pellegrino, M.W. & Haynes, C.M. 2015, "Mitophagy and the mitochondrial unfolded protein response in neurodegeneration and bacterial infection", *BMC Biology*, vol. 13, pp. 10.1186/s12915-015-0129-1.
- Pette, D. & Staron, R.S. 2000, "Myosin isoforms, muscle fiber types, and transitions", *Microscopy research and technique*, vol. 50, no. 6, pp. 500-509. Review.
- Piantadosi, C.A. & Suliman, H.B. 2012, "Redox regulation of mitochondrial biogenesis", *Free radical biology & medicine*, vol. 53, no. 11, pp. 2043-2053. Review.
- Pinti, M.V., Hathaway, Q.A. & Hollander, J.M. 2016, "Role of MicroRNA in Metabolic Shift During Heart Failure", *American journal of physiology. Heart and circulatory physiology*, , pp. ajpheart.00341.2016. Review.
- Plas, D.R. & Thompson, C.B. 2005, "Akt-dependent transformation: there is more to growth than just surviving", *Oncogene*, vol. 24, no. 50, pp. 7435-7442. Review.

- Platts, A.E., Dix, D.J., Chemes, H.E., Thompson, K.E., Goodrich, R., Rockett, J.C., Rawe, V.Y., Quintana, S., Diamond, M.P., Strader, L.F. & Krawetz, S.A. 2007, "Success and failure in human spermatogenesis as revealed by teratozoospermic RNAs", *Human molecular genetics*, vol. 16, no. 7, pp. 763-773.
- Prigione, A., Fauler, B., Lurz, R., Lehrach, H. & Adjaye, J. 2010, "The senescence-related mitochondrial/oxidative stress pathway is repressed in human induced pluripotent stem cells", *Stem cells (Dayton, Ohio)*, vol. 28, no. 4, pp. 721-733.
- Pullman, M.E. & Monroy, G.C. 1963, "A Naturally Occurring Inhibitor of Mitochondrial Adenosine Triphosphatase", *The Journal of biological chemistry*, vol. 238, pp. 3762-3769.
- Rai, A.K., Spolaore, B., Harris, D.A., Dabbeni-Sala, F. & Lippe, G. 2013, "Ectopic FOF1 ATP synthase contains both nuclear and mitochondrially-encoded subunits", *Journal of Bioenergetics and Biomembranes*, vol. 45, no. 6, pp. 569-579.
- Rakieten, N., Rakieten, M.L. & Nadkarni, M.R. 1963, "Studies on the diabetogenic action of streptozotocin (NSC-37917)", *Cancer chemotherapy reports*, vol. 29, pp. 91-98.
- Ramsey, M.R. & Sharpless, N.E. 2006, "ROS as a tumour suppressor?", *Nature cell biology*, vol. 8, no. 11, pp. 1213-1215.
- Rawson S., Harrison M.A., Muench S.P. 2016, "Rotating with the brakes on and other unresolved features of the vacuolar ATPase", *Biochem Soc Trans.* Jun 15; 44(3): 851–855.
- Revel, J.P., Fawcett, D.W. & Philpott, C.W. 1963, "Observations on mitochondrial structure: Angular Configurations of the Cristae", *The Journal of cell biology*, vol. 16, no. 1, pp. 187-195.
- Rhodes, D.R., Yu, J., Shanker, K., Deshpande, N., Varambally, R., Ghosh, D., Barrette, T., Pandey, A. & Chinnaiyan, A.M. 2004, "ONCOMINE: a cancer microarray database and integrated data-mining platform", *Neoplasia (New York, N.Y.)*, vol. 6, no. 1, pp. 1-6.
- Rizzuto, R., De Stefani, D., Raffaello, A. & Mammucari, C. 2012, "Mitochondria as sensors and regulators of calcium signalling", *Nature reviews.Molecular cell biology*, vol. 13, no. 9, pp. 566-578.
- Rodriguez-Acevedo, A.J., Ferreira, M.A., Benton, M.C., Carless, M.A., Goring, H.H., Curran, J.E., Blangero, J., Lea, R.A. & Griffiths, L.R. 2015, "Common polygenic variation contributes to risk of migraine in the Norfolk Island population", *Human genetics*, vol. 134, no. 10, pp. 1079-1087.
- Rothenberg, S.M., Mohapatra, G., Rivera, M.N., Winokur, D., Greninger, P., Nitta, M., Sadow, P.M., Sooriyakumar, G., Brannigan, B.W., Ullman, M.J., Perera, R.M., Wang, R., Tam, A., Ma, X.J., Erlander, M., Sgroi, D.C., Rocco, J.W., Lingen, M.W., Cohen, E.E., Louis, D.N., Settleman, J. & Haber, D.A. 2010, "A genome-wide screen for microdeletions reveals disruption of polarity complex genes in diverse human cancers", *Cancer research*, vol. 70, no. 6, pp. 2158-2164.

- Runswick, M.J., Bason, J.V., Montgomery, M.G., Robinson, G.C., Fearnley, I.M. & Walker, J.E. 2013, "The affinity purification and characterization of ATP synthase complexes from mitochondria", *Open biology*, vol. 3, no. 2, pp. 120160.
- Rustin, P., Chretien, D., Bourgeron, T., Gerard, B., Rotig, A., Saudubray, J.M. & Munnich, A. 1994, "Biochemical and molecular investigations in respiratory chain deficiencies", *Clinica chimica acta; international journal of clinical chemistry*, vol. 228, no. 1, pp. 35-51.
- Saltiel, A.R. & Kahn, C.R. 2001, "Insulin signalling and the regulation of glucose and lipid metabolism", *Nature*, vol. 414, no. 6865, pp. 799-806.
- Sanchez-Arago, M., Formentini, L., Martinez-Reyes, I., Garcia-Bermudez, J., Santacatterina, F., Sanchez-Cenizo, L., Willers, I.M., Aldea, M., Najera, L., Juarranz, A., Lopez, E.C., Clofent, J., Navarro, C., Espinosa, E. & Cuezva, J.M. 2013a, "Expression, regulation and clinical relevance of the ATPase inhibitory factor 1 in human cancers", *Oncogenesis*, vol. 2, pp. e46.
- Sanchez-Arago, M., Garcia-Bermudez, J., Martinez-Reyes, I., Santacatterina, F. & Cuezva, J.M. 2013b, "Degradation of IF1 controls energy metabolism during osteogenic differentiation of stem cells", *EMBO reports*, vol. 14, no. 7, pp. 638-644.
- Sanchez-Cenizo, L., Formentini, L., Aldea, M., Ortega, A.D., Garcia-Huerta, P., Sanchez-Arago, M. & Cuezva, J.M. 2010, "Up-regulation of the ATPase inhibitory factor 1 (IF1) of the mitochondrial H⁺-ATP synthase in human tumors mediates the metabolic shift of cancer cells to a Warburg phenotype", *The Journal of biological chemistry*, vol. 285, no. 33, pp. 25308-25313.
- Satake, H., Tamura, K., Furihata, M., Anchi, T., Sakoda, H., Kawada, C., Iiyama, T., Ashida, S. & Shuin, T. 2010, "The ubiquitin-like molecule interferon-stimulated gene 15 is overexpressed in human prostate cancer", *Oncology reports*, vol. 23, no. 1, pp. 11-16.
- Scarpulla, R.C., Vega, R.B. & Kelly, D.P. 2012, "Transcriptional integration of mitochondrial biogenesis", *Trends in endocrinology and metabolism: TEM*, vol. 23, no. 9, pp. 459-466. Review.
- Seelert, H. & Dencher, N.A. 2011, "ATP synthase superassemblies in animals and plants: two or more are better", *Biochimica et biophysica acta*, vol. 1807, no. 9, pp. 1185-1197. Review.
- Selak, M.A., Armour, S.M., MacKenzie, E.D., Boulahbel, H., Watson, D.G., Mansfield, K.D., Pan, Y., Simon, M.C., Thompson, C.B. & Gottlieb, E. 2005, "Succinate links TCA cycle dysfunction to oncogenesis by inhibiting HIF-alpha prolyl hydroxylase", *Cancer cell*, vol. 7, no. 1, pp. 77-85.
- Selga, E., Morales, C., Noe, V., Peinado, M.A. & Ciudad, C.J. 2008, "Role of caveolin 1, E-cadherin, Enolase 2 and PKCalpha on resistance to methotrexate in human HT29 colon cancer cells", *BMC medical genomics*, vol. 1, pp. 35-8794-1-35.

- Semenza, G.L. 2010, "HIF-1: upstream and downstream of cancer metabolism", *Current opinion in genetics & development*, vol. 20, no. 1, pp. 51-56.
- Sena, L.A. & Chandel, N.S. 2012, "Physiological roles of mitochondrial reactive oxygen species", *Molecular cell*, vol. 48, no. 2, pp. 158-167. Review.
- Servidei, S. 2002, "Mitochondrial encephalomyopathies: gene mutation", *Neuromuscular disorders : NMD*, vol. 12, no. 1, pp. 101-110. Review.
- Shoshan-Barmatz, V. & Mizrachi, D. 2012, "VDAC1: from structure to cancer therapy", *Frontiers in oncology*, vol. 2, pp. 164. Review.
- Sos, M.L., Michel, K., Zander, T., Weiss, J., Frommolt, P., Peifer, M., Li, D., Ullrich, R., Koker, M., Fischer, F., Shimamura, T., Rauh, D., Mermel, C., Fischer, S., Stuckrath, I., Heynck, S., Beroukhim, R., Lin, W., Winckler, W., Shah, K., LaFramboise, T., Moriarty, W.F., Hanna, M., Tolosi, L., Rahnenfuhrer, J., Verhaak, R., Chiang, D., Getz, G., Hellmich, M., Wolf, J., Girard, L., Peyton, M., Weir, B.A., Chen, T.H., Greulich, H., Barretina, J., Shapiro, G.I., Garraway, L.A., Gazdar, A.F., Minna, J.D., Meyerson, M., Wong, K.K. & Thomas, R.K. 2009, "Predicting drug susceptibility of non-small cell lung cancers based on genetic lesions", *The Journal of clinical investigation*, vol. 119, no. 6, pp. 1727-1740.
- Stamer, K., Vogel, R., Thies, E., Mandelkow, E. & Mandelkow, E.M. 2002, "Tau blocks traffic of organelles, neurofilaments, and APP vesicles in neurons and enhances oxidative stress", *The Journal of cell biology*, vol. 156, no. 6, pp. 1051-1063.
- Steffens, A.A., Hong, G.M. & Bain, L.J. 2011, "Sodium arsenite delays the differentiation of C2C12 mouse myoblast cells and alters methylation patterns on the transcription factor myogenin", *Toxicology and applied pharmacology*, vol. 250, no. 2, pp. 154-161.
- Sullivan, L.B., Martinez-Garcia, E., Nguyen, H., Mullen, A.R., Dufour, E., Sudarshan, S., Licht, J.D., Deberardinis, R.J. & Chandel, N.S. 2013, "The proto-oncometabolite fumarate binds glutathione to amplify ROS-dependent signaling", *Molecular cell*, vol. 51, no. 2, pp. 236-248.
- Suva, M.L., Riggi, N. & Bernstein, B.E. 2013, "Epigenetic reprogramming in cancer", *Science (New York, N.Y.)*, vol. 339, no. 6127, pp. 1567-1570. Review.
- Szkudelski, T. 2001, "The mechanism of alloxan and streptozotocin action in B cells of the rat pancreas", *Physiological research*, vol. 50, no. 6, pp. 537-546.
- Takahashi, A., Ohtani, N., Yamakoshi, K., Iida, S., Tahara, H., Nakayama, K., Nakayama, K.I., Ide, T., Saya, H. & Hara, E. 2006, "Mitogenic signalling and the p16INK4a-Rb pathway cooperate to enforce irreversible cellular senescence", *Nature cell biology*, vol. 8, no. 11, pp. 1291-1297.
- Talbot, L.J., Bhattacharya, S.D. & Kuo, P.C. 2012, "Epithelial-mesenchymal transition, the tumor microenvironment, and metastatic behavior of epithelial malignancies", *International journal of biochemistry and molecular biology*, vol. 3, no. 2, pp. 117-136. Review.

- Teixeira, F.K., Sanchez, C.G., Hurd, T.R., Seifert, J.R., Czech, B., Preall, J.B., Hannon, G.J. & Lehmann, R. 2015, "ATP synthase promotes germ cell differentiation independent of oxidative phosphorylation", *Nature cell biology*, vol. 17, no. 5, pp. 689-696.
- Teslaa, T. & Teitell, M.A. 2015, "Pluripotent stem cell energy metabolism: an update", *The EMBO journal*, vol. 34, no. 2, pp. 138-153. Review.
- Tormos, K.V., Anso, E., Hamanaka, R.B., Eisenbart, J., Joseph, J., Kalyanaraman, B. & Chandel, N.S. 2011, "Mitochondrial complex III ROS regulate adipocyte differentiation", *Cell metabolism*, vol. 14, no. 4, pp. 537-544.
- Vacirca, D., Delunardo, F., Matarrese, P., Colasanti, T., Margutti, P., Siracusano, A., Pontecorvo, S., Capozzi, A., Sorice, M., Francia, A., Malorni, W. & Ortona, E. 2012, "Autoantibodies to the adenosine triphosphate synthase play a pathogenetic role in Alzheimer's disease", *Neurobiology of aging*, vol. 33, no. 4, pp. 753-766.
- Valenta, T., Hausmann, G. & Basler, K. 2012, "The many faces and functions of beta-catenin", *The EMBO journal*, vol. 31, no. 12, pp. 2714-2736. Review.
- Valle, A., Oliver, J. & Roca, P. 2010, "Role of uncoupling proteins in cancer", *Cancers*, vol. 2, no. 2, pp. 567-591. Review.
- van Lunteren, E. & Moyer, M. 2007, "Oxidoreductase, morphogenesis, extracellular matrix, and calcium ion-binding gene expression in streptozotocin-induced diabetic rat heart", *American journal of physiology. Endocrinology and metabolism*, vol. 293, no. 3, pp. E759-68.
- Vencio, E.F., Nelson, A.M., Cavanaugh, C., Ware, C.B., Milller, D.G., Garcia, J.C., Vencio, R.Z., Loprieno, M.A. & Liu, A.Y. 2012, "Reprogramming of prostate cancer-associated stromal cells to embryonic stem-like", *The Prostate*, vol. 72, no. 13, pp. 1453-1463.
- Viale, A., Pettazoni, P., Lyssiotis, C.A., Ying, H., Sanchez, N., Marchesini, M., Carugo, A., Green, T., Seth, S., Giuliani, V., Kost-Alimova, M., Muller, F., Colla, S., Nezi, L., Genovese, G., Deem, A.K., Kapoor, A., Yao, W., Brunetto, E., Kang, Y., Yuan, M., Asara, J.M., Wang, Y.A., Heffernan, T.P., Kimmelman, A.C., Wang, H., Fleming, J.B., Cantley, L.C., DePinho, R.A. & Draetta, G.F. 2014, "Oncogene ablation-resistant pancreatic cancer cells depend on mitochondrial function", *Nature*, vol. 514, no. 7524, pp. 628-632.
- Vicent, D., Piper, M., Gammeltoft, S., Maratos-Flier, E. & Kahn, C.R. 1998, "Alterations in skeletal muscle gene expression of ob/ob mice by mRNA differential display", *Diabetes*, vol. 47, no. 9, pp. 1451-1458.
- Walker, J.E. 2013, "The ATP synthase: the understood, the uncertain and the unknown", *Biochemical Society transactions*, vol. 41, no. 1, pp. 1-16.
- Walker, J.E., Lutter, R., Dupuis, A. & Runswick, M.J. 1991, "Identification of the subunits of F1F0-ATPase from bovine heart mitochondria", *Biochemistry*, vol. 30, no. 22, pp. 5369-5378.

- Wallace, D.C. 2012, "Mitochondria and cancer", *Nature reviews.Cancer*, vol. 12, no. 10, pp. 685-698. Review.
- Wang, L., Zhu, H., Wu, J., Li, N. & Hua, J. 2014, "Characterization of embryonic stem-like cells derived from HEK293T cells through miR302/367 expression and their potentiality to differentiate into germ-like cells", *Cytotechnology*, vol. 66, no. 5, pp. 729-740.
- Warburg, O. 1956, "On the origin of cancer cells", *Science (New York, N.Y.)*, vol. 123, no. 3191, pp. 309-314.
- Warburg, O., Wind, F. & Negelein, E. 1927, "The Metabolism of Tumors in the Body", *The Journal of general physiology*, vol. 8, no. 6, pp. 519-530.
- Wei, H., Liu, L. & Chen, Q. 2015, "Selective removal of mitochondria via mitophagy: distinct pathways for different mitochondrial stresses", *Biochimica et biophysica acta*, vol. 1853, no. 10 Pt B, pp. 2784-2790.
- Welle, S., Brooks, A.I., Delehanty, J.M., Needler, N. & Thornton, C.A. 2003, "Gene expression profile of aging in human muscle", *Physiological genomics*, vol. 14, no. 2, pp. 149-159.
- Wheaton, W.W. & Chandel, N.S. 2011, "Hypoxia. 2. Hypoxia regulates cellular metabolism", *American journal of physiology.Cell physiology*, vol. 300, no. 3, pp. C385-93.
- Wu, Z., Puigserver, P., Andersson, U., Zhang, C., Adelmant, G., Mootha, V., Troy, A., Cinti, S., Lowell, B., Scarpulla, R.C. & Spiegelman, B.M. 1999, "Mechanisms controlling mitochondrial biogenesis and respiration through the thermogenic coactivator PGC-1", *Cell*, vol. 98, no. 1, pp. 115-124.
- Xu, X., Duan, S., Yi, F., Ocampo, A., Liu, G.H. & Izpisua Belmonte, J.C. 2013, "Mitochondrial regulation in pluripotent stem cells", *Cell metabolism*, vol. 18, no. 3, pp. 325-332. Review.
- Yang, J., Mani, S.A., Donaher, J.L., Ramaswamy, S., Itzykson, R.A., Come, C., Savagner, P., Gitelman, I., Richardson, A. & Weinberg, R.A. 2004, "Twist, a master regulator of morphogenesis, plays an essential role in tumor metastasis", *Cell*, vol. 117, no. 7, pp. 927-939.
- Yang, M., Soga, T. & Pollard, P.J. 2013, "Oncometabolites: linking altered metabolism with cancer", *The Journal of clinical investigation*, vol. 123, no. 9, pp. 3652-3658. Review.
- Yechoor, V.K., Patti, M.E., Saccone, R. & Kahn, C.R. 2002, "Coordinated patterns of gene expression for substrate and energy metabolism in skeletal muscle of diabetic mice", *Proceedings of the National Academy of Sciences of the United States of America*, vol. 99, no. 16, pp. 10587-10592.
- Yechoor, V.K., Patti, M.E., Ueki, K., Laustsen, P.G., Saccone, R., Rauniyar, R. & Kahn, C.R. 2004, "Distinct pathways of insulin-regulated versus diabetes-regulated gene expression: an in vivo analysis in MIRKO mice", *Proceedings of the*

National Academy of Sciences of the United States of America, vol. 101, no. 47, pp. 16525-16530.

Yen, Y.P., Tsai, K.S., Chen, Y.W., Huang, C.F., Yang, R.S. & Liu, S.H. 2010, "Arsenic inhibits myogenic differentiation and muscle regeneration", *Environmental health perspectives*, vol. 118, no. 7, pp. 949-956.

Yeung, T.M., Gandhi, S.C., Wilding, J.L., Muschel, R. & Bodmer, W.F. 2010, "Cancer stem cells from colorectal cancer-derived cell lines", *Proceedings of the National Academy of Sciences of the United States of America*, vol. 107, no. 8, pp. 3722-3727.

Zeisberg, M. & Neilson, E.G. 2009, "Biomarkers for epithelial-mesenchymal transitions", *The Journal of clinical investigation*, vol. 119, no. 6, pp. 1429-1437. Review.

Zhang, B.B., Wang, D.G., Guo, F.F. & Xuan, C. 2015, "Mitochondrial membrane potential and reactive oxygen species in cancer stem cells", *Familial cancer*, vol. 14, no. 1, pp. 19-23.

Zhang, J., Khvorostov, I., Hong, J.S., Oktay, Y., Vergnes, L., Nuebel, E., Wahjudi, P.N., Setoguchi, K., Wang, G., Do, A., Jung, H.J., McCaffery, J.M., Kurland, I.J., Reue, K., Lee, W.N., Koehler, C.M. & Teitell, M.A. 2011, "UCP2 regulates energy metabolism and differentiation potential of human pluripotent stem cells", *The EMBO journal*, vol. 30, no. 24, pp. 4860-4873.

Zhang, L., Marsboom, G., Glick, D., Zhang, Y., Toth, P.T., Jones, N., Malik, A.B. & Rehman, J. 2014, "Bioenergetic shifts during transitions between stem cell states (2013 Grover Conference series)", *Pulmonary circulation*, vol. 4, no. 3, pp. 387-394. Review.

Zhang, L., Yu, C., Vasquez, F.E., Galeva, N., Onyango, I., Swerdlow, R.H. & Dobrowsky, R.T. 2010, "Hyperglycemia alters the schwann cell mitochondrial proteome and decreases coupled respiration in the absence of superoxide production", *Journal of proteome research*, vol. 9, no. 1, pp. 458-471.

10 SUPPLEMENTS

Supplement 1. Sequences of the probes used in Northern blot

2Ad (213 bp) – Aldolase A (identity 98%)

GACCGCTTGTCAAGGAAAGTACACTCCAAGTGGCCAGTCTGGAGCCGCAGCCAG
TGAATCTCTTTCATCTCTAACCATGCCTACTAACCAGAGCTGATCTAAGGCTGCT
CCATCGACACTCCAGGCCCTGCCTACCCACTTGCTATTGAAGAGGGGCCCTTCAG
GCTCTTTCCCAACCCTCTTGCTGCCCTCGTGTGTCAGTGTTGTCTGTGAATGCTAA
ATCTGCCATCCCTTCCAGCCCACTGCCAATAAACAGCTATTTAAGGGGGTGTCAA
AAAAAAAAAAAAA

13Cc2 (303 bp) – Nme2 (identity 87%)

AGTTAGGCACCATTTCGTGGGGATAGNTGCAAATCAAGTCGGCAGCGAACATCAT
TCACGGCAGTGATTCAGTAGGAGAGTGCCGAGAAAGAGATCTGGTACTATGGTT
TAAGCCCGAAGAACTGATTGACTATAAGTCTTGTAGCCCATGGACTGGGCAGTA
TAAGTCGACGAGGCAAAAACCAGAAGTACTTTTCAGCACTACTGATGGGGTTCA
TGAACACAGATAGGCATCCCACTGACTGAATAGACCATCGTTTAATAAAACAATT
AAGACTTTAAAAC TGCAAAAAAACACAAAAA

13Cc1 (312 bp) – Atp6V0d1 (identity 95%)

AGTTAGGCACCTTTCCCTAGTCAAGAATGGACCAAGATCCCCTCTAGAGCAAAA
AAGGAACCCAGCCCTATGTTTACAGCCACTGACATGTCTAAGAACTGAGTGAC
TTTTATGTCCCTCCCTAACCTGAGAACCCTGGGGACAGTTTCCATTCTGTCTTA
GGTCATTCCCAGAACCATGACCTGTGGGAAAAATAGAGAATATGTATACTTGGG
GTATTGGAAGCAGCAACTGCAGCCCTCTCCATCAGCTCTGCCCTCTGAGACA
ATAAAATTGCCCTCTTTAAAAGAAAAA

12Gd (314 bp) – Nnt (identity 99%)

TGCTGACCTGTTCTCTTGCATTTTAGCCGTAGTCTGGATTGATCATGCCAATTCCA
TATCAGGTTTTTAGCCTTCACTCTAGACTCTAGATTCCAAAGACCTATTTTCTCAC
TTCTATTTAATATGTAGAAGATCTAGATAGTCTAAGTAATAACTTAAAAGGAAT
AAGTTGTATTTTTAAAAGTCCCATGCCAATTGGTCTCTTTAATTTCAATCAATTAA
GTGCTCTTGAATGGTCTGTATTAAGTGTCTTGAATGGAATGCAACCATTTGAGT
AATAAATGAGTTCATCATGTTCCCAAAAAAAAAAAAAA

13Gc4 (242 bp) – Ndufs2 (identity 97%)

AGTTAGGCACCCAGGATCTTGTATTTGGAGAAATAGACCGATGAGCAAAAGCAC
AGCCTGTGAGCTCCCTTGCCTGTCAGCTGCTTCATCGAGCGAGGCCTTTGTGAG
GGTGGGAAACGAGGCTGTGTTTCAGCAAACATACATGTA CTCTGTTGACTTAGCT
GCACAGGCTTTCTGTGCATGTACTNNAAGGAGAAATTATATTAATTAGCCAC
CTTTGGCCCCCAAAAAAAAAAAAAA

3Gc6 (221 bp) – Cox7c (identity 99%)

AGGTGACCGTGTACTTTGGATCTGGATTTGCTGCTCCTTTCTTTATAGTAGGGCA
CCAGCTACTTAAAAATAAGGATATTTAATTCATCCCATTAACAGAATGAAGAAA
GTTTAAGAGATATGATCTGGAACTGGATTAACTCTTGA ACTCTTATACTAGAA
AAAAATGTAATAAACTAATGATATAAATATTTAATGCCAAAAAAAAAAAAAAAAA

9Ac4 (246 bp) – Atp5a1 (identity 98%)

CGGGCAATATTCAGGTCTGATGGGAAAATCTCAGAACAGTCGGATGCAAAGCTG
AAGGNAATCGTAACAACTTCTTGGCTGGGTTTGAACCTTAAAGCCCTNCCACTG
TCACCAGACACTGCTTTGGTTTTGTCATTTATTGTGGTAAAATCAGCACCATTTGT
AAAGGTTTACTCTTGTACTCCCTGATGTACAGAAATCACATGAATAAAAGTTCCA
TATTGAGTGAAAAAAAAAAAAAAAAA

8Gd (213 bp) – PP1G (identity 98%)

GGATTGTGCGGTGACATTGAGGCTTATAAATCAAAGGAACTAACTTGCCGTCC
ACCGGTTTATACAGAACTCACAGTATCTATGACTTTTTTAACTACGACCTGTTAA
AATGAATCCGTTTCCACAGATGCCCGTGTACAATGCCATGTGCTAAGAATGATTT
CAGACTTATTAATGCGAGCTTGTTAACCTGCCAAAAAAAAAAAAAAAAA

20Cc2 (228 bp) – DAPIT (identity 100%)

GTGATCGGACGAAGAAGATTGAAGTCATGGCTGGCCCAGAAAGTGATGGCCAA
TTCCAGTTCACTGGTATTAATAAATATTTCAACTCTTATACCCTCACAGGTAGAAT
GAATTGTGTCTGGCCACATATGGAGGCATTGCTTTGTTGGTCCTATACTTTAAG
TTAAGGCCTAAAAAACCCCAGCTGTGAAAGCAACATAAATGGATTTTGAAATGT
CTGGCCTTATCTGTAAAGTCCCACGCCTGAAGAAGCTGATGTGAACTCATCATGT
AATACTCAATTTGTACAATAAATTATGAACCTGGAAAAAAAAAAAAAAAA

13Gc2(1) (255 bp) – YEATS4 (identity 99%)

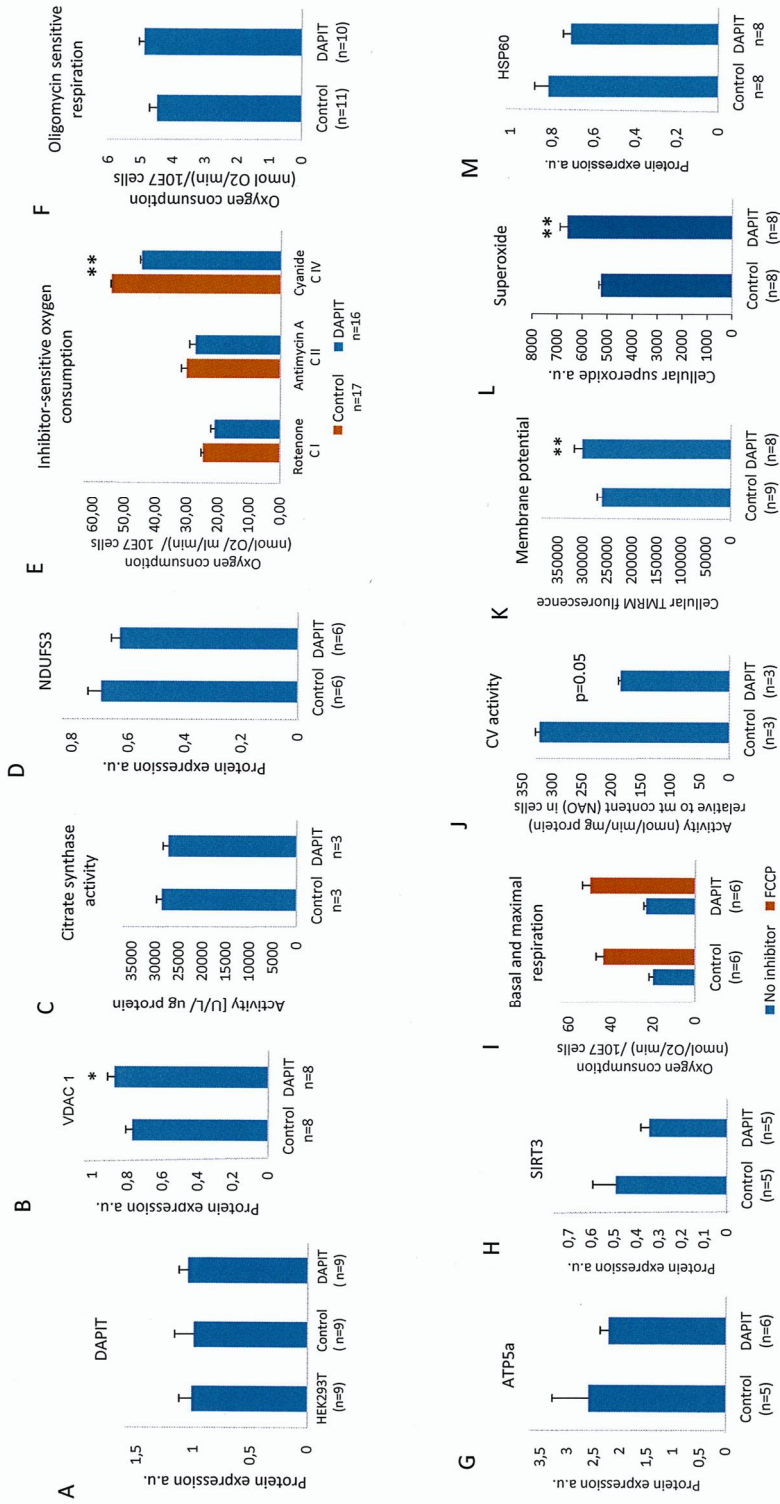
AGTTAGGCACAACCTTTTAAATTTTTGTTTTGTTTTTAAATTGAACTATATGTAT
AGTTTATTTTCCTTCGGGCAGGATTGAAAATTCTGTTATAAAGTCTTACTTGTGC
NGACTTTGTACTTCTCTACTATAGAATTAGTGATTAGTATGGTGTGTTAGTTCTT
CAGGCTCACGTCTGCCCCGCTACCTCTTTTGTATATGATGTGTCTAGGAAGTATT
TAATAAATGTTTACTGCTCCCAAAAAAAAAAAAAA

13Gc2(7) (257 bp) – OPTN (identity 96%)

AGTTAGGCACGAATATCACNTGATGTCTCTTACATGTGGACCCTGAAGAAACATA
GTTCATAGATATTGAGAGCTGAATAGTGGTTTGCAGGACAGGAGGGAAGGTGT
GGGAAGGGTGAGATGTTGCTCAAAGGTACGAAGTCTAGGAGGGATAAACTGTA
GTGATCTACTGTACCAGAGTGAAGTGAATAATTTGTATATTAAGGCTATATCCCC
AGTTTAGTAAACAACCTTGNNAAACCAAAAAAAAAAAAAA

6Gd2 (244bp) – Crb1 (identity 96%)

AATCGATGGAAGGATCACGGATACCAGAAGCTGCAGGTCTACTAGCTGTGGACC
CCAAGAAAGGCCTCTTGCTCTTCTGGGTGGCTGATGAAACAGTTCTCTGTGCC
TACGAGAGTTAGGACTATACCAGAAAGGCCTAAAAGCAGCGTGTGTATCCGTCA
TGCTCGTATCACAGCCTCAGTGTGTTTCATTATGGGATAGCTGAAATGAATAAAT
AGTATGTCTGGCCAAAAAAAAAAAAAAAA



Supplement 2. Mitochondrial metabolism (activity) of DAPIT cells at cellular level. Protein levels estimated by Western blot of (A) DAPIT and (B) VDAC. (C) Citrate synthase activity. (D) Protein level of NDUFS3. Inhibitor-sensitive oxygen consumption of (E) complexes I, II, IV and (F) complex V in digitonin-permeabilized and intact cells. Protein level of (G) ATP5a and (H) Sirt3. (I) Basal and maximal respiration. (J) H⁺-ATP synthase activity measured by spectrophotometric analysis. Mitochondrial (K) membrane potential and (L) superoxide levels at cellular level measured by flow cytometry of TMRM (200nM, 30', 37°C) and Mitosox (2.5 μM, 45', 37°C) stained cells. (M) Protein level of HSP60. The error bars are S.D. and asterisks indicate: **p<0.01.

11 ORIGINAL PUBLICATIONS

Cellular and tissue expression of DAPIT, a phylogenetically conserved peptide

H. Kontro,^{1,2} J.J. Hulmi,³ P. Rakkila,⁴ H. Kainulainen³

¹Institute of Biomedical Technology, University of Tampere

²Pediatric Research Center, University of Tampere;

³Department of Biology of Physical Activity, University of Jyväskylä;

⁴Department of Health Sciences, University of Jyväskylä, Finland

Abstract

DAPIT (Diabetes Associated Protein in Insulin-sensitive Tissues) is a small, phylogenetically conserved, 58 amino acid peptide that was previously shown to be down-regulated at mRNA level in insulin-sensitive tissues of type 1 diabetes rats. In this study we characterize a custom made antibody against DAPIT and confirm the mitochondrial presence of DAPIT on cellular level. We also show that DAPIT is localized in lysosomes of HUVEC and HEK 293T cells. In addition, we describe the histological expression of DAPIT in several tissues of rat and man and show that it is highly expressed especially in cells with high aerobic metabolism and epithelial cells related to active transport of nutrients and ions. We propose that DAPIT, in addition to indicated subunit of mitochondrial F-ATPase, is also a subunit of lysosomal V-ATPase suggesting that it is a common component in different proton pumps.

Introduction

DAPIT is a 58 amino acid peptide, which was previously discovered in insulin-sensitive tissues of rats that were rendered diabetic by streptozotocin.¹ Afterwards, it was shown that it is a component of mitochondrial ATP synthase^{2,3} (also called F-ATPase) and regulates ATP synthase population in mitochondria.⁴ DAPIT is the protein product of *Usmg5* (also called *Dapit*) gene that is conserved from insects to vertebrates. It contains a single presumed α -helix spanning from amino acid 23 to 45. The predicted length of the α -helix varies marginally (1-3 amino acids), depending on the software used. In addition, DAPIT has a poor but recognizable similarity with a putative yeast ortholog.³ This similarity over the species depicts the conceivable importance

and conserved function of DAPIT. The chromosomal location of *Usmg5* gene is 1q54 in rat, 19D1 in mouse and 10q24 in man.

Since proteomics approach has identified DAPIT as a subunit of F-ATPase,^{2,3} we wanted to confirm this result on cellular level in human and rodent cells. F-ATPase and vacuolar-ATPase (V-ATPase) are related to each other structurally and mechanistically wise,^{5,6} therefore, we also studied the DAPIT involvement with V-ATPase by immunofluorescence. We previously investigated the mRNA expression of DAPIT in insulin-sensitive tissues of normal and streptozotocin diabetic rats;¹ in the present study we investigated the DAPIT protein expression in this type 1 diabetic model and show its histological expression in several normal rat and human tissues. Based on the results of all these studies, we confirm the mitochondrial location of DAPIT and show its new localization in lysosomes containing V-ATPase. In addition, we describe DAPIT expression in the insulin-sensitive tissues of diabetic rat and mouse, and its histological expression in several rat and human tissues.

Materials and Methods

DAPIT antibody

For the detection of DAPIT, polyclonal IgG antibodies α D15N and α D15C against the amino- and carboxyterminal peptides (MAGPESDGGQFQTGI and YFKLRPKKTPAVKAT, respectively) of rat DAPIT were raised in rabbits (Davids Biotechnologie, Regensburg, Germany). The animals were immunized once intra-dermally followed by four intra-muscular immunizations. The sera were collected for the affinity purification of IgG. The concentrations of affinity purified IgG fractions were determined by ELISA being 0.38 mg/mL for α D15N and 0.16 mg/mL for α D15C. All the experiments utilizing these antibodies were repeated three times, except the Western blot of rat and mouse tissues. This was repeated twice with two pairs of control and diabetic rats and 2-3 times with mouse samples.

Animals and human samples

The control and streptozotocin diabetic rats were described previously.¹ Diabetes was confirmed by serum glucose that was >600 mg/dL 7 days after the injection of streptozotocin (STZ). The control and STZ-mice were reported in detail elsewhere.⁷ Human tissue samples were collected during resection of carcinomas. Healthy appearing pieces of the liver adenocarcinoma sample of a 48-year-old female and kidney clear cell carcinoma of a 68-year-old male were used for immunohistochemistry.

Correspondence: Prof. Heikki Kainulainen, Department of Biology of Physical Activity, University of Jyväskylä, PO Box 35, FIN-40014. Tel. +358.50.3302901 – Fax: +358.14.2602071. E-mail: Heikki.Kainulainen@sport.jyu.fi

Key words: DAPIT, mitochondrion, V-ATPase, type 1 diabetes.

Acknowledgments: this work was supported by the *Competitive Research Funding* of the Pirkanmaa Hospital District, the *Diabetes Research Foundation*, the *Finnish Cultural Foundation*, *Pirkanmaa Regional fund*, and the *Academy of Finland*. The authors would like to thank Eric Dufour for his critical view of the manuscript and Marja-Leena Koskinen for her skillful technical assistance.

Contributions: HKa, HKo, study design, coordination, cell and rat experiments planning and carrying out, manuscript drafting; JJH, mouse protein studies carrying out; PR, mouse microscopy. All authors read and approved the final manuscript.

Conflict of interests: the authors declare no conflict of interests.

Received for publication: 12 December 2011.

Accepted for publication: 13 March 2012.

This work is licensed under a Creative Commons Attribution NonCommercial 3.0 License (CC BY-NC 3.0).

©Copyright H. Kontro et al., 2012

Licensee PAGEPress, Italy

European Journal of Histochemistry 2012; 56:e18

doi:10.4081/ejh.2012.e18

Cell lines and cell culture

Human embryonic kidney-derived HEK 293T cells were a kind gift from the laboratory of Howard T. Jacobs, Institute of Biomedical Technology, Tampere, Finland. The cells were cultured in Dulbecco's modified Eagle medium (Sigma-Aldrich, Ayshire, UK, or Gibco brl, Paisley, Scotland, UK), containing 4.5 g/L of D-glucose, 10% foetal calf serum (Sigma), 50 μ g/mL uridine, 1 mM sodium pyruvate, 2 mM L-glutamine, and 100 U penicillin and 100 μ g/mL of streptomycin (Gibco) at 37°C in an incubator with 5% CO₂ in air. Mouse myoblasts (C2C12) were a kind gift from Antero Salminen, University of Kuopio, Finland. These cells were maintained in Dulbecco's modified Eagle's medium (DMEM/F12, Gibco) containing 4.5 g/L D-glucose, 10% foetal calf serum, 0.075% sodium bicarbonate (Gibco), and 100 U penicillin and 100 μ g/mL streptomycin. Cells were passaged routinely every 3-4 days at 1:10 and 1:4 dilution. HEK 293T cells were detached by pipetting and C2C12 by treat-

ment with Trypsin-EDTA (Gibco). Human Umbilical Vein Endothelial Cells (HUVEC) were purchased from Lonza (Cambrex Bio Science, Walkersville, MD, USA), maintained in HuMedia-EGM™ (EGM-1) (Clonetics®, San Diego, CA, USA) and subdivided 1:6 when confluent. In all experiments performed, the cells were used between passages 2 and 6.

All cells were seeded on cover slips or in culture slides (BD Biosciences, Erembodegem, Belgium) one to three day prior to use. The glassware was coated with 20% poly-L-lysine (Sigma) when needed.

Fluorescence microscopy

For the staining of mitochondria and lysosomes, the cells were washed with PBS and incubated in a medium containing 100 nM Mitotracker Red or LysoTracker Red (Invitrogen Molecular Probes, Leiden, The Netherlands) for 10-30 min at 37°C. After washing, normal medium was added to the Mitotracker stained cells and incubated for further 30-60 min at 37°C. For transient translation of amino- and carboxyterminal fusion proteins of DAPIT and GFP in HEK 293T cells, DAPIT was cloned into pEGFP-N3 and pEGFP-C1 vectors (Clontech Laboratories, Palo Alto, CA, USA). In immunofluorescence, the Tris Buffered Saline-Tween (TBS-T) (10 mM Tris, 0.9% NaCl, pH 8.0, 0.1% Tween 20, Sigma) was used. The cells were fixed at room temperature with 4% paraformaldehyde (Sigma) for 15 min, permeabilized with 0.5% Triton X-100 (Sigma) for 10 min and blocked with 5% w/v non-fat milk powder and 2% BSA (Sigma) for 30 min. The cells were single- or double-stained with the rabbit polyclonal antibody against DAPIT (reported above, α D15N 1:800, α D15C 1:320 and antibodies preincubated overnight at 4°C with 4x excess of peptide of issue) and goat

polyclonal antibody against V-ATPase subunit H (SC-21228, Santa Cruz, CA, USA, 1:800) for 2 h. After intensive washing with TBS-T the primary antibodies were detected by donkey anti-

rabbit IgG conjugated with Alexa Fluor 488 (Invitrogen, 1:4000) and donkey anti-goat IgG conjugated with Alexa Fluor 555 (Invitrogen, 1:4000) for 1 h. After washes the coverslips

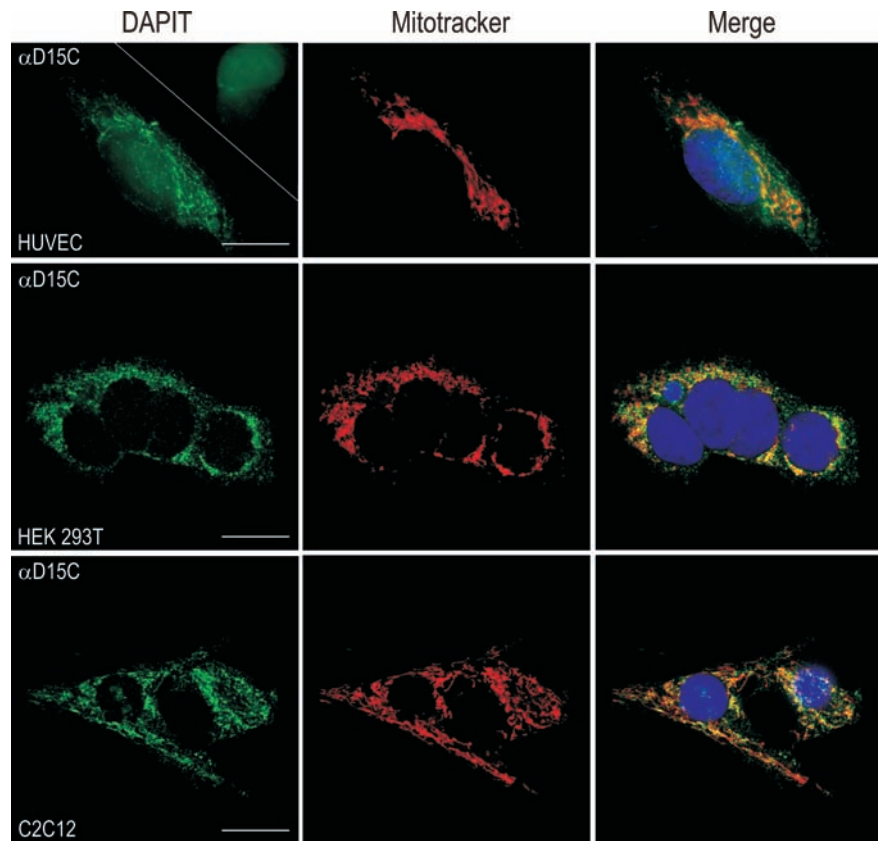


Figure 1. DAPIT locates into mitochondria in HUVEC, HEK 293T and C2C12 cells. In the upper right corner of the green picture in HUVEC is shown the staining with peptide-blocked C-terminal antibody. The pictures of HUVEC cells were taken by traditional fluorescence microscope, and the ones of HEK 293T and C2C12 cells by confocal microscope. Nuclei-staining with DAPI. Scale bars 25 μ m.

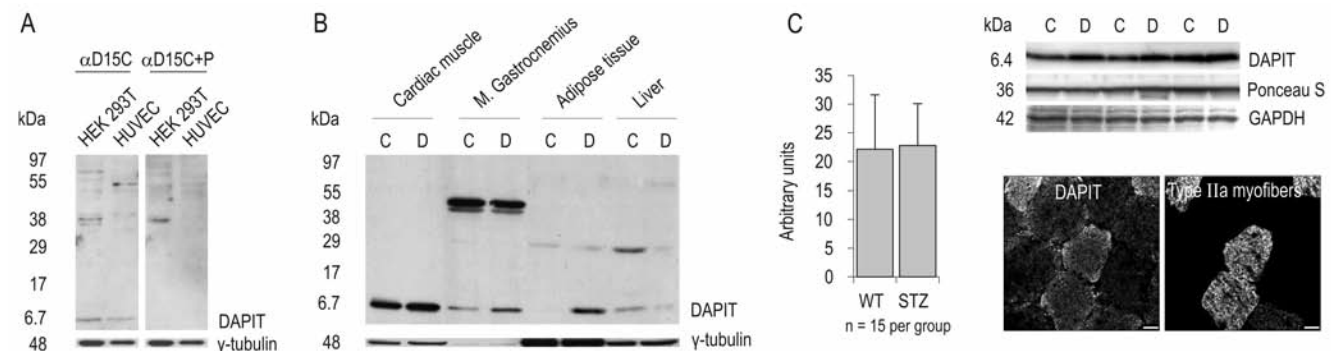


Figure 2. DAPIT expression in protein level. SDS-PAGE with: A) antibody and peptide-blocked antibody against DAPIT; B) healthy and early stage diabetic insulin-sensitive tissues of rat; C) DAPIT in healthy and STZ-induced diabetic insulin-sensitive calf muscle complex of mice (C, control; D, diabetic). Cross-section of mouse skeletal muscle shows more DAPIT in type IIa (highly oxidative) myofibers, which contain more mitochondria, than other myofibers. Scale bars: 20 μ m.

were mounted on slides using Vectashield mounting medium (Vector Laboratories, Burlingame, CA, USA). All samples were examined at 100x magnification by confocal microscopy, using a Perkin Elmer-Cetus/Wallac UltraView LCI system (Wellesly, MA, USA) equipped with appropriate excitation and emission filters and an Andor iXon DV885 EMCCD camera and the Andor iQ software (Andor, Belfast, UK), or a traditional fluorescence microscope, ColorView III camera and the Cell imaging software (Olympus BX60, Olympus Corp., Tokyo, Japan). Images were further processed using Corel Photo-Paint 11 (Corel Corp., Ottawa, ON, Canada).

Ten micrometer thick cryosections from mouse *gastrocnemius* muscle were fixed with 4% PFA for 15 min, permeabilized with 0.5% Triton-X100 for 10 min and blocked with 3% BSA for 1 h. Sections were double-stained with a mouse monoclonal antibody against fast myosin type II a developed by Dr. H.M Blau⁸ (SC-71, Developmental Studies Hybridoma Bank, University of Iowa, Iowa City, USA, 1:50) to detect most oxidative fibers and C-terminal rabbit polyclonal DAPI antibody (*see above*) for 1 h at room temperature. After intensive washing with PBS the primary antibodies were detected by a mixture of goat anti-mouse antibody conjugated with Alexafluor 488 (Invitrogen, 1:400) and the polyclonal antibody with goat anti-rabbit antibody conjugated with Alexafluor 546 (Invitrogen, 1:400) for 1 h. After washing with PBS the sections were mounted with Mowiol (Sigma) including 2.5% DABCO (Sigma). The samples were viewed with Olympus BX 51 epifluorescence microscope. Images were captured by ColorView III camera and Analysis Five software (Olympus Corp.).

Immunohistochemistry

Sections of paraffin-embedded tissues from the rat myocardium, skeletal muscle, adipose tissue, liver, kidney, brain and small bowel, and human liver and kidney were used for immunohistochemical staining applying the standard immunoperoxidase method. Briefly, 4 μ m thick paraffin sections were cut and deparaffinized. The antigen retrieval of the sections was performed by boiling in a microwave oven for 15 min in 0.01 M citrate buffer (pH 6.0) followed by cooling to room temperature. After washing in PBS, non-specific binding sites were blocked by incubating the sections in normal goat serum for 1 h. Subsequently, the sections were incubated overnight at 4°C with α D15C antibody (dilution 1:150-1:200) followed by an incubation in the secondary antibody (biotinylated anti-rabbit IgG, Vector Laboratories, 1:100) for 30 min. Endogenous peroxidase activity was removed using 0.3%

H₂O₂ for 30 min. ABC-reaction was done with the Vectabond TM reagent (Vector Laboratories) for 30 min at room temperature. Antigen-antibody complexes were visualized using diaminobenzidine (DAB DacoCytomation Inc., Carpinteria, CA, USA) as the chromogen. Finally, the sections were counterstained with Mayer's hematoxylin (Merck KGaA, Darmstadt, Germany), washed with tap water, dehydrated and mounted with Pertex mounting medium. Sections incubated with the peptide-blocked antibody or without the primary antibody served as negative controls.

Western blot analysis

The expression level of DAPIT was studied by Western blot in HEK 293T and HUVEC cells, in healthy and diabetic rat myocardium and *m. gastrocnemius*, epididymal adipose tissue and liver, and also in mouse calf muscle complex (*gastrocnemius*, *soleus*, *plantaris*). The tissue samples were incubated or homogenized in 0.5 ml of buffer containing (1% Triton X100 in standard PBS, protease inhibitor mixture (Roche Applied Science, Rotkreuz, Switzerland) and 3 mM phenylmethylsulfonyl fluoride (PSMF) (Calbiochem/Merck) followed by an incubation on ice for 30 min and centrifugation at 12,000 g for 1 min. The cells from confluent 100x20mm cell culture dishes were treated in a similar way without homogeniza-

tion.

The protein concentration was determined by Bradford method. Twenty μ g (rat and cellular) and 30 μ g (mouse) of protein, was heated at 95 °C for 5 min in SDS-PAGE sample buffer⁹ prior to loading on the gel, run on 12% acrylamide SDS-PAGE according to standard protocol¹⁰ and blotted electrophoretically at 100 V for 1 h at 4°C to Hybond-C extra nitrocellulose membrane (Amersham Int. plc, Buckinghamshire, UK). Blots were blocked with TBS-T containing 5% freeze-dried fat-free milk powder for 1 h and incubated with primary antibody (α D15C 1:160 and peptide blocked antibody, mouse monoclonal antibody against γ -tubulin (T5326, Sigma) 1:4000, ATP synthase subunit alpha monoclonal antibody produced in mouse (MS502, Abcam, Eugene, OR, USA) 1:4000 and goat polyclonal IgG against cytochrome C (Sc-8385, Santa Cruz, CA, USA) 1:1000) for 2 h. After washings, the blots were incubated in the secondary antibody (peroxidase-conjugated swine anti-rabbit and rabbit anti-mouse (DAKO, Clostrup, Denmark) 1:2000, and Peroxidase Horse Anti-Goat IgG (H+L) (Vector Laboratories, 1:10000) for 1 h. Subsequently, the blots were washed and the signal was detected by enhanced chemiluminescent ECLTM reagent (Amersham Int.) according to the manufacturer's protocol. The blots were visualized on Super RX medical X-

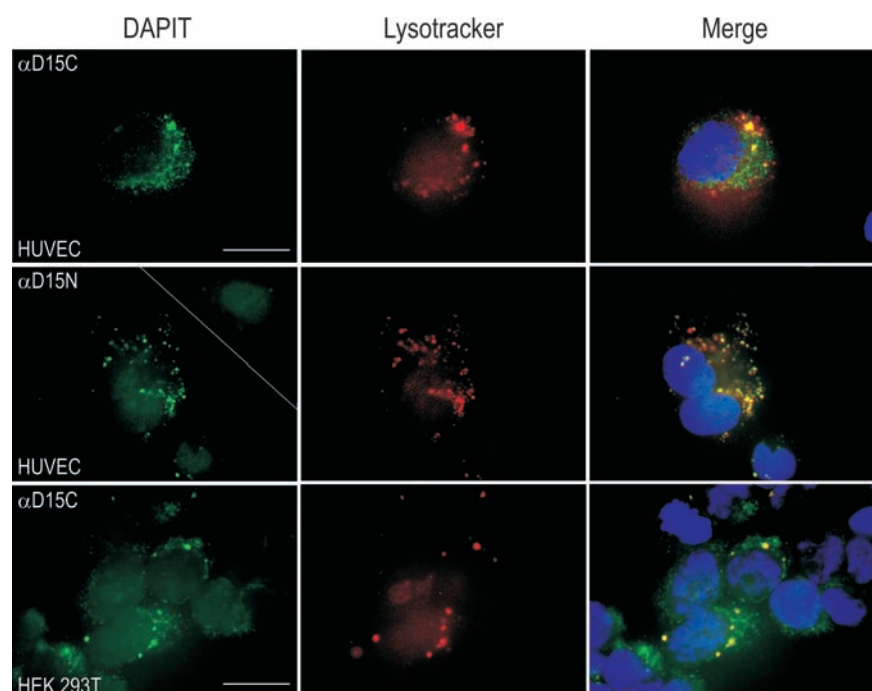


Figure 3. DAPI locates into lysosomes in HUVEC, HEK 293T and C2C12 cells. In the upper right corner of the green picture in the middle row is shown the staining with peptide-blocked N-terminal antibody. Nuclei-staining with DAPI. Scale bars: 25 μ m.

ray film (Fujifilm Corp., Tokyo, Japan) using 3–20 min exposure times.

Ethical permissions

Animal experiments were approved by the Animal Experimentation Committee of the University of Tampere and Jyväskylä. The Ethical Committee of Tampere University Hospital approved the use of human tissues.

Results

Specificity of α D15N and α D15C antibodies

We used a custom made α D15N and α D15C polyclonal antibody against amino- and carboxyterminus of DAPIT, a small, phylogenetically conserved protein. In transient transfection studies in HEK 293T cells, α D15C colocalized with DAPIT fused to the C-terminus of GFP and, respectively, α D15N recognized DAPIT fused to the N-terminus of GFP (*results not shown*).

We further studied the specificity of α D15C antibody by immunofluorescence microscopy in human HUVEC endothelial and HEK 293T kidney cells, and mouse C2C12 myocytes. Incubation of the cell samples with the antigen-blocked antibody abolished all DAPIT staining as shown in left upper panel in Figure 1. The cross-over reactions between anti-rabbit and anti-goat IgG secondary antibodies with the non-corresponding primary antibody were negative. The approximately 6.7 kDa band corresponding to the calculated molecular weight of DAPIT (6.407 kD) disappeared also in SDS-PAGE upon peptide blocking of the antibody (Figure 2A). The α D15N antibody was specific in HUVEC-cells by immunofluorescence (Figure 3, middle panel). The specificity of the C-terminal antibody was also studied by Western blot in rat cardiac and skeletal muscle (Figure 2B). The antibody recognized DAPIT in both muscle types. In skeletal muscle also a protein of ca 50 kDa was seen. All bands disappeared upon peptide blocking of the antibody. In mouse this size of protein was not detected.

Also DAPIT staining in histological samples was negative after the omission of secondary antibody and peptide-blocking of the α D15C confirming further the specificity of the α D15C antibody (Figure 4).

Cellular localization of DAPIT

We confirmed DAPIT localization to mitochondria by immunofluorescence in human and rodent cell lines. DAPIT colocalized with Mitotracker (*i.e.* mitochondria) in HUVEC, HEK 293T and C2C12 cells (Figure 1). Due to

the reported similarity of the structure of F-ATPase and V-ATPase, we studied DAPIT localization in vacuoles like lysosomes, which are known to contain a lot of hydrogen pumps. Our amino- and carboxyterminal antibodies against DAPIT colocalized with Lysotracker (Figure 3) and V-ATPase (Figure 5) in HUVEC and HEK 293T cells. The N-terminal antibody against DAPIT did not recognize the mitochondrial form of the protein in HUVEC cells, whereas in HEK 293T cells the antibody did not recognize any specific structures (*results not shown*). The vacuolar expression of DAPIT was more abundant in HUVEC than in HEK 293T cells. The lysosomal localization of DAPIT in both cell lines was also detected with N- and C-

terminal GFP-fusionproteins and with Lysotracker and antibodies against LAMP 24 h after transient transfections (*results not shown*).

Tissue expression of DAPIT

The expression of DAPIT was investigated in several healthy rat and human tissues by immunohistochemistry (Figure 4). The antibody against carboxyterminal end of the protein was used. The expression of DAPIT varied in intensity within a tissue and from one tissue to another, showing mainly cytoplasmic staining and also occasional staining in some nuclei. The expression in cytoplasm varied exhibiting both smeary and finely granular

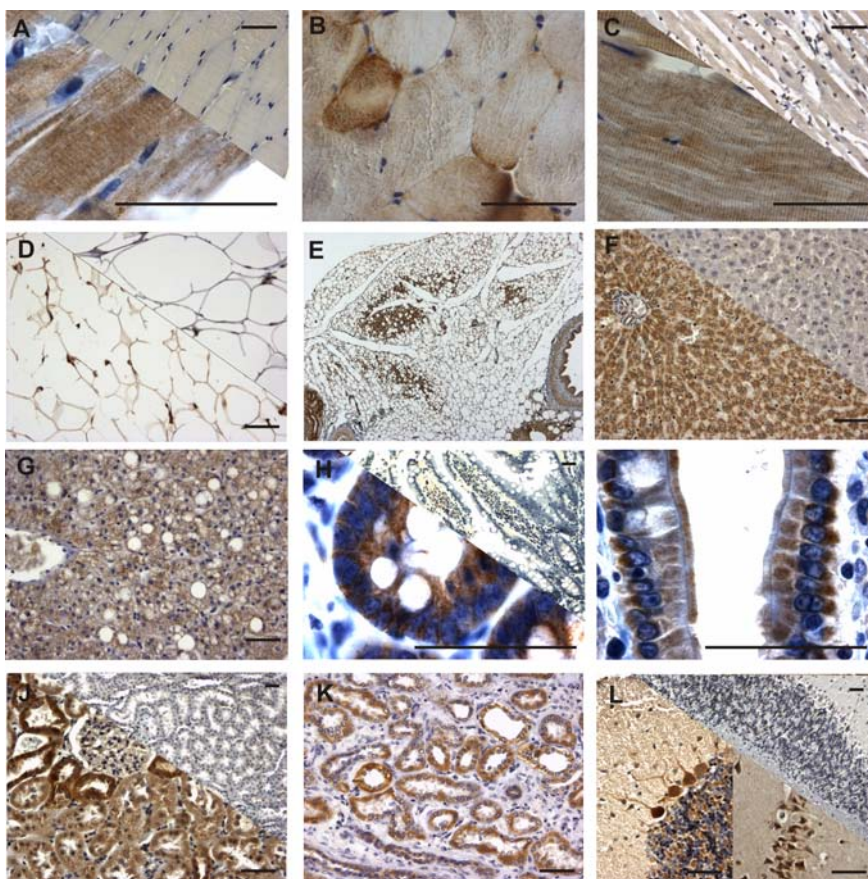


Figure 4. Immunohistochemical staining of DAPIT with α D15C antibody in rat and human tissues. Negative control stainings were performed using antigen-blocked antibody or by omitting the primary antibody (upper right corner of A, C, D, F, H, J and L). A,B) Myofibers of rat skeletal muscle; longitudinal section (A) shows sarcomere-like staining; in crosssections (B) differential staining of fibers is notable. C) In rat myocardium sarcomere-like staining was also seen. D,E) Adipocytes of rat epididymal adipose tissue (D) and adipose tissue surrounding kidney showed cytoplasmic staining; islands of brown adipose tissue (E) seen within the white adipose tissue were strongly stained. F) Rat and G) human hepatocytes showed granular cytoplasmic staining that was more intense in hepatocytes surrounding veins and bile ducts. H) Crypt and I) villus epithelial cells of the rat small intestine exhibited cytoplasmic and also some nuclear staining. In the villi the staining was seen specifically both in basal and apical sides of the nuclei. J) In the rat and K) human kidneys variable staining was seen in the epithelial cells of convoluted proximal tubules. L) In the rat, especially Purkinje cells of the cerebellum (left) and pyramidal neurons in the hippocampus were strongly stained. Scale bars: 50 μ m.

staining patterns.

In general, the strongest DAPIT expression was observed in insulin-sensitive and epithelial cells as well as in neurons. Cardiocytes and myofibers showed strong expression of DAPIT complying the sarcomeric structure (Figure 4A-C). Skeletal muscle cells showed considerable differences in their staining intensities. Double staining with type IIa-specific myosin antibody demonstrated that DAPIT was more abundant in highly oxidative (type IIa) than in less oxidative or glycolytic muscle fibers and located preferentially under the sarcolemma (Figure 2C). Adipocytes of white and brown adipose tissue (Figure 4D,E) showed distinct cytoplasmic staining that was considerably stronger in brown fat. In hepatocytes, granular cytoplasmic staining was observed (Figure 4F,G). This staining and granularity tended to be more intensive in the cells surrounding blood vessels and bile ducts. Epithelial cells of rat small intestine were stained from the base of the crypt to the villus tips showing also some nuclear staining (Figure 4H,I). The epithelial cells of proximal tubuli in kidney were intensively stained (Figure 4J,K) showing, however, considerable difference in staining intensity from cell to cell. Purkinje cells of cerebellum and pyramidal cells of hippocampus were

strongly stained in rat brain (Figure 4L). The stainings with the antibody against aminoterminal end of DAPIT were similar to those of the carboxyterminal antibody (*results not shown*).

Previously, we showed that DAPIT mRNA is down-regulated in the rat skeletal muscle and myocardium in streptozotocin-induced diabetes.¹ Here we studied first qualitatively the level of protein expression of DAPIT in insulin-sensitive tissues of two pairs of control and diabetic rats. We found that DAPIT was up-regulated in the diabetic myocardium, m. gastrocnemius and epididymal adipose tissue but down-regulated in the liver in the early stage of diabetes in rat (Figure 2B). We also found up-regulated DAPIT expression in diabetic *m. soleus* and down-regulation in *m. plantaris* (*results not shown*). Western blot showed also two tissue specific bands of ~50 kDa in skeletal muscle but not in the other tissues.

In contrast to rats, no changes in quantified expression of DAPIT was seen in comparing healthy and diabetic calf muscle complexes (gastrocnemius, soleus, plantaris) of mice with diabetes for 1-5 weeks (Figure 2C). Notably, however, DAPIT correlated well with the mitochondrial proteins cytochrome c ($r=0.450$, $P=0.014$) and ATP synthase subunit

alpha ($r=0.689$, $P\leq 0.001$) in mouse skeletal muscle.

Discussion

DAPIT is 58 amino acid peptide with single transmembrane helical span that in mRNA level is down-regulated in insulin-sensitive tissues in streptozotocin-induced diabetes.¹ In this study we show by peptide-blocking that our custom made antibody against aminoterminal end of DAPIT recognizes the vacuolar structures in immunofluorescence in HUVEC. The carboxyterminal antibody against DAPIT is specific in Western blot, immunofluorescence and immunohistochemistry. It recognizes the right size of the protein, the reported mitochondrial location of the protein, and also previously unreported vacuolar structures. However, in skeletal muscle of rat but not mouse, the carboxyterminal DAPIT antibody detected also a ~50 kDa protein. At the moment, protein databases do not recognize any proteins of greater size than DAPIT with the antigenic sequence used to raise the specific antibody. It remains to be shown if a still unknown longer isoform of DAPIT or an unknown skeletal muscle-specific protein exists. Therefore, it cannot be ruled out that the antibody detects also another protein in skeletal muscle in immunohistochemistry.

Previously, DAPIT was shown to associate with the ATP synthase from bovine heart mitochondria^{2,3} and suggested to contribute to the formation of this enzyme.² In the present study we confirmed the mitochondrial location of DAPIT in three different cell lines by immunofluorescence microscopy using the specific polyclonal antibody that was raised against the carboxy terminus of DAPIT. Significant correlations of DAPIT with cytochrome c and ATP synthase subunit alpha further supported the observed close association of DAPIT with mitochondria.

In addition, we could detect DAPIT also in other structures than mitochondria that prompted us to study its possible colocalization with other organelles. DAPIT colocalized abundantly with acidic organelles labelled by LysoTracker and antibody against V-ATPase in HUVEC and HEK 293T cells. Vacuolar ATPases are structurally and mechanistically related to mitochondrial F-ATPase.^{5,6} Both F-ATPase and V-ATPase consist of a membrane domain V_0 and a catalytic domain V_1 , and operate *via* rotary mechanism.¹¹ V-ATPases are ATP-driven proton pumps that acidify intracellular compartments and transport protons across the plasma membrane. V-ATPases have been identified *e.g.* in lysosomes, secretory vesicles and plasma membrane, and they are involved in

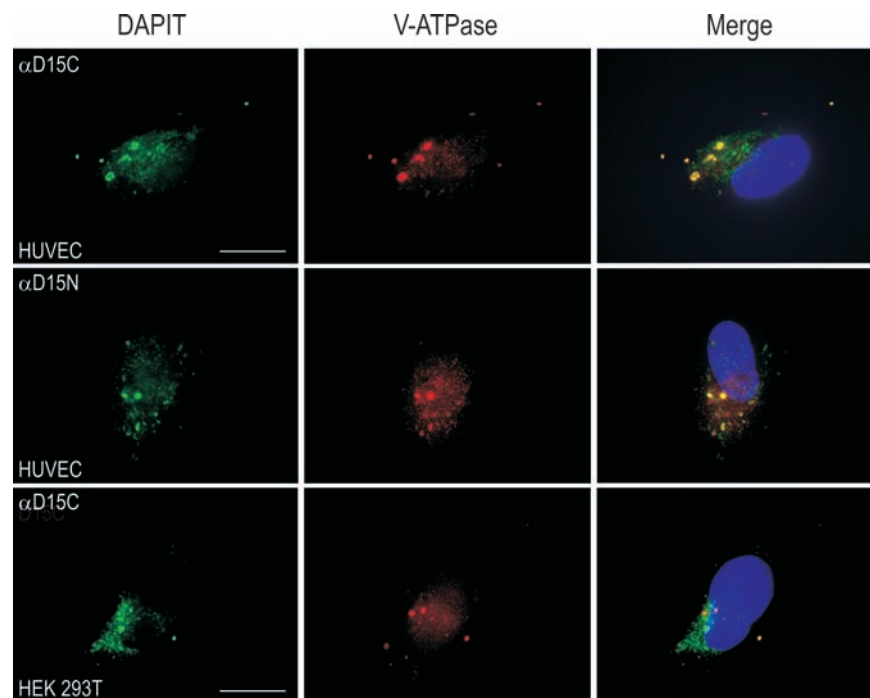


Figure 5. DAPIT locates into vacuoles containing V-ATPase in HUVEC and HEK 293T cells. Nuclei-staining with DAPI. Scale bars: 25 μ m.

various disease processes.¹² We ascertained by microscopy that DAPIT localizes to lysosomes, which are acidified by V-ATPase.

Our finding promotes the idea that DAPIT could be a component of V-ATPase complex. Since DAPIT has a predicted transmembrane helical span it presumably participates in the formation of the V_0 subunit of the proton pump. Our N-terminal antibody against DAPIT recognized vacuolar protein in HUVEC cells whereas the carboxyterminal both in HUVEC and HEK 293T cells. This suggests that different cell types may have variation in the structure of V-ATPase. Whether DAPIT is a mere structural component or it has a regulatory function in V-ATPases remains to be shown.

DAPIT amino acid sequence is conserved from the yeast to mammalia^{1,3} implying its fundamental significance for organisms. In histological studies, we showed the DAPIT expression in several healthy rat and human tissues. In all studied tissues DAPIT showed smeary and granular-type expression, which was most intensive in tissues known to contain copious mitochondria, such as cardiac and skeletal muscle cells and hepatocytes, and epithelial cells related to active transport of nutrients and ions.

The expression of DAPIT requires further studies in insulin-sensitive tissues of diabetic rat and mouse. Previously we showed that DAPIT mRNA was down-regulated in the myocardium and skeletal muscle in early type I diabetes.¹ However, the protein level was regulated differentially. DAPIT was up-regulated in insulin-sensitive rat tissues, except in liver. However, no change in DAPIT protein expression was seen in mouse calf muscle complex after 1-5 weeks of streptozotocin-induced diabetes. This seemingly contradicting data may be due to sample heterogeneity since these muscles have different compositions highly oxidative type I and type II fibers containing plenty of mitochondria and glycolytic type IIb fibers that contain only a low amount of mito-

chondria. Differential expression of mRNA and protein in rat suggests that DAPIT is post-transcriptionally regulated. Since DAPIT is a component of mitochondrial oxidative machinery, one might expect to observe down-regulation of DAPIT in diabetes that is accompanied with impaired mitochondrial function and number in myocardium and skeletal muscles.¹³ The significance of the differential DAPIT expression in diabetic tissues and how DAPIT may be implicated in the etiology of diabetes remains to be shown.

In the present study, we characterized custom-made antibodies against DAPIT. In addition to DAPIT protein, the antibody specific for the carboxyterminus of DAPIT recognizes also a larger, unrecognized protein in rat skeletal muscle. Furthermore, we confirmed the presence of DAPIT in mitochondria and showed that it is also located in lysosomes and in other acidic vacuoles. We propose that in addition to being a component of mitochondrial ATP synthase DAPIT is also a subunit of V-ATPase. The significance and possible functions of DAPIT remain to be elucidated.

References

1. Päivärinne H, Kainulainen H. DAPIT, a novel protein down-regulated in insulin-sensitive tissues in streptozotocin-induced diabetes. *Acta Diabetol* 2001;38: 83-6.
2. Chen R, Runswick MJ, Carroll J, Fearnley IM, Walker JE. Association of two proteolipids of unknown function with ATP synthase from bovine heart mitochondria. *FEBS Lett* 2007;581:3145-8.
3. Meyer B, Wittig I, Trifilieff E, Karas M, Schagger H. Identification of two proteins associated with mammalian ATP synthase. *Mol Cell Proteomics* 2007;6:1690-9.
4. Ohsakaya S, Fujikawa M, Hisabori T, Yoshida M. Knockdown of DAPIT (diabetes-associated protein in insulin-sensitive tissue) results in loss of ATP synthase in mitochondria. *J Biol Chem* 2011;286: 20292-6.
5. Imamura H, Nakano M, Noji H, Muneyuki E, Ohkuma S, Yoshida M, et al. Evidence for rotation of V1-ATPase. *Proc Natl Acad Sci USA* 2003;100:2312-5.
6. Hirata T, Iwamoto-Kihara A, Sun-Wada GH, Okajima T, Wada Y, Futai M. Subunit rotation of vacuolar-type proton pumping ATPase: Relative rotation of the G and C subunits. *J Biol Chem* 2003;278:23714-9.
7. Hulmi JJ, Silvennoinen M, Lehti M, Kivelä R, Kainulainen H. Altered REDD1, myostatin and Akt/mTOR/FoxO/MAPK signaling in streptozotocin-induced diabetic muscle atrophy. *Am J Physiol Endocrinol Metab* 2012;302:E307-15.
8. Hughes SM, Cho M, Karsch-Mizrachi I, Travis M, Silberstein L, Leinwand LA, et al. Three slow myosin heavy chains sequentially expressed in developing mammalian skeletal muscle. *Dev Biol* 1993;158:183-99.
9. Schagger H, Aquila H, Von Jagow G. Coomassie blue-sodium dodecyl sulfate-polyacrylamide gel electrophoresis for direct visualization of polypeptides during electrophoresis. *Anal Biochem* 1988;173: 201-5.
10. Laemmli UK. Cleavage of structural proteins during the assembly of the head of bacteriophage T4. *Nature* 1970;227:680-5.
11. Jefferies KC, Cipriano DJ, Forgac M. Function, structure and regulation of the vacuolar (H⁺)-ATPases. *Arch Biochem Biophys* 2008;476:33-42.
12. Hinton A, Bond S, Forgac M. V-ATPase functions in normal and disease processes. *Pflugers Arch* 2009;457:589-98.
13. Patti ME, Corvera S. The role of mitochondria in the pathogenesis of type 2 diabetes. *Endocr Rev* 2010;31:364-95.

RESEARCH ARTICLE

DAPIT Over-Expression Modulates Glucose Metabolism and Cell Behaviour in HEK293T Cells

Heidi Kontro¹, Giuseppe Cannino², Pierre Rustin^{3,4}, Eric Dufour², Heikki Kainulainen^{5*}

1 Tampere Centre for Child Health Research, University of Tampere, Tampere, Finland, **2** Institute of Biomedical Technology, University of Tampere, Tampere, Finland, **3** INSERM UMR 1141, Paris, France, **4** Université Paris 7, Paris, France, **5** Department of Biology of Physical Activity, University of Jyväskylä, Jyväskylä, Finland

* heikki.s.o.kainulainen@ju.fi



OPEN ACCESS

Citation: Kontro H, Cannino G, Rustin P, Dufour E, Kainulainen H (2015) DAPIT Over-Expression Modulates Glucose Metabolism and Cell Behaviour in HEK293T Cells. PLoS ONE 10(7): e0131990. doi:10.1371/journal.pone.0131990

Editor: Mauro Salvi, University of Padova, ITALY

Received: July 10, 2014

Accepted: June 9, 2015

Published: July 10, 2015

Copyright: © 2015 Kontro et al. This is an open access article distributed under the terms of the [Creative Commons Attribution License](https://creativecommons.org/licenses/by/4.0/), which permits unrestricted use, distribution, and reproduction in any medium, provided the original author and source are credited.

Data Availability Statement: All relevant data are within the paper and its Supporting Information files.

Funding: The study was financially supported by the Competitive Research Funding of the Pirkanmaa Hospital District grant 9G030, HKo; Finnish Cultural Foundation, Pirkanmaa Regional fund, HKo; Finnish Diabetes Research Foundation, HKo; Academy of Finland, HKA; Finnish Cultural Foundation Central Fund, HKA. The funders had no role in study design, data collection and analysis, decision to publish, or preparation of the manuscript. The URLs of funding sources are as follows in the order they are mentioned: <http://www.pshp.fi/default.aspx?nodeid=10066&contentlan=2>, <https://www.skr.fi/en/finnish->

Abstract

Introduction

Diabetes Associated Protein in Insulin-sensitive Tissues (DAPIT) is a subunit of mitochondrial ATP synthase and has also been found to associate with the vacuolar H⁺-ATPase. Its expression is particularly high in cells with elevated aerobic metabolism and in epithelial cells that actively transport nutrients and ions. Deletion of DAPIT is known to induce loss of mitochondrial ATP synthase but the effects of its over-expression are obscure.

Results

In order to study the consequences of high expression of DAPIT, we constructed a transgenic cell line that constitutively expressed DAPIT in human embryonal kidney cells, HEK293T. Enhanced DAPIT expression decreased mtDNA content and mitochondrial mass, and saturated respiratory chain by decreasing H⁺-ATP synthase activity. DAPIT over-expression also increased mitochondrial membrane potential and superoxide level, and translocated the transcription factors hypoxia inducible factor 1 α (Hif1 α) and β -catenin to the nucleus. Accordingly, cells over-expressing DAPIT used more glucose and generated a larger amount of lactate compared to control cells. Interestingly, these changes were associated with an epithelial to mesenchymal (EMT)-like transition by changing E-cadherin to N-cadherin and up-regulating several key junction/adhesion proteins. At physiological level, DAPIT over-expression slowed down cell growth by G1 arrest and migration, and enhanced cell detachment. Several cancers also showed an increase in genomic copy number of *Usmg5* (gene encoding DAPIT), thereby providing strong correlative evidence for DAPIT possibly having oncogenic function in cancers.

Conclusions

DAPIT over-expression thus appears to modulate mitochondrial functions and alter cellular regulations, promote anaerobic metabolism and induce EMT-like transition. We propose

cultural-foundation/regional-funds/pirkanmaa-regional-fund, <http://www.diabetestutkimus.fi/en>, <http://www.aka.fi/en-GB/A/Funding-and-guidance/Funding/>, <https://www.skr.fi/en/grants>.

Competing Interests: The authors have declared that no competing interests exist.

that DAPIT over-expression couples the changes in mitochondrial metabolism to physiological and pathophysiological regulations, and suggest it could play a critical role in H⁺-ATP synthase dysfunctions.

Introduction

DAPIT is a 58 amino acid peptide first discovered in insulin-sensitive tissues of the streptozotocin-diabetic rat model [1]. It is a component of the F_o subunit of the mitochondrial H⁺-ATP synthase (F-ATPase) [2–4] and its knock-down results in the loss of this enzyme [5]. Recently we found that DAPIT is also a component of the vacuolar proton pump (V-ATPase) [6].

The gene encoding DAPIT is *Usmg5* that is well conserved from insects to vertebrates underlining its potentially important function. A histological analysis of DAPIT in rat and human tissues revealed an elevated expression in cells with a high aerobic metabolism and in epithelial cells involved in the active transport of nutrients and ions [6].

Interestingly, DAPIT expression appears to be modulated in various disease models. Streptozotocin (STZ) induction of diabetes in rats caused a down-regulation of DAPIT mRNA in insulin-sensitive tissues [1], but it increased DAPIT protein levels, suggesting post-transcriptional regulation [6]. In diabetic neuropathies, hyperglycaemia up-regulates the DAPIT protein in the Schwann cells of neonatal rats [7]. DAPIT is also enriched in the brain synaptosomes of a murine model of Parkinson's disease [8]. In addition, Gene Expression Omnibus [GEO] database [9] screening suggests that the *Usmg5* transcript is up-regulated in various cancers (GEO accession GDS1792 [10], GDS3330 [11], GDS3754 [12], GDS2755 [13]), in adipose tissue of high weight gainers (GDS 2319 [14]) and in cardiac deficiencies (GDS487, GDS696); but, since post-transcriptional regulations seem to play an important role in DAPIT synthesis, it is difficult to estimate the consequences this upregulation could have at the functional level.

As a component of the H⁺-ATP synthase, DAPIT is involved in mitochondrial oxidative phosphorylation (OXPHOS), which is the major source of ATP in aerobic organisms. In various diseases, including cancer, diabetes, cardiopathies and degenerative diseases, metabolic stress lead to changes in OXPHOS activity and properties, altering mitochondrial parameters such as respiration, membrane potential, ATP production, ROS generation and mitochondrial mass. Such changes can be either beneficial (partly complementing the defects caused by the disease) or detrimental (precipitating its pathological consequences). In addition, changes in OXPHOS activity are known to elicit retrograde regulations, further altering the cellular metabolism. For example, tumour cells shift from oxidative ATP generation to glycolytic production of energy, even under normoxic conditions (the so-called Warburg effect) [15,16]. A key regulator of this effect is the nuclear stabilization of hypoxia-inducible factor 1 α (Hif1 α). Hif1 signalling up-regulates glycolysis and controls mitochondrial function, cell proliferation and angiogenesis while repressing apoptosis [15,17]. Hif1 α activation usually requires hypoxia, but it is also observed in normoxic conditions in response to increased mitochondrial ROS production and/or accumulation on tricarboxylic acid cycle (TCA) intermediates [18,19]. Changes in respiratory chain function can also be sensed by mitochondrial sirtuins (Sirt 3–5) that modulate the activity of metabolic enzymes via protein deacetylation or mono-ADP-ribosylation [20]. In particular, Sirt3, a NAD⁺-dependent deacetylase is able to activate many protein targets, including respiratory chain complex I, acetyl-CoA synthetase 2 and glutamate dehydrogenase, leading to enhanced function of TCA and increased respiration [21,22].

As *Usmg5* mRNA or DAPIT is up-regulated in various diseases and metabolic disorders known to be associated with mitochondrial functions, we aimed to study the effects of DAPIT over-expression at the cellular level. DAPIT was stably transfected into human embryonic kidney cells, HEK293T, and we studied cell morphology-, mitochondria-, nuclei-, cell junction-, behaviour- and metabolism-related parameters. We show that DAPIT over-expression modulates mitochondrial activity causing a cellular regulation that promote glycolysis and induce EMT-like transition.

Materials and Methods

Plasmid DNA constructs

The full-length DAPIT cDNA was originally cloned in pCR-TOPO vector (Invitrogen, Carlsbad, CA, USA) [1]. The DAPIT coding sequence—including ten nucleotides from the 5' NCR—was recloned by PCR with the pEGFP sequence of the pIRES2-EGFP vectors (Clontech Laboratories, Palo Alto, CA, USA). The primers used were 5'- acgaattcgattgaagtcattgctggccca -3' and 5'- tcgggatccttatgttgctttcacagctggggg -3'. The PCR reactions consisted of cycles at 96°C for 2 min, 4x (96°C for 30 s, 50°C for 1 min, 72°C for 30 s), 25x (96°C for 30 s, 60°C for 1 min, 72°C for 30 s) and 72°C for 10 min. The DAPIT amplicon was purified, cloned into the pIRES2-EGFP vector with *EcoRI* and *BamHI* restriction enzymes (MBI Fermentas GmbH, Leon-Rot, Germany; Clontech Laboratories, Palo Alto, CA, USA) and amplified in One Shot TOP 10 bacteria (Invitrogen). The insert size (~204 bp) was confirmed by restriction enzyme digestion, and the insert DNA was fully sequenced. The construct was used for stable transfection of HEK293T cells.

Cell culture, transfections and RT-PCR

HEK293T cells (ATCC, crl-3216) were cultured in Dulbecco's modified Eagle's medium (Sigma-Aldrich, Ayshire, UK or Gibco BRL, Paisley, Scotland, UK), containing 4.5 g/l of D-glucose, 10% foetal calf serum (Sigma), 50 µg/ml uridine, 1 mM sodium pyruvate, 2 mM L-glutamine, 100 U penicillin and 100 µg/ml of streptomycin (Gibco BRL) at 37°C in an incubator with 5% CO₂. Transfections were performed using Lipofectamine according to the manufacturer's protocol (Invitrogen). Transfection efficiency was estimated by flow cytometry using GFP fluorescence. Twenty-five Geneticin-resistant clones (Calbiochem/Merck KGaA, Darmstadt, Germany; 2 mg/ml) were selected and combined to form the polyclonal cell line. Total RNAs from pIRES2-EGFP and DAPIT-pIRES2-EGFP stably transfected cells were extracted by RNeasy Mini Kit (Qiagen), and 1 µg total RNA was used for RT-PCR using M-MuLV reverse transcriptase, as suggested by the provider (MBI Fermentas). The obtained cDNAs of control and transgenic cells were multiplied by PCR as indicated above.

Fluorescence microscopy

For live imaging of mitochondria and lysosomes, the cells grown on poly-L-lysine coated cover slips (Sigma) were washed with PBS and incubated in a medium containing 100 nM Mito-tracker Red (Invitrogen) or 100 nM LysoTracker red (Invitrogen) for 10–30 min at 37°C. Mito-tracker-stained cells were PBS washed and maintained in DMEM medium for 1 hour at 37°C before observation. For immunofluorescence microscopy, cells fixed in 4% paraformaldehyde (Sigma) for 15 min were permeabilized with 0.5% Triton X-100 (MP Biomedicals, Illkirch, France) in TBS (10mM Tris, 0.9% NaCl, pH 8.0 (Sigma)) for 10 min. Non-specific epitopes were blocked by using 5% w/v non-fat milk powder, 2% w/v BSA (Sigma) for 30 min. Samples were incubated in TBS-T (TBS with 0.1% Tween (Sigma)) with the primary antibody (αD15C,

1:300) [5] for 2 h at room temperature, washed for 3x5min and incubated in Alexa Fluor 488 or 568 goat anti-rabbit, Alexa Fluor 568 goat anti-mouse or Alexa Fluor 549 chicken anti-mouse IgG secondary antibodies (Molecular Probes, Eugene, Oregon, USA, 1:4000) for 1 hour. Coverslips were mounted on slides using Vectashield mounting medium (Vector Laboratories, Burlingame, CA, USA), and samples were examined by confocal microscopy at 100x magnification using a Perkin Elmer-Cetus/Wallac UltraView LCI system (Wellesley, MA, USA) equipped with appropriate excitation and emission filters, an Andor iXon DV885 EMCCD camera and the Andor iQ software (Andor, Belfast, UK), or with a conventional fluorescence microscope at 40x and 60x magnification (Olympus BX60, Olympus Corporation, Japan). Images were further processed using Corel Photo-Paint 11 (Corel Corporation).

Mitochondrial copy number calculation and citrate synthase activity

For mtDNA copy-number analysis, total DNA was prepared as reported in Fukuoh et. al. [23]. The isolated DNA from 0.4×10^6 cells were resuspended in TE buffer (pH 8.0), purified and quantified by Nanodrop. Relative mtDNA copy number was measured by real-time qPCR using primers for mitochondrial COXII subunit (Forward cgtctgaactatcctgcccg, Reverse tggttaagggaggatcgttg) and nuclear APP (Forward ttttgtgtctctcccaggctc, Reverse tggctactggtttggc) in a StepOnePlus instrument (Applied Biosystems) using Fast SYBR Green Master Mix (Applied Biosystems) under the manufacturer's recommended conditions, with 20 sec of enzyme activation at 95°C, followed by 40 cycles of 95°C for 3 sec and 60°C for 30 sec.

The activity of citrate synthase of cells was measured using a kit (Sigma-Aldrich, CS0720) according to the manufacturer's instructions with an automated KoneLab device (Thermo Scientific, Vantaa, Finland).

Oxygen consumption and fluorescence biomarkers

The mitochondrial measurements in living cells were performed as in Cannino et. al. [24]. Oxygen consumption was measured with a Clark-type electrode (Oxygraph, Hansatech Instruments Ltd, Norfolk, UK). Intact cell respiration was recorded from 1×10^7 cells suspended in 500 μ l of DMEM medium at 37°C. Maximum respiration was obtained by FCCP titration (5–9 μ M). Oxygen consumption was stopped with 150 nM rotenone, 30 ng/ml antimycin A, 100 μ M Cyanide or 100–200 nM Oligomycin (Sigma). Oxygen consumption from 1×10^7 cells permeabilized by 80 μ g/ml digitonin was recorded in respiratory buffer A (225 mM sucrose, 75 mM mannitol, 10 mM Tris-buffer pH 7.4, 10 mM KCl, 10 mM KH_2PO_4 , 5 mM MgCl_2 , 1mg/ml BSA (Sigma)) at 37°C. The substrate concentrations were 10 mM ADP, 5 mM pyruvate + 5 mM malate for complex I, 10 mM succinate for complex II, and 50 μ M TMPD and 1 mM ascorbate for complex IV. All measurements were corrected by subtracting the residual oxygen consumption present after full inhibition of the respiratory chain.

For the mitochondrial mass, membrane potential and superoxide measurements, flow cytometry assays were used. In the absence of G418, 4×10^5 (Vector) and 4.5×10^5 (DAPIT) cells were seeded in culture medium. After overnight culture, the subconfluent cells were treated with 200 nM 10-nonyl acridine orange (NAO; Invitrogen,) for 30 min at 37°C, 200nM tetramethyl rhodamine methyl ester (TMRM; Invitrogen,) for 30 min at 37°C or 2.5 μ M MitoSox (Invitrogen,) for 45 min at 37°C. The staining was stopped by replacing the medium with 1xPBS, and cells were kept at 37°C (NAO and TMRM) or on ice (MitoSox) until measured. Negative controls for mitochondrial membrane potential were obtained by adding 10 μ M FCCP before flow cytometry analysis.

The fluorescence was counted from 40,000 cells using a BD Accuri C6 flow cytometry (BD Biosciences). The region of interest was defined by using the forward scatter/side scatter values, excluding the debris and dead cells. The staining was measured either by using 488 nm (band-pass) excitation and emission of FL2 (585 ± 40 nm) for NAO and TMRM, FL3 (620 ± 15 nm) for Mitosox and FL1 (533 ± 40 nm) for GFP. The fluorescence compensations were estimated independently for each series of experiments. All measurements provided as “relative to mitochondrial (mt) content” were normalized by NAO quantification, whereas measurements provided as “per cell” were normalized to the cell count.

Isolation of mitochondria and complex V activity

For crude extraction of mitochondria, the cells from four 17.5 cm^2 or 8–10 10 cm^2 culture plates were collected by centrifugation at $250 g$ for 3 min at room temperature. The rest of the protocol was carried out in a cold room ($+4^\circ\text{C}$) on ice. The cells were bloated in 5.5 ml of hypotonic buffer (10mM NaCl, 1.5mM MgCl₂, 10mM Tris-HCl pH 7.5 (Sigma), protease inhibitor cocktail (Roche, Mannheim, Germany)) for 8–13 min, ruptured with eight strokes of teflon pestle. 4 ml of 2.5X MS buffer (700 mM sucrose, 2.5 mM EDTA, 12.5 mM Tris-HCl pH 7.5, protease inhibitors) was added. To remove nuclei and cell debris, the samples were centrifuged at $1,300 g$ for 10 min. Mitochondria from the supernatant was pelleted by centrifugation at $17,000 g$ for 15 min, and diluted to 0.5–1 ml of 1X MS buffer (0.28 mM sucrose, 5 mM Tris-HCl, 1 mM EDTA pH 7.5, protease inhibitors).

Fifteen ml of 1.5 M and 1.0 M sucrose in buffer (10mM Tris-HCl pH 7.4, 1 mM EGTA, 0.1% BSA, protease inhibitors) were layered in ultracentrifuge tubes. The crude extract of mitochondria was added on the top of sucrose layers and centrifuged at $60,000 g$ for 20 min at 4°C . The resulting fraction of mitochondria in the interphase of sucrose layers was collected, the volume measured and slowly (15–20 min) diluted on ice for 4X with 0.2M mannitol in Tris-EGTA-BSA buffer. Finally, the mitochondria were pelleted at $17,000 g$ for 15 min at 4°C , diluted to 40–50 μl of 1X MS buffer and stored at -80°C .

The oligomycin-sensitive complex V activity was spectrophotometrically measured in the backward direction using lactic dehydrogenase and pyruvate kinase as coupling enzymes, as essentially described elsewhere [25,26].

Cell growth, mortality, and synchronization

Fifteen thousand cells were seeded on a 24-well culture plate (Nunclon, Thermo Scientific) in 500 μl of culture medium in the presence of antibiotics (Penicillin-Streptomycin & G418). Cell proliferation and mortality were followed for five days by counting the living and dead cells in a Burkert hemocytometer after trypan blue labelling (0.4%; Sigma).

The control and DAPIT overexpressing cells were synchronized by a double thymidine block method (DIAMONDS Deliverable 1-D1.1.3, [ResearchGate.net](https://www.researchgate.net)) for more accurate follow up of cell division. At 30% confluence in 24-well culture plate, the cells were washed twice with 1x PBS and 1 ml of cell culture medium supplemented with 2 mM thymidine (Sigma) was added for 18 hours. Thymidine was washed out and the cell divisions were released by adding fresh cell culture medium for nine hours. This was followed by another thymidine step for 17 hours after which the cells progress synchronously through G₂- and mitotic phase. Upon the release from the thymidine block, the cells were cultured in normal medium for 4, 8, 12, 16 and 24 hours in order to follow the cell cycle progress. At each time point the cells were collected, pelleted, stained with 250 μl of PI staining solution (25 $\mu\text{g/ml}$ propidium iodide, 100 $\mu\text{g/ml}$ RNase A, 0.1% sodium citrate, 0.1% Triton X-100 (Sigma)) for 20 min on ice and measured by flow cytometry (488 nm excitation, >670 nm emission; FL3). The number of cells (arbitrary

units) was blotted against the DNA content at each time point. The test was repeated for four times.

Migration and adhesion

The migration was studied by scratch wound test in a 12-well culture plate (Nunclon). The cells were grown confluent, and fresh medium was provided three hours prior to starting the test. After 1 hour-treatment with 20 $\mu\text{g/ml}$ Mitomycin C (Sigma) cells were scratched with a tip, washed and incubated overnight at 37°C. After fixation with 4% PFA for 15 min and PBS washing, cells were stained with crystal violet (0.5 mM) for 5 min in 70% ethanol. The cells migrating in the scratched area were counted using a phase contrast microscope (Axiovert 200 M, Zeiss). Cell attachment was studied using PMS/MTS (Promega, Madison, WI, USA) according to the manufacturer's protocol. Detachment was determined according to the protocol used in migration assays in a 48-well culture plate (Nunclon). The empty areas of detached cells in the bottom of wells were quantified by ImageJ (imagej.nih.gov/ij) analysis.

Western blot analysis

Proteins from subconfluent (approximately 50–70%) cells were extracted in PBS containing 1% Triton X100 and protease, followed by incubation on ice for 30 min and centrifugation at 12,000 *g* for 1 minute. The protocol applied by Teittinen et al. [27] was followed to obtain nuclear extracts. Briefly, subconfluent cells were washed with PBS and collected by centrifugation. The cells were resuspended in 5 ml hypotonic buffer (10 mM Hepes (pH 7.9), 10 mM KCl, 1.5 mM MgCl_2 , 0.5 mM DTT (Sigma)) and broken on ice using a Dounce homogenizer. Nuclei were pelleted by centrifugation (228 *g*, 5 min, +4°C) and purified by isopycnic centrifugation (1,430 *g*, 5 min, +4°C) on a two-step sucrose gradient: 250 mM sucrose, 10 mM MgCl_2 vs 880 mM sucrose, 0.5 mM MgCl_2 . The proteins of this nuclear fraction were extracted as described above.

The protein concentration was determined by the Bradford method [28]. Then, 20 μg of cellular and 50 μg of nuclear protein were used for SDS-PAGE analysis according to Laemmli et al. [29] and transferred to Hybond-C extra nitrocellulose membrane (Amersham plc, Buckinghamshire, UK). Non-specific epitopes were masked, exposing membranes to 5% freeze-dried fat-free milk in TBS-T for 1 hour. Primary antibodies (see Table 1) were incubated for 2 hours. After washings, the blots were incubated with the secondary antibody: peroxidase-conjugated swine anti-rabbit and rabbit anti-mouse (DAKO, Clostrup, Denmark) 1:2,000, or Peroxidase Horse Anti-Goat IgG (H+L; Vector Laboratories) 1:10,000 for 1 hour. Subsequently, the blots were washed, and the signal was detected by enhanced chemiluminescent ECL reagent (Amersham) according to the manufacturer's protocol. The blots were visualized on Super RX medical X-ray film (Fujifilm Corporation, Tokyo, Japan) and the bands quantitated by Kodak imaging software (Eastman Kodak Company, US). The protein expression was normalized to the house-keeping protein gamma-tubulin, and additionally to mitochondrial content (NAO result) in the case of the mitochondrial proteins.

Glucose and lactate test

The glucose consumption and lactate production were measured from culture media of the cell proliferation test and results were normalized with concomitant cell number. Glucose and lactate levels were analysed using the enzymatic-amperometric method and chip-sensor technology (Biosen C-line Sport, EKF Diagnostic, Magdeburg, Germany).

Table 1. List of primary antibodies and dilutions used in Western blot.

Antibody	Dilution	Host	Manufacturer
ATP5a	1:4000	Mouse monoclonal	Abcam, #MS502
β-actin	1:5000	Mouse monoclonal	Sigma, #A5316
β-catenin	1:400	Mouse monoclonal	Transduction Laboratories, BD Biosciences, #610153
Connexin 43	1:1000	Rabbit polyclonal	Sigma, #C6219
αD15C (anti-DAFIT)	1:160	Rabbit polygonal	Custom made [5]
E-cadherin	1:1000	Rabbit polyclonal	Santa Cruz, #sc-7870
γ-tubulin	1:4000	Mouse monoclonal	Sigma, #T5326
GFP	1:10000	Mouse monoclonal	Zymed, #33–2600
Hif1α	1:1000	Mouse monoclonal	Abcam, #10625, ab8366
Histone H1	1:500	Mouse monoclonal	Santa Cruz, #sc-8030
HSP60	1:600	Mouse monoclonal	Sigma, #4149
Integrin α2	1:200	Mouse monoclonal	Santa Cruz, #sc-13546
N-cadherin	1:1000	Mouse monoclonal	Sigma, #C2542
NDUFS3	1:10000	Mouse monoclonal	Abcam, # 14711
PGC1α	1:3000	Rabbit polyclonal	Millipore, #516557
RhoA	1:200	Mouse monoclonal	Santa Cruz, #sc-418
Sirt3	1:400	Goat polyclonal	Abcam, #118334
Smooth muscle actin	1:200	Mouse monoclonal	Sigma, #A5228
VDAC1/Porin	1:1000	Mouse monoclonal	Nordic BioSite, #MSA03
Vimentin	1:200	Goat polyclonal	Millipore, #AB1620
Zo-1	1:300	Mouse monoclonal	Invitrogen, #339100

doi:10.1371/journal.pone.0131990.t001

Oncomine data analysis

We used the Oncomine Cancer Genomics Data Analysis tool [30] to mine *Usmg5* copy number profiles in a large subset of carcinomas and cancer cell lines [31–48]. In the dataset information of cancers both significant differences ($p \leq 0.05$) and fold changes (≥ 1) were reported. The number of DNA copies ($= 2^*(2^{\wedge}y\text{-axis value})$) were calculated as advised in Oncomine instructions.

Statistical analysis

Comparisons between cell lines were performed by using Mann-Whitney U test.

Results

For the sake of simplicity, from now on we will call “control cells” the cells transfected with empty pIRES2-EGFP vector and “DAFIT cells” the ones over-expressing transgenic DAFIT. The transgene is co-transcribed with a cytosolic GFP reporter, independent from fusion protein.

Mitochondrial mass, mtDNA and DAFIT over-expressing cells

As DAFIT was reported a Fo subunit of H⁺-ATP synthase, the immunofluorescence analysis of DAFIT cells showed clear co-localization of mitochondrial and DAFIT signals (Fig 1A). Importantly, we observed very few DAFIT-positive lysosomes. Knowing that mitochondria that are targeted for degradation (e.g. through mitophagy) would lead to a transient localization of DAFIT into lysotracker positive compartments, our results suggest a pure mitochondrial location of this protein.

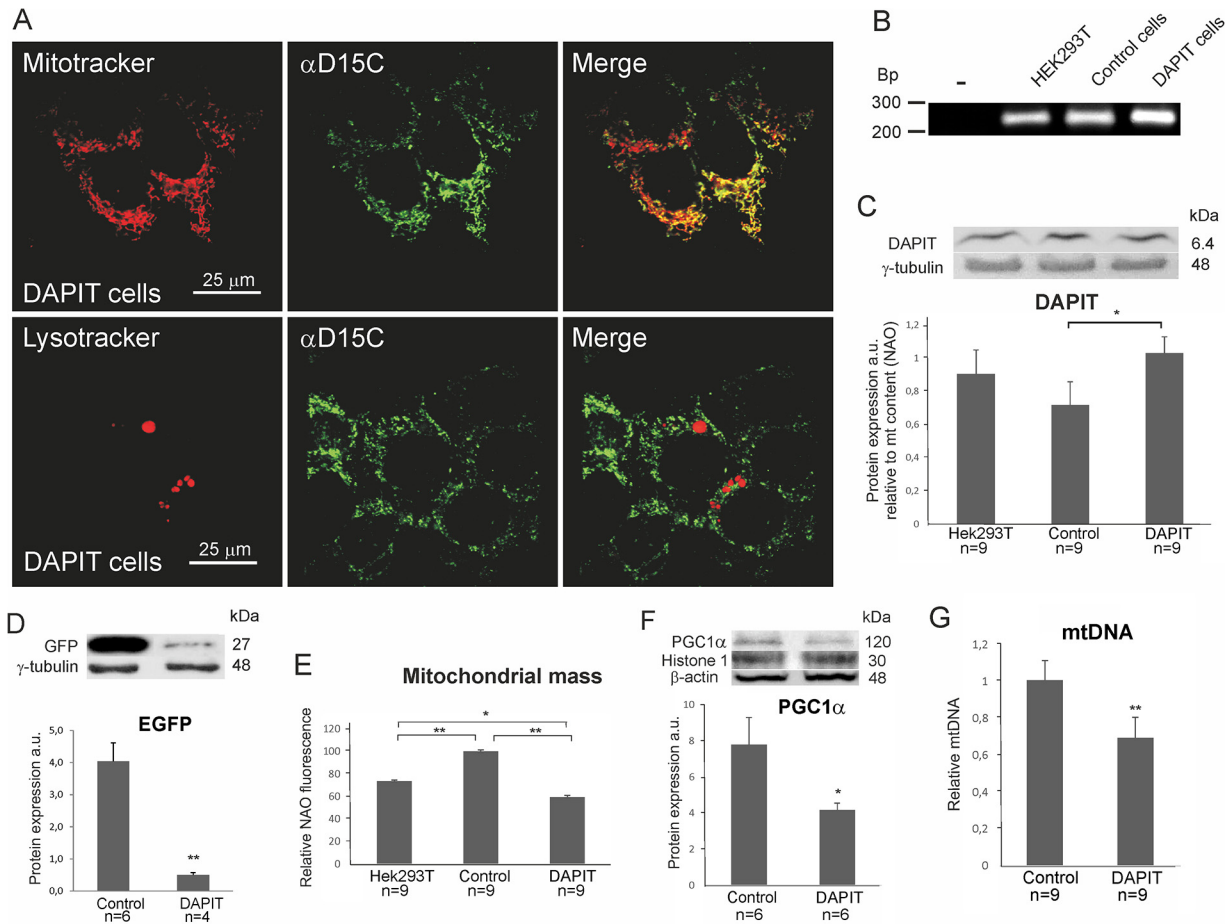


Fig 1. DAPIT over-expression decreased mitochondrial mass and mtDNA content in DAPIT cells. (A) Representative confocal microscopy images of cells stained by Mitotracker and Lysotracker (100 nM, 10–30', 37°C) and anti-DAPIT antibody, α D15C. (B) mRNA expression of the *Usmg5* by semi-quantitative RT-PCR. Protein levels estimated by Western blot of (C) DAPIT and (D) EGFP. (E) Mitochondrial mass was measured by flow cytometry of NAO stained cells (200nM, 30', 37°C). (F) Protein level of PGC1 α from nuclear extract. (G) mtDNA content by quantitative PCR. The error bars are S.D. and asterisks indicate: * p <0.05, ** p <0.01.

doi:10.1371/journal.pone.0131990.g001

In this study, we emphasize the comparison of DAPIT cells to control ones due to vector transduction and following culture conditions. For assuring our cell model, the mRNA and protein level and mitochondrial mass from HEK293T cells are also reported. As mitochondrial mass is sensitive to H^+ -ATP synthase impairments [23,49,50], the concomitant differences in mass between cell lines are normalized into reported mitochondrial parameters.

The expression of transgene was controlled by reverse transcriptase-PCR (RT-PCR) and Western blot analysis. DAPIT cells presented higher level of *Usmg5* messenger RNA compared to the HEK293T and control cells (Fig 1B) demonstrating the functionality of the DAPIT construct.

The expression of DAPIT protein in the three cell lines is shown in Fig 1C. DAPIT expression was slightly decreased in control cells (vehicle) as compared to HEK293T cells. A mild but not significant increase was seen between HEK293T and DAPIT cells, but significantly higher expression was observed in DAPIT than in control cells (p <0.05). The green fluorescent protein expression appeared lower in DAPIT cells (Fig 1D) indicating that translation from the 5' RNA CAP is more efficient than internal ribosome entry, as previously reported [51].

In order to study the effect of DAPIT over-expression on mitochondrial physiology, we measured mitochondrial mass using the mitochondria specific dye NAO in HEK293T, control and DAPIT cell lines (Fig 1E). Mitochondrial mass in DAPIT cells was significantly lower than in control and HEK293T cells, while it was intermediate in HEK293T cells.

To verify the mitochondrial mass in control and DAPIT cells, we measured mtDNA copy number and nuclear level of mitochondrial biogenesis regulating transcription factor PGC1 α . In line with NAO results, both the translocation of PGC1 α to the nuclei and the mtDNA content were decreased in DAPIT cells (Fig 1F and 1G). These results indicate that mitogenesis is decreased in DAPIT cells.

Metabolic activity of mitochondria

We next estimated the effect of DAPIT over-expression on mitochondrial protein transport, TCA cycle activity, respiratory chain activity in intact cells and oxygen consumption driven by complexes I, II and IV in permeabilized cells. The results are reported both at cellular level (S1 Fig) and in relation to mitochondrial content (NAO normalized results, Fig 2).

The expression of VDAC1 (Fig 2A and 2M) and the activity of citrate synthase (Fig 2B) were increased significantly upon DAPIT over-expression ($p = 0.001$ and 0.05 , respectively). These results could indicate increased transport or reduced turn-over of cytosolic substrates suitable for enhanced oxidation by TCA cycle, thereby facilitating the demands of respiratory chain.

The protein expression of C1 subunit NDUFS3 ($p = 0.004$) was increased in DAPIT cells (Fig 2C and 2M). In addition, both the oxygen consumption from complexes I, II and IV in digitonin-permeabilized cells and respiration of intact cells (Fig 2D and 2E) were significantly increased ($p = 0.044, 0.000, 0.002, 0.000$), respectively. However, the expression of F₁ complex subunit ATP5a was unaltered (Fig 2F and 2M) suggesting that enhanced oxygen consumption seen in DAPIT cells is not due to increase in CV content. Instead, the changes in respiratory chain function are supported by unchanged expression of Sirt3 (Fig 2G and 2M), a modulator of the activity of metabolic enzymes. In addition, DAPIT cells exhibit increased basal and maximal respiration ($p = 0.003$ and 0.004 , respectively) (Fig 2H) and decreased activity of ATP synthase ($p = 0.005$) (Fig 2I). These results suggest enhanced substrate availability and increased activity of TCA cycle, efficient respiration, active coupling but decreased H⁺-ATP synthase activity in DAPIT cells. Accordingly, the membrane potential ($p = 0.001$) and superoxide ($p = 0.001$) levels were increased (Fig 2J and 2K). When assessed at cell level (S1 Fig), respiration and TCA cycle activity remained unchanged between cell lines but VDAC1 expression, CV activity, membrane potential and superoxide showed the same changes as when normalized to mitochondrial mass. Taken together, these results suggest the saturation of respiratory chain due to DAPIT over-expression. The protein level of HSP60 increased significantly ($p = 0.009$) in DAPIT cells (Fig 2L and 2M), indicative of an appropriate maintenance of the mitochondrial proteins.

Nuclear proteins

We observed increased nuclear translocation of the Hif1 α transcription factor in DAPIT cells (Fig 3A and 3C). We also observed an increased protein expression of nuclear β -catenin (Fig 3B and 3C) and relocation of E-cadherin from cell junctions to the cytosol in DAPIT cells (Fig 3D, upper panel). Altogether, these results suggest major remodeling of cellular functions in response to DAPIT over-expression, since Hif1 α and β -catenin level are known to be involved in cellular dedifferentiation [52].

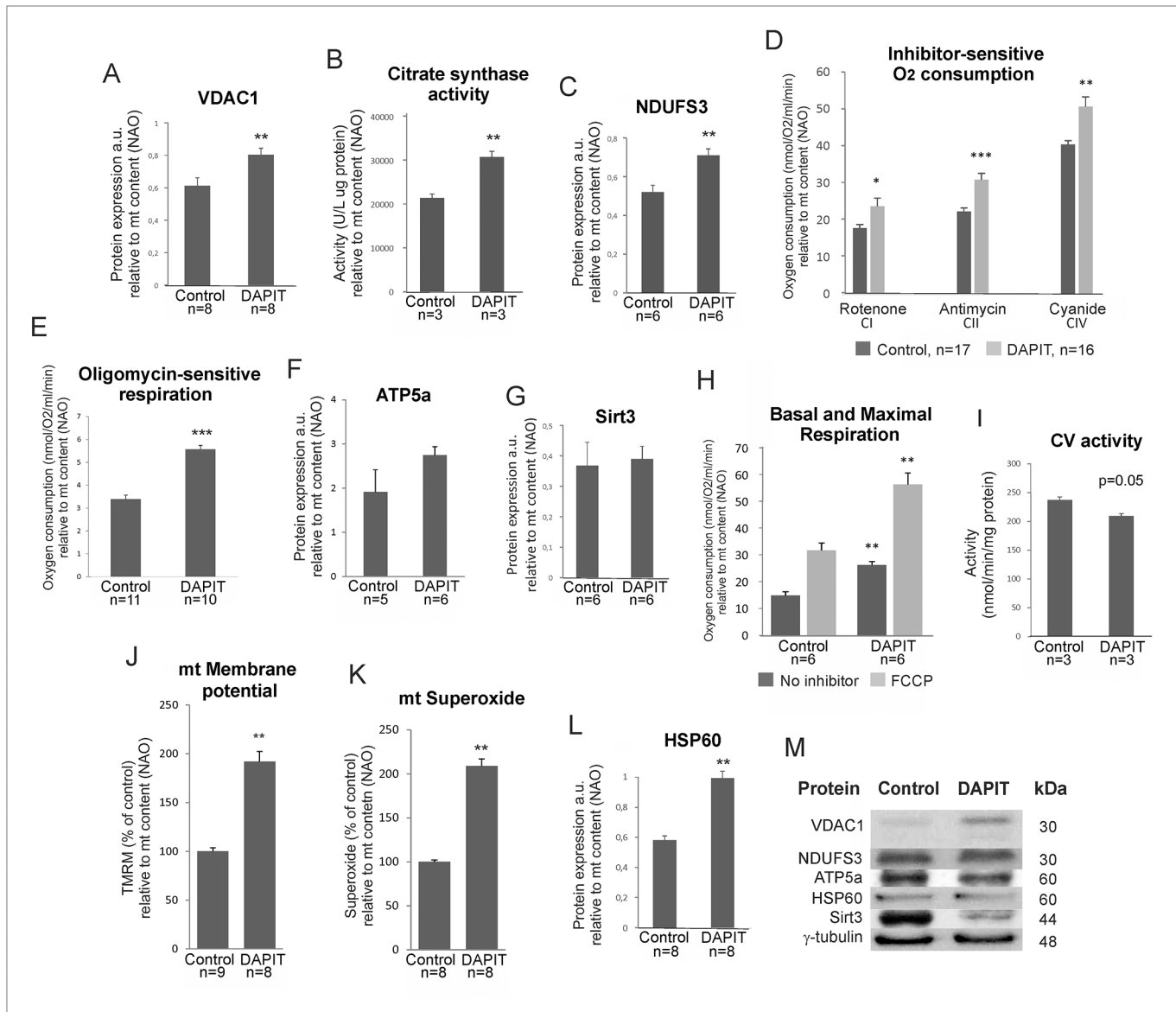


Fig 2. Mitochondrial activity in DAPIT over-expression (relative to mitochondrial mass (NAO)). (A) Protein level of VDAC1 by Western blot of cellular lysates. (B) Citrate synthase activity was measured by spectrophotometric analysis from protein extracts of control and DAPIT cells. (C) Protein level of NDUFS3. (D) Inhibitor-sensitive oxygen consumption of complexes I, II, IV and (E) complex V in digitonin-permeabilized and intact cells. Protein level of (F) ATP5a and (G) Sirt3. (H) Basal and maximal respiration by oxygen consumption of living cells. (I) Spectrophotometric analysis applied for measuring CV activity in backward direction using lactic dehydrogenase and pyruvate kinase as coupling enzymes. Mitochondrial (J) membrane potential and (K) superoxide levels measured by flow cytometry of TMRM (200nM, 30', 37°C) and Mitosox (2.5 μM, 45', 37°C) stained cells. (L) Protein expression of HSP60. (M) Representative immunoblots. The error bars are S.D. and asterisks indicate: *p < 0.05, **p < 0.01 and ***p < 0.001.

doi:10.1371/journal.pone.0131990.g002

Morphological analysis of cell junction and adhesion proteins in DAPIT over-expressing cells

The over-expression of DAPIT induced changes in cell morphology, from a regular cuboidal epithelial-like (control cells) to an irregularly sized and shaped morphology (DAPIT cells) with decreased intercellular separation, showing a polygonal, sheet-like appearance but unaffected cell projections (Fig 3D, lower panel), thereby suggesting an epithelial to mesenchymal transition (EMT).

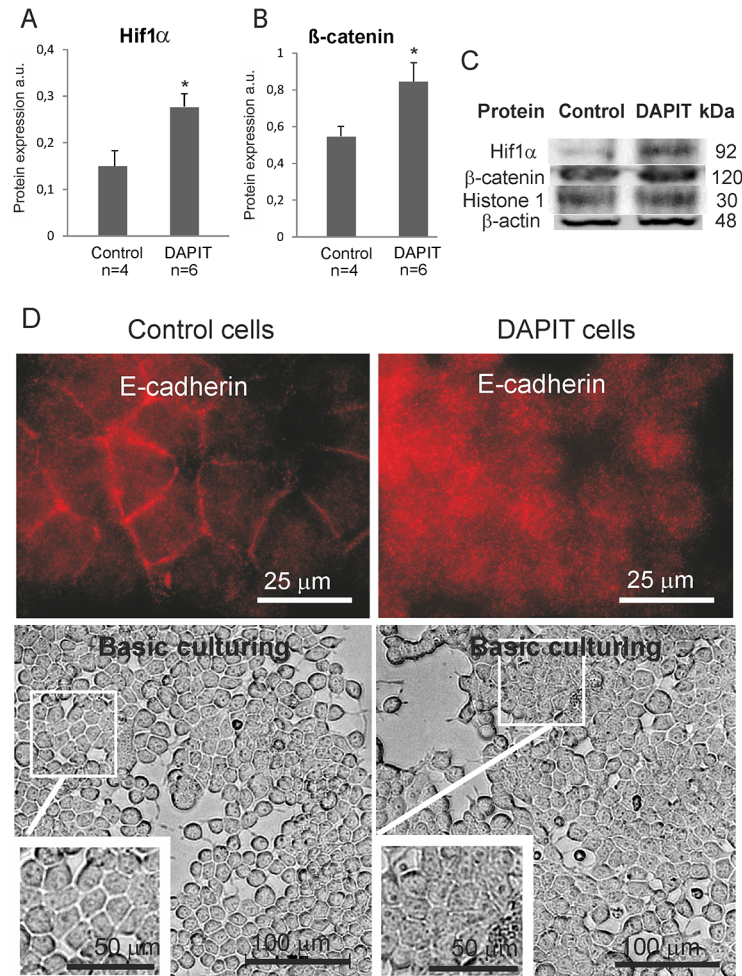


Fig 3. DAPIT over-expression regulates nuclear translocation of Hif1 α and β -catenin leading to morphological changes. Nuclear protein level of (A) Hif1 α and (B) β -catenin by Western blot. (C) Representative immunoblots. (D) Immunofluorescence of E-cadherin (upper panel, 100x magnification) and microscope view of living control and DAPIT cells (lower panel, 20x magnification). The error bars are S.D. and asterisk indicates * $p < 0.05$.

doi:10.1371/journal.pone.0131990.g003

Due to morphological changes in DAPIT cells, we investigated the expression of several cell junction and adhesion proteins (Fig 4). Protein levels of E-cadherin decreased significantly (Fig 4A and 4I), while N-cadherin, Connexin 43, ZO-1, Vimentin, Integrin $\alpha 2$, and their modulator RhoA GTPase were all increased (Fig 4B–4G and 4I). We also observed increased (although non-significant) expression of the SMA (Fig 4H and 4I). Interestingly, such pattern of expression is reminiscent of the EMT observed, for example, in embryogenesis, wound healing and cancer.

Cell growth, mortality, migration and adhesion

In order to study the effect of DAPIT over-expression on cell physiology and to clarify the consequences of the EMT-like phenotype, we examined cell growth, mortality, cell cycle, migration and adhesion capacity (Fig 5). According to hemocytometer calculation, DAPIT cells showed slower growth during the active growing phase (Fig 5A, days 1–3). Since the mortality rate, measured at day 2, was not altered (Fig 5B), we attribute the slower cell proliferation to a

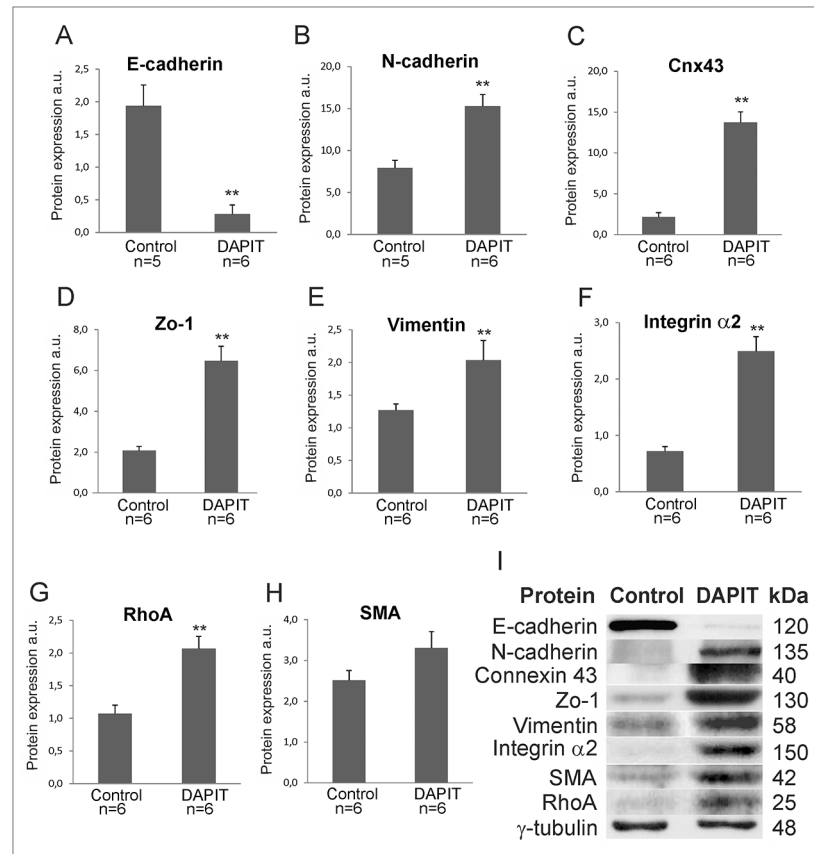


Fig 4. Modification in cell junction and adhesion proteins correspond to EMT-like changes in DAPIT cells. (A-H) Modulation of cell junction proteins and RhoA. Protein expression by Western blot in 20µg of cell lysate. (I) Representative immunoblots. The error bars are S.D. and asterisks indicates **p<0.01.

doi:10.1371/journal.pone.0131990.g004

reduced proliferation rather than increased cell death. To test this premise, we followed the cell cycle in synchronized cells. After withdrawal of thymidine, DAPIT cells entered the G1 phase approximately four hours later than control cells (seen at time point 4 h) (Fig 5C, dark grey). This retardation results also significant difference in S phase from 12 h on (light grey) and in G2 (medium grey) at 4 h onwards, thereby confirming the slower growth of DAPIT cells.

The unexpected decreased migration capacity (Fig 5D) of DAPIT cells is in contradiction with EMT and suggests a suppressive trait. The attachment capacity of the cells remained unchanged, whereas cell detachment was enhanced (Fig 5E and 5F), indicating adhesion characteristics typical of EMT.

Glucose consumption and lactate production

The miss-functional ATP-synthase, reduced growth and HIF1α stabilization in DAPIT cells suggested a metabolic shift from aerobic respiration to glycolysis. Therefore, we measured, in parallel, glucose consumption and lactate production in DAPIT cells. As we anticipated, DAPIT cells consumed more glucose and produced more lactate during the exponential stage of their growth at days 1–3 (Fig 5G and 5H). Cell growth reached a plateau at day 4, and this was associated with a decreased glucose consumption and lactate production, a metabolic switch attributable to cell quiescence (see Valcourt et al. [53] for a review).

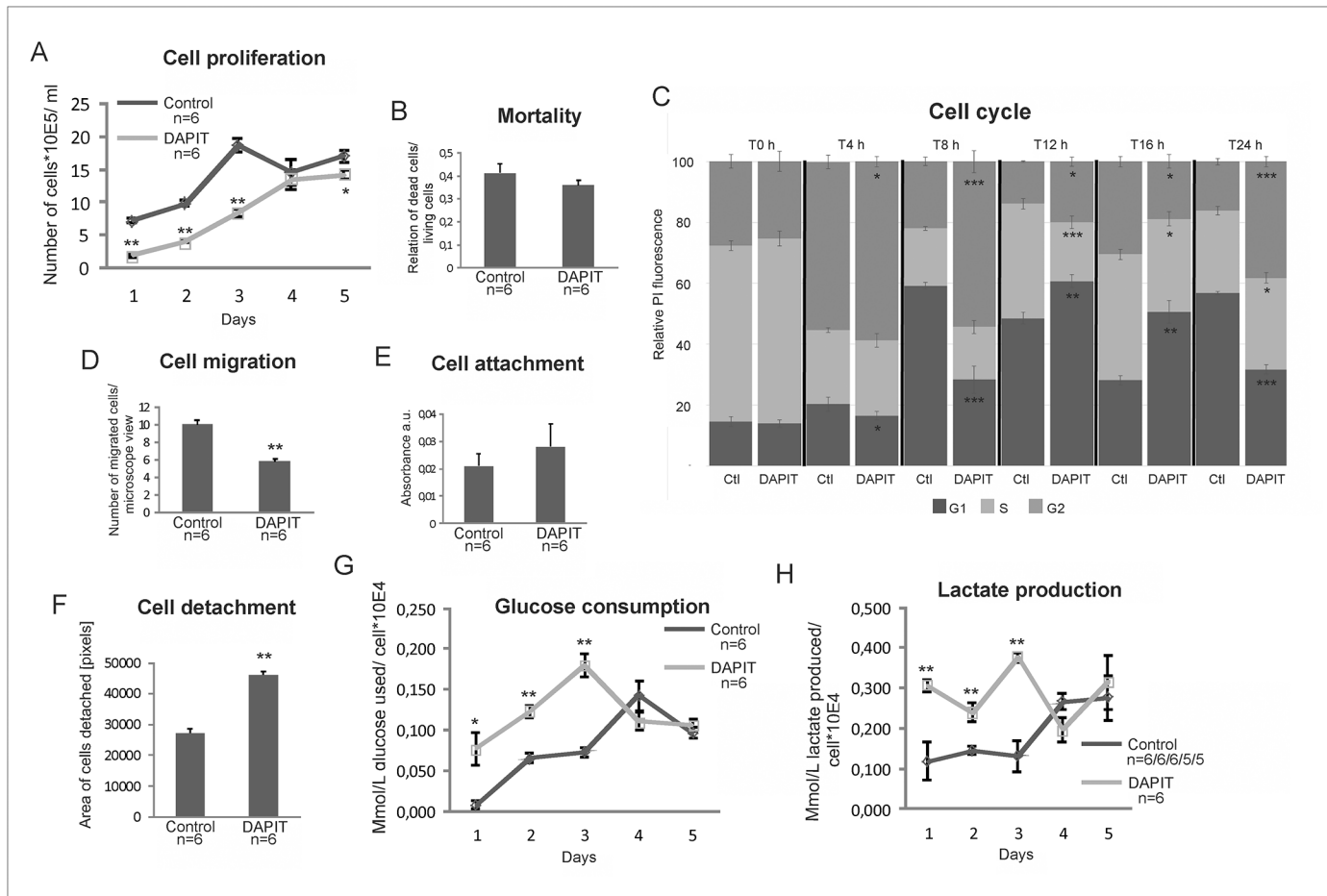


Fig 5. Characteristics of cell behaviour and metabolism of DAPIT over-expressing cells. (A) Cell proliferation by cell counting. (B) Mortality rate at day two of culture. (C) Flow cytometric analysis of cell cycle progression after double thymidine synchronization of the cells. (D) Cell migration by scratch wound assay. Cell adhesion capacity; (E) attachment measured by PMS/MTS test and (F) detachment according to migration test. (G) Glucose consumption and (H) lactate production measured in parallel from the culture medium of the cell proliferation test. The error bars are S.D. and asterisks indicate: * $p < 0.05$ and ** $p < 0.01$.

doi:10.1371/journal.pone.0131990.g005

Usmg5 copy number in cancers

Since DAPIT over-expression induced EMT and glycolytic switch in HEK293T cells, we tested if DAPIT is over-presented in cancers. The Oncomine Cancer Genomics database revealed a duplication (4 copies) of *Usmg5* copy number in a large panel of cancers (Table 2). *Usmg5* was ranked within 10% of top genes duplicated in various brain, pancreas and liver cancers, within 15% in sarcomas, kidney, lung and gastric cancers, and within approximately 20% in leukemia, lymphoma, and breast- and ovarian cancers. These data strongly suggest a role for DAPIT over-expression in cancers.

Discussion

The OXPHOS system comprises five multi-subunit enzymes known as complexes I, II, III, IV and V. The electron transfer through complexes I-IV is coupled to proton translocation across the inner membrane. This results transmembrane electrochemical potential which is converted into chemical energy in the form of ATP by H^+ -ATP synthase (CV).

Table 2. Cancers expressing increased genomic *Usmg5* copy number in Oncomine cancer genomics database.

Classification	Cancer type	DNA copy number	*Gene rank %	Oncomine datasets
Brain	Astrocytoma	4,40	1	Beroukhim Brain [31]
	Astrocytoma	4,50	3	TCGA Brain 2 [N/A]
	Astrocytoma	4,36	4	Kotliarov Brain [32]
	Astrocytoma	4,07	12	Northcott Brain 4 [33]
	Head and Neck Cancer Cell Line	4,13	2	Beroukhim Multi-cancer [34]
	Head and Neck Cancer	4,11	5	Beroukhim Multi-cancer [34]
	Head and Neck Cancer	4,13	24	Barretina CellLine 2 [35]
	Mixed Glioma	4,89	1	TCGA Brain 2 [N/A]
	Oligodendroglial Tumor	4,73	2	Kotliarov Brain [32]
	Oligodendroglial Tumor	5,07	3	TCGA Brain 2 [N/A]
	Oligodendroglial Tumor	4,29	7	Beroukhim Brain [31]
Pancreas	Pancreatic Cancer	4,19	6	Barretina CellLine 2 [35]
Liver	Liver Cancer	4,33	4	Rothenberg CellLine [38]
	Liver Cancer	4,18	7	Barretina CellLine 2 [35]
	Liver Cancer Precursor	4,10	29	Chiang Liver 2 [46]
Sarcoma	Dedifferentiated Liposarcoma	4,12	9	Barretina Sarcoma 2 [37]
	Myxoid/Round Cell Liposarcoma	4,12	15	Barretina Sarcoma 2 [37]
	Sarcoma	4,12	8	Barretina CellLine 2 [35]
	Sarcoma	4,12	12	Wooster CellLine 2 [N/A]
	Sarcoma	4,10	13	Rothenberg CellLine [38]
	Sarcoma Cell Line	4,14	24	Beroukhim Multi-cancer [34]
Kidney	Kidney Cancer	4,67	2	Neale Multi-cancer 2 [43]
	Kidney Cancer	4,20	12	Barretina CellLine 2 [35]
	Hereditary Clear Cell Renal Cell Carcinoma	4,07	26	Beroukhim Renal 2 [47]
Lung	Non-Small Cell Lung Carcinoma	4,13	10	Weiss Lung [40]
	Non-Small Cell Lung Carcinoma	4,18	12	TCGA Lung 2 [N/A]
Gastric	Gastric Adenocarcinoma	4,06	14	Deng Gastric [36]
	Gastric Mixed Adenocarcinoma vs. Normal	4,10	15	Deng Gastric [36]
	Gastrointestinal Stromal Tumor	4,40	17	Barretina Sarcoma 4 [37]
	Colon Adenocarcinoma	4,06	14	TCGA Colorectal 2 [N/A]
	Colorectal Cancer	4,13	13	Rothenberg CellLine [38]
	Colorectal Cancer	4,07	18	Barretina CellLine 2 [35]
	Colorectal Cancer	4,28	13	Jaiswal Multi-cancer [39]
	Leukemia	Leukemia	4,46	5
Leukemia	Refractory Anemia with Excess Blasts-1 vs. Normal	4,13	13	Yoshida Leukemia [44]
	Chronic Myelomonocytic Leukemia-1 vs. Normal	4,12	14	Yoshida Leukemia [44]
	Leukemia Cell Line	4,17	20	Beroukhim Multi-cancer [34]
	Plasma Cell Leukemia	4,09	21	Chapman Myeloma 2 [45]
	Breast	Mixed Lobular and Ductal Breast Carcinoma	4,11	7
Breast	Papillary Breast Carcinoma	4,08	11	TCGA Breast 2 [N/A]
	Mucinous Breast Carcinoma	4,08	20	Curtis Breast 2 [42]
	Lobular Breast Carcinoma	4,07	23	TCGA Breast 2 [N/A]
	Ductal Breast Carcinoma in Situ	4,06	24	Curtis Breast 2 [42]
	Ovarian	Ovarian Cancer	4,09	16
Ovarian	Endometrial Endometrioid Adenocarcinoma vs. Normal	4,10	17	TCGA Endometrium [N/A]
	Endometrial Serous Adenocarcinoma vs. Normal	4,16	29	TCGA Endometrium [N/A]

(Continued)

Table 2. (Continued)

Classification	Cancer type	DNA copy number	*Gene rank %	Oncomine datasets
Lymphoma	Lymphoma	4,15	21	Wooster CellLine 2 [N/A]
	Lymphoma	4,08	28	Barretina CellLine 2 [35]
Other	Oral Cavity Squamous Cell Carcinoma vs. Normal	4,03	48	Peng Head-Neck 2 [48]

N/A indicating not available.

* Indicating % of top genes duplicated, within which *Usmg5* was ranked.

doi:10.1371/journal.pone.0131990.t002

DAPIT has been shown to be a structural component of H⁺-ATP synthase and its deletion resulted in the loss of H⁺-ATP synthase [2–5]. As DAPIT mRNA and/or protein levels are increased in various diseases [6–8, 10–14] we hypothesized that in addition to its structural role, DAPIT could also be a regulatory component of H⁺-ATP synthase. In consequence, DAPIT up-regulation could lead to both structural changes and alteration in respiratory chain regulation. In the present study, we stably transfected DAPIT into HEK293T cells. The strategy we used permits both the transgene and an EGFP reporter to be translated from a single bicistronic mRNA without formation of a fusion protein. The DNA sequence of the DAPIT transgene appeared unaltered and the expression of the protein was confirmed. We emphasized the effect of DAPIT over-expression on mitochondrial level by normalizing the reported mitochondrial parameters with concomitant mass. Accordingly, DAPIT up-regulation did not alter the mitochondrial H⁺-ATP synthase levels in terms of the expression of ATP5a (a subunit of the H⁺-ATP synthase enzymatic channel). Still, DAPIT cells showed an increased basal respiration and inhibitor-sensitive oxygen consumption of complexes I, II and IV, but decreased activity of H⁺-ATP-synthase. This result is in line with cellular increase in lactate production. Therefore, we suggest that increased maximal respiration is due to increased capacity of complexes I-IV. Since mitochondrial mass was decreased, we conclude that DAPIT positively modulates respiration. In agreement with this hypothesis, we observed increased membrane potential together with citrate synthase activity and VDAC1 expression, an issue suggesting increased availability and use of respiratory chain substrates. As DAPIT cells are glycolytic, these may have altered their catabolic balance in order to fuel the respiration. Accordingly, an accumulation of superoxide production per mitochondria and DAPIT cell was also observed. Interestingly, it was recently reported that intracellular balance of respiratory substrates contribute to the cell decision between differentiation and stemness [54].

Most of the energy needed by human cells is provided by mitochondria in the form of ATP through oxidative phosphorylation. Mitochondrial adenosine triphosphate (ATP) synthesis, while essential to maintain homeostasis, is sensitive to oxidative damages and other cellular injuries [49], and alterations of H⁺-ATP synthase biogenesis increases ROS production while decreasing energy production [55]. ROS damages could disrupt mitochondrial integrity and lead to apoptosis or necrosis, depending on cellular energy status. Regardless of increased mitochondrial respiration and good coupling, the activity of H⁺-ATP-synthase was decreased in DAPIT cells. This decrease could be due to diminished number of H⁺-ATP-synthase complexes in mitochondrial inner membrane, the down-regulation of its enzymatic/hydrolytic activity or both. The decreased H⁺-ATP-synthase activity is well documented in human tumors where the Inhibitory Factor 1 (IF1) of H⁺-ATP-synthase mediates the metabolic shift of cancer cells to aerobic glycolysis with mitochondrial hyperpolarization and subsequent production of superoxide radical [56,57], the mitochondrial characteristics also seen in DAPIT cells. Moreover, the regulated degradation of IF1 controlled energy metabolism during osteogenic

differentiation of human mesenchymal stem cells by hindering their self-renewal, but favouring differentiation [58]. These reported studies clarify a mito-cellular mechanism by which the activity of H⁺-ATP-synthase is physiologically regulated in stemness, differentiation and cancer, process where DAPIT over-expression might be involved in. Altogether, these results fit with the idea that DAPIT over-expression accelerates mitochondrial respiration although, or because, inactivating H⁺-ATP synthase.

Cells can adapt to mitochondrial dysfunctions and energy depletion by regulating mitochondrial biogenesis [49,50]. We observed significant decrease in mtDNA level due to inactivation of mitogenesis in impaired H⁺-ATP-synthase DAPIT cells.

Hif1 induction is reported to shift aerobic cellular metabolism to glycolysis [15–17,59]. Accordingly, translocation of Hif1a to the nucleus was induced in DAPIT cells, and both glucose consumption and lactate production were significantly enhanced. Interestingly, these changes are reminiscent of the Warburg effect observed in many cancers and stem cells.

Hif1 α stabilization is also involved in EMT, which is a process of epithelial cells losing cell-cell junctions and baso-apical polarity while acquiring plasticity, mobility, invasive capacity, stem-like characteristics and resistance to apoptosis [60–62]. This cell biology program is active in embryos, fibrosis, wound healing and in promoting metastasis in cancer. In addition to Hif1a, the Wnt/ β -catenin pathway signalling also controls EMT upon hypoxic stress in cancer [60,61]. One of the hallmarks of EMT in cancer is the disappearance of E-cadherin from the cellular membrane and its replacement with N-cadherin. Several key transcription factors regulating E-cadherin expression and/or the fate of other epithelial molecules are direct or indirect transcriptional targets of the canonical Wnt pathway [61]. Accordingly, we saw E-cadherin shift to N-cadherin (and regulation of various other proteins) in DAPIT cells and nuclear expression of β -catenin indicating activation of Wnt signalling. All these molecular findings provide evidence that supports the involvement of DAPIT over-expression in altered mitochondrial function in cancer and stemness.

EMT resembling change in DAPIT cells induced transformation of regular cuboidal epithelial-like cells into irregularly sized and shaped cells showing a polygonal, tightly packed, sheet-like appearance with short projections reminiscent of mesenchymal-like cells. However, in contrast to mesenchymal cells, DAPIT cells presented an unexpected decrease in migration capacity. This suggests that some of the defects caused by DAPIT over-expression suppressed the normally improved migratory capacity of mesenchymal-like cells. However, if cell adhesion was unaltered, dissociation from the surface was more frequent.

DAPIT cells grew slower while presenting normal viability. We studied the cell-cycle progression by thymidine synchronization and found that DAPIT cells were arrested in G1. Previously it was shown that the activation of Hif1 α (which occurred in DAPIT cells) in embryonic stem cells and colon cancer cells under hypoxia inhibited transcriptional activity of β -catenin resulting in G1 arrest [63,64]. Taken together, the physiological properties of DAPIT cells resemble an EMT-like phenotype with mitochondrial impairment leading to glycolytic metabolism, decreased cell proliferation and migration, and an increase in cell dissociation from the surface, the issues active in varying conditions of cancer and stem cells. Interestingly, searching in the Oncomine cancer genomics database revealed a duplication in *Usmg5* copy number in various cancers (Table 2). This was ranked within 15% of top of duplicated genes in classified brain, pancreas, liver, sarcoma, kidney, lung, gastric, leukemia, breast and ovarian cancers. Despite the link between DAPIT and the tumorigenic capacity has not been sufficiently demonstrated, this result strengthens a correlative involvement of DAPIT in cancer and suggests a possible oncogenic function for it.

In summary, we have characterized the effect of a stable over-expression of DAPIT in a cell culture model; at the level of morphology, molecular biology, metabolic homeostasis and cell

behavior. The over-expression of DAPIT in HEK293T cells impaired mitochondria promoting the activation of Hif1 α and Wnt/ β -catenin signaling, which resulted in a shift of aerobic metabolism to more glycolytic direction and in cell dedifferentiation resembling EMT. We suggest that DAPIT over-expression couples changes in mitochondrial metabolism to physiological and pathophysiological activities at the cellular level, possibly including cancer.

Supporting Information

S1 Fig. Mitochondrial metabolism (activity) at cellular level. Protein levels estimated by Western blot of (A) DAPIT and (B) VDAC. (C) Citrate synthase activity. (D) Protein level of NDUFS3. Inhibitor-sensitive oxygen consumption of (E) complexes I, II, IV and (F) complex V in digitonin-permeabilized and intact cells. Protein level of (G) ATP5a and (H) Sirt3. (I) Basal and maximal respiration. (J) H⁺-ATP synthase activity measured by spectrophotometric analysis. Mitochondrial (K) membrane potential and (L) superoxide levels at cellular level measured by flow cytometry of TMRM (200nM, 30', 37°C) and MitoSox (2,5 μ M, 45', 37°C) stained cells. (M) Protein level of HSP60. Representative immunoblots are shown in [Fig 2M](#). The error bars are S.D. and asterisks indicate: **p<0.01. (PDF)

Acknowledgments

The authors would like to thank Cristina Nadalutti, Kaisa Teittinen, Mervi Matero and Risto Puurtinen for technical help and useful discussions.

Author Contributions

Conceived and designed the experiments: H. Kontro H. Kainulainen. Performed the experiments: H. Kontro GC PR ED. Analyzed the data: H. Kontro GC PR ED. Contributed reagents/materials/analysis tools: H. Kontro ED PR H. Kainulainen. Wrote the paper: H. Kontro GC PR ED H. Kainulainen. Set up and optimized the method for HEK293T cells used in membrane potential and superoxide analysis: GC.

References

1. Paivarinne H, Kainulainen H. DAPIT, a novel protein down-regulated in insulin-sensitive tissues in streptozotocin-induced diabetes. *Acta Diabetol.* 2001; 38(2):83–86. PMID: [11757806](#)
2. Chen R, Runswick MJ, Carroll J, Fearnley IM, Walker JE. Association of two proteolipids of unknown function with ATP synthase from bovine heart mitochondria. *FEBS Lett.* 2007; 581(17):3145–3148. doi: [10.1016/j.febslet.2007.05.079](#) PMID: [17570365](#)
3. Meyer B, Wittig I, Trifilieff E, Karas M, Schagger H. Identification of two proteins associated with mammalian ATP synthase. *Mol Cell Proteomics.* 2007; 6(10):1690–1699. doi: [10.1074/mcp.M700097-MCP200](#) PMID: [17575325](#)
4. Lee J, Ding S, Walpole TB, Holding AN, Montgomery MG, Fearnley IM, et al. Organisation of Subunits in the Membrane Domain of the Bovine F-ATPase Revealed by Covalent Cross-linking. *J Biol Chem.* 2015 Apr 7. doi: [10.1074/jbc.M115.645283](#)
5. Ohsakaya S, Fujikawa M, Hisabori T, Yoshida M. Knockdown of DAPIT (diabetes-associated protein in insulin-sensitive tissue) results in loss of ATP synthase in mitochondria. *J Biol Chem.* 2011; 286(23):20292–20296. doi: [10.1074/jbc.M110.198523](#) PMID: [21345788](#)
6. Kontro H, Hulmi JJ, Rahkila P, Kainulainen H. Cellular and tissue expression of DAPIT, a phylogenetically conserved peptide. *Eur J Histochem.* 2012; 56(2):e18. doi: [10.4081/ejh.2012.18](#) PMID: [22688299](#)
7. Zhang L, Yu C, Vasquez FE, Galeva N, Onyango I, Swerdlow RH, et al. Hyperglycemia alters the schwann cell mitochondrial proteome and decreases coupled respiration in the absence of superoxide production. *J Proteome Res.* 2010; 9(1):458–471. doi: [10.1021/pr900818g](#) PMID: [19905032](#)

8. McFarland MA, Ellis CE, Markey SP, Nussbaum RL. Proteomics analysis identifies phosphorylation-dependent alpha-synuclein protein interactions. *Mol Cell Proteomics*. 2008; 7(11):2123–2137. doi: [10.1074/mcp.M800116-MCP200](https://doi.org/10.1074/mcp.M800116-MCP200) PMID: [18614564](https://pubmed.ncbi.nlm.nih.gov/18614564/)
9. Barrett T, Wilhite SE, Ledoux P, Evangelista C, Kim IF, Tomashevsky M, et al. NCBI GEO: Archive for functional genomics data sets—update. *Nucleic Acids Res*. 2013; 41(Database issue):D991–5. doi: [10.1093/nar/gks1193](https://doi.org/10.1093/nar/gks1193) PMID: [23193258](https://pubmed.ncbi.nlm.nih.gov/23193258/)
10. Lee CH, Bang SH, Lee SK, Song KY, Lee IC. Gene expression profiling reveals sequential changes in gastric tubular adenoma and carcinoma in situ. *World J Gastroenterol*. 2005; 11(13):1937–1945. PMID: [15800983](https://pubmed.ncbi.nlm.nih.gov/15800983/)
11. Selga E, Morales C, Noe V, Peinado MA, Ciudad CJ. Role of caveolin 1, E-cadherin, enolase 2 and PKCalpha on resistance to methotrexate in human HT29 colon cancer cells. *BMC Med Genomics*. 2008; 1:35-8794-1-35. doi: [10.1186/1755-8794-1-35](https://doi.org/10.1186/1755-8794-1-35)
12. Li M, Balch C, Montgomery JS, Jeong M, Chung JH, Yan P, et al. Integrated analysis of DNA methylation and gene expression reveals specific signaling pathways associated with platinum resistance in ovarian cancer. *BMC Med Genomics*. 2009; 2:34-8794-2-34. doi: [10.1186/1755-8794-2-34](https://doi.org/10.1186/1755-8794-2-34)
13. Chang TC, Wentzel EA, Kent OA, Ramachandran K, Mullendore M, Lee KH, et al. Transactivation of miR-34a by p53 broadly influences gene expression and promotes apoptosis. *Mol Cell*. 2007; 26(5):745–752. doi: [10.1016/j.molcel.2007.05.010](https://doi.org/10.1016/j.molcel.2007.05.010) PMID: [17540599](https://pubmed.ncbi.nlm.nih.gov/17540599/)
14. Koza RA, Nikonova L, Hogan J, Rim JS, Mendoza T, Faulk C, et al. Changes in gene expression foreshadow diet-induced obesity in genetically identical mice. *PLoS Genet*. 2006; 2(5):e81. doi: [10.1371/journal.pgen.0020081](https://doi.org/10.1371/journal.pgen.0020081) PMID: [16733553](https://pubmed.ncbi.nlm.nih.gov/16733553/)
15. Cairns RA, Harris IS, Mak TW. Regulation of cancer cell metabolism. *Nat Rev Cancer*. 2011; 11(2):85–95. doi: [10.1038/nrc2981](https://doi.org/10.1038/nrc2981) PMID: [21258394](https://pubmed.ncbi.nlm.nih.gov/21258394/)
16. Wallace DC. Mitochondria and cancer. *Nat Rev Cancer*. 2012; 12(10):685–698. doi: [10.1038/nrc3365](https://doi.org/10.1038/nrc3365) PMID: [23001348](https://pubmed.ncbi.nlm.nih.gov/23001348/)
17. Sena LA, Chandel NS. Physiological roles of mitochondrial reactive oxygen species. *Mol Cell*. 2012; 48(2):158–167. doi: [10.1016/j.molcel.2012.09.025](https://doi.org/10.1016/j.molcel.2012.09.025) PMID: [23102266](https://pubmed.ncbi.nlm.nih.gov/23102266/)
18. Wheaton WW, Chandel NS. Hypoxia. 2. hypoxia regulates cellular metabolism. *Am J Physiol Cell Physiol*. 2011; 300(3):C385–93. doi: [10.1152/ajpcell.00485.2010](https://doi.org/10.1152/ajpcell.00485.2010) PMID: [21123733](https://pubmed.ncbi.nlm.nih.gov/21123733/)
19. Sullivan LB, Martinez-Garcia E, Nguyen H, Mullen AR, Dufour E, Sudarshan S, et al. The proto-oncogene metabolite fumarate binds glutathione to amplify ROS-dependent signaling. *Mol Cell*. 2013; 51(2):236–248. doi: [10.1016/j.molcel.2013.05.003](https://doi.org/10.1016/j.molcel.2013.05.003) PMID: [23747014](https://pubmed.ncbi.nlm.nih.gov/23747014/)
20. Huang JY, Hirschev MD, Shimazu T, Ho L, Verdin E. Mitochondrial sirtuins. *Biochim Biophys Acta*. 2010; 1804(8):1645–1651. doi: [10.1016/j.bbapap.2009.12.021](https://doi.org/10.1016/j.bbapap.2009.12.021) PMID: [20060508](https://pubmed.ncbi.nlm.nih.gov/20060508/)
21. Hallows WC, Lee S, Denu JM. Sirtuins deacetylate and activate mammalian acetyl-CoA synthetases. *Proc Natl Acad Sci U S A*. 2006; 103(27):10230–10235. doi: [10.1073/pnas.0604392103](https://doi.org/10.1073/pnas.0604392103) PMID: [16790548](https://pubmed.ncbi.nlm.nih.gov/16790548/)
22. Schlicker C, Gertz M, Papatheodorou P, Kachholz B, Becker CF, Steegborn C. Substrates and regulation mechanisms for the human mitochondrial sirtuins Sirt3 and Sirt5. *J Mol Biol*. 2008; 382(3):790–801. doi: [10.1016/j.jmb.2008.07.048](https://doi.org/10.1016/j.jmb.2008.07.048) PMID: [18680753](https://pubmed.ncbi.nlm.nih.gov/18680753/)
23. Fukuoh A, Cannino G, Gerards M, Buckley S, Kazancioglu S, Scialo F, et al. Screen for mitochondrial DNA copy number maintenance genes reveals essential role for ATP synthase. *Mol Syst Biol*. 2014; 10(6):734. doi: [10.15252/msb.20145117](https://doi.org/10.15252/msb.20145117)
24. Cannino G, El-Khoury R, Pirinen M. Glucose modulates respiratory complex I activity in response to acute mitochondrial dysfunction. *J Biol Chem*. 2012; 287(46):38729–38740. doi: [10.1074/jbc.M112.386060](https://doi.org/10.1074/jbc.M112.386060) PMID: [23007390](https://pubmed.ncbi.nlm.nih.gov/23007390/)
25. Rustin P, Chretien D, Bourgeron T, Gérard B, Rötig A, Saudubray JM, et al. Biochemical and molecular investigations in respiratory chain deficiencies. *Clin Chim Acta*. 1994; 228(1):35–51. PMID: [7955428](https://pubmed.ncbi.nlm.nih.gov/7955428/)
26. Benit P, Goncalves S, Philippe Dassa E, Briere JJ, Martin G, Rustin P. Three spectrophotometric assays for the measurement of the five respiratory chain complexes in minuscule biological samples. *Clin Chim Acta*. 2006; 374(1–2):81–86. doi: [10.1016/j.cca.2006.05.034](https://doi.org/10.1016/j.cca.2006.05.034) PMID: [16828729](https://pubmed.ncbi.nlm.nih.gov/16828729/)
27. Teittinen KJ, Karkkainen P, Salonen J, Rönholm G, Korkeamäki H, Vihinen M, et al. Nucleolar proteins with altered expression in leukemic cell lines. *Leuk Res*. 2012; 36(2):232–236. doi: [10.1016/j.leukres.2011.06.038](https://doi.org/10.1016/j.leukres.2011.06.038) PMID: [21783252](https://pubmed.ncbi.nlm.nih.gov/21783252/)
28. Bradford MM. A rapid and sensitive method for the quantitation of microgram quantities of protein utilizing the principle of protein-dye binding. *Anal Biochem*. 1976; 72:248–254. PMID: [942051](https://pubmed.ncbi.nlm.nih.gov/942051/)
29. Laemmli UK. Cleavage of structural proteins during the assembly of the head of bacteriophage T4. *Nature*. 1970; 227(5259):680–685. PMID: [5432063](https://pubmed.ncbi.nlm.nih.gov/5432063/)

30. Rhodes DR, Yu J, Shanker K, Deshpande N, Varambally R, Ghosh D, et al. ONCOMINE: A cancer microarray database and integrated data-mining platform. *Neoplasia*. 2004; 6(1):1–6. PMID: [15068665](#)
31. Beroukhim R, Getz G, Nghiemphu L, Barretina J, Hsueh T, Linhart D, et al. Assessing the significance of chromosomal aberrations in cancer: Methodology and application to glioma. *Proc Natl Acad Sci U S A*. 2007; 104(50):20007–20012. doi: [10.1073/pnas.0710052104](#) PMID: [18077431](#)
32. Kotliarov Y, Steed ME, Christopher N, Walling J, Su Q, Center A, et al. High-resolution global genomic survey of 178 gliomas reveals novel regions of copy number alteration and allelic imbalances. *Cancer Res*. 2006; 66(19):9428–9436. doi: [10.1158/0008-5472.CAN-06-1691](#) PMID: [17018597](#)
33. Northcott PA, Shih DJ, Peacock J, Garzia L, Morrissy AS, Zichner T, et al. Subgroup-specific structural variation across 1,000 medulloblastoma genomes. *Nature*. 2012; 488(7409):49–56. doi: [10.1038/nature11327](#) PMID: [22832581](#)
34. Beroukhim R, Mermel CH, Porter D, Wei G, Raychaudhuri S, Donovan J, et al. The landscape of somatic copy-number alteration across human cancers. *Nature*. 2010; 463(7283):899–905. doi: [10.1038/nature08822](#) PMID: [20164920](#)
35. Barretina J, Caponigro G, Stransky N, Venkatesan K, Margolin AA, Kim S, et al. The cancer cell line encyclopedia enables predictive modelling of anticancer drug sensitivity. *Nature*. 2012; 483(7391):603–607. doi: [10.1038/nature11003](#) PMID: [22460905](#)
36. Deng N, Goh LK, Wang H, Das K, Tao J, Tan IB, et al. A comprehensive survey of genomic alterations in gastric cancer reveals systematic patterns of molecular exclusivity and co-occurrence among distinct therapeutic targets. *Gut*. 2012; 61(5):673–684. doi: [10.1136/gutjnl-2011-301839](#) PMID: [22315472](#)
37. Barretina J, Taylor BS, Banerji S, Ramos AH, Lagos-Quintana M, Decarolis PL, et al. Subtype-specific genomic alterations define new targets for soft-tissue sarcoma therapy. *Nat Genet*. 2010; 42(8):715–721. doi: [10.1038/ng.619](#) PMID: [20601955](#)
38. Rothenberg SM, Mohapatra G, Rivera MN, Winokur D, Greninger P, Nitta M, et al. A genome-wide screen for microdeletions reveals disruption of polarity complex genes in diverse human cancers. *Cancer Res*. 2010; 70(6):2158–2164. doi: [10.1158/0008-5472.CAN-09-3458](#) PMID: [20215515](#)
39. Jaiswal BS, Janakiraman V, Kljavin NM, Chaudhuri S, Stern HM, Wang W, et al. Somatic mutations in p85alpha promote tumorigenesis through class IA PI3K activation. *Cancer Cell*. 2009; 16(6):463–474. doi: [10.1016/j.ccr.2009.10.016](#) PMID: [19962665](#)
40. Weiss J, Sos ML, Seidel D, Peifer M, Zander T, Heuckmann JM, et al. Frequent and focal FGFR1 amplification associates with therapeutically tractable FGFR1 dependency in squamous cell lung cancer. *Sci Transl Med*. 2010; 2(62):62ra93. doi: [10.1126/scitranslmed.3001451](#)
41. Nikolsky Y, Sviridov E, Yao J, Dosymbekov D, Ustyansky V, Kaznacheev V, et al. Genome-wide functional synergy between amplified and mutated genes in human breast cancer. *Cancer Res*. 2008; 68(22):9532–9540. doi: [10.1158/0008-5472.CAN-08-308](#) PMID: [19010930](#)
42. Curtis C, Shah SP, Chin SF, Turashvili G, Rueda OM, Dunning MJ, et al. The genomic and transcriptomic architecture of 2,000 breast tumours reveals novel subgroups. *Nature*. 2012; 486(7403):346–352. doi: [10.1038/nature10983](#) PMID: [22522925](#)
43. Neale G, Su X, Morton CL, Phelps D, Gorlick R, Lock RB, et al. Molecular characterization of the pediatric preclinical testing panel. *Clin Cancer Res*. 2008; 14(14):4572–4583. doi: [10.1158/1078-0432.CCR-07-5090](#) PMID: [18628472](#)
44. Yoshida K, Sanada M, Shiraishi Y, Nowak D, Nagata Y, Yamamoto R, et al. Frequent pathway mutations of splicing machinery in myelodysplasia. *Nature*. 2011; 478(7367):64–69. doi: [10.1038/nature10496](#) PMID: [21909114](#)
45. Chapman MA, Lawrence MS, Keats JJ, Cibulskis K, Sougnez C, Schinzel AC, et al. Initial genome sequencing and analysis of multiple myeloma. *Nature*. 2011; 471(7339):467–472. doi: [10.1038/nature09837](#) PMID: [21430775](#)
46. Chiang DY, Villanueva A, Hoshida Y, Peix J, Newell P, Minguez B, et al. Focal gains of VEGFA and molecular classification of hepatocellular carcinoma. *Cancer Res*. 2008; 68(16):6779–6788. doi: [10.1158/0008-5472.CAN-08-0742](#) PMID: [18701503](#)
47. Beroukhim R, Brunet JP, Di Napoli A, Mertz KD, Seeley A, Pires MM, et al. Patterns of gene expression and copy-number alterations in von-hippel lindau disease-associated and sporadic clear cell carcinoma of the kidney. *Cancer Res*. 2009; 69(11):4674–4681. doi: [10.1158/0008-5472.CAN-09-0146](#) PMID: [19470766](#)
48. Peng CH, Liao CT, Peng SC, Chen YJ, Cheng AJ, Juang JL, et al. A novel molecular signature identified by systems genetics approach predicts prognosis in oral squamous cell carcinoma. *PLoS One*. 2011; 6(8):e23452. doi: [10.1371/journal.pone.002345](#) PMID: [21853135](#)
49. Piantadosi CA, Suliman HB. Redox regulation of mitochondrial biogenesis. *Free Radic Biol Med*. 2012; 53(11):2043–2053. doi: [10.1016/j.freeradbiomed.2012.09.014](#) PMID: [23000245](#)

50. Scarpulla RC, Vega RB, Kelly DP. Transcriptional integration of mitochondrial biogenesis. *Trends Endocrinol Metab.* 2012; 23(9):459–466. doi: [10.1016/j.tem.2012.06.006](https://doi.org/10.1016/j.tem.2012.06.006) PMID: [22817841](https://pubmed.ncbi.nlm.nih.gov/22817841/)
51. Stein I, Itin A, Einat P, Skaliter R, Grossman Z, Keshet E. Translation of vascular endothelial growth factor mRNA by internal ribosome entry: Implications for translation under hypoxia. *Mol Cell Biol.* 1998; 18(6):3112–3119. PMID: [9584152](https://pubmed.ncbi.nlm.nih.gov/9584152/)
52. Czerwinska P, Kaminska B. Regulation of breast cancer stem cell features. *Contemp Oncol (Pozn).* 2015; 19(1A):A7–A15. doi: [10.5114/wo.2014.47126](https://doi.org/10.5114/wo.2014.47126)
53. Valcourt JR, Lemons JM, Haley EM, Kojima M, Demuren OO, Collier HA. Staying alive: Metabolic adaptations to quiescence. *Cell Cycle.* 2012; 11(9):1680–1696. doi: [10.4161/cc.19879](https://doi.org/10.4161/cc.19879) PMID: [22510571](https://pubmed.ncbi.nlm.nih.gov/22510571/)
54. Carey BW, Finley LW, Cross JR, Allis CD, Thompson CB. Intracellular alpha-ketoglutarate maintains the pluripotency of embryonic stem cells. *Nature.* 2015; 518(7539):413–416. doi: [10.1038/nature13981](https://doi.org/10.1038/nature13981) PMID: [25487152](https://pubmed.ncbi.nlm.nih.gov/25487152/)
55. Geromel V, Kadhom N, Cebalos-Picot I, Ouari O, Polidori A, Munnich A, et al. Superoxide-induced massive apoptosis in cultured skin fibroblasts harboring the neurogenic ataxia retinitis pigmentosa (NARP) mutation in the ATPase-6 gene of the mitochondrial DNA. *Hum Mol Genet.* 2001; 10(11):1221–1228. PMID: [11371515](https://pubmed.ncbi.nlm.nih.gov/11371515/)
56. Sanchez-Cenizo L, Formentini L, Aldea M, Ortega AD, García-Huerta P, Sánchez-Aragó M, et al. Up-regulation of the ATPase inhibitory factor 1 (IF1) of the mitochondrial H⁺-ATP synthase in human tumors mediates the metabolic shift of cancer cells to a Warburg phenotype. *J Biol Chem.* 2010; 285(33):25308–25313. doi: [10.1074/jbc.M110.146480](https://doi.org/10.1074/jbc.M110.146480) PMID: [20538613](https://pubmed.ncbi.nlm.nih.gov/20538613/)
57. Formentini L, Sanchez-Arago M, Sanchez-Cenizo L, Cuezva JM. The mitochondrial ATPase inhibitory factor 1 triggers a ROS-mediated retrograde prosurvival and proliferative response. *Mol Cell.* 2012; 45(6):731–742. doi: [10.1016/j.molcel.2012.01.008](https://doi.org/10.1016/j.molcel.2012.01.008) PMID: [22342343](https://pubmed.ncbi.nlm.nih.gov/22342343/)
58. Sanchez-Arago M, Garcia-Bermudez J, Martinez-Reyes I, Santacatterina F, Cuezva JM. Degradation of IF1 controls energy metabolism during osteogenic differentiation of stem cells. *EMBO Rep.* 2013; 14(7):638–644. doi: [10.1038/embor.2013.72](https://doi.org/10.1038/embor.2013.72) PMID: [23722655](https://pubmed.ncbi.nlm.nih.gov/23722655/)
59. Yang M, Soga T, Pollard PJ. Oncometabolites: Linking altered metabolism with cancer. *J Clin Invest.* 2013; 123(9):3652–3658. doi: [10.1172/JCI67228](https://doi.org/10.1172/JCI67228) PMID: [23999438](https://pubmed.ncbi.nlm.nih.gov/23999438/)
60. Talbot LJ, Bhattacharya SD, Kuo PC. Epithelial-mesenchymal transition, the tumor microenvironment, and metastatic behavior of epithelial malignancies. *Int J Biochem Mol Biol.* 2012; 3(2):117–136. PMID: [22773954](https://pubmed.ncbi.nlm.nih.gov/22773954/)
61. Valenta T, Hausmann G, Basler K. The many faces and functions of beta-catenin. *EMBO J.* 2012; 31(12):2714–2736. doi: [10.1038/emboj.2012.150](https://doi.org/10.1038/emboj.2012.150) PMID: [22617422](https://pubmed.ncbi.nlm.nih.gov/22617422/)
62. Zeisberg M, Neilson EG. Biomarkers for epithelial-mesenchymal transitions. *J Clin Invest.* 2009; 119(6):1429–1437. doi: [10.1172/JCI36183](https://doi.org/10.1172/JCI36183) PMID: [19487819](https://pubmed.ncbi.nlm.nih.gov/19487819/)
63. Carmeliet P, Dor Y, Herbert JM, Fukumura D, Brusselmans K, Dewerchin M, et al. Role of HIF-1alpha in hypoxia-mediated apoptosis, cell proliferation and tumour angiogenesis. *Nature.* 1998; 394(6692):485–490. doi: [10.1038/28867](https://doi.org/10.1038/28867) PMID: [9697772](https://pubmed.ncbi.nlm.nih.gov/9697772/)
64. Kaidi A, Williams AC, Paraskeva C. Interaction between beta-catenin and HIF-1 promotes cellular adaptation to hypoxia. *Nat Cell Biol.* 2007; 9(2):210–217. doi: [10.1038/ncb1534](https://doi.org/10.1038/ncb1534) PMID: [17220880](https://pubmed.ncbi.nlm.nih.gov/17220880/)

CORRECTION

Correction: DAPIT Over-Expression Modulates Glucose Metabolism and Cell Behaviour in HEK293T Cells

Heidi Kontro, Giuseppe Cannino, Pierre Rustin, Eric Dufour, Heikki Kainulainen

There are errors in the “Oncomine data analysis” section of the Materials and Methods. It should read:

Oncomine and CCLE data analysis

We used the Oncomine Cancer Genomics Data Analysis tool [30] and Cancer Cell Line Encyclopedia, CCLE [35] to mine *Usmg5* copy number profiles in a large subset of cancer cell lines [31, 34, 35, 38, 41, 65–69]. In the dataset, the $\log_2 (\geq 0,34)$ values were analyzed. The number of DNA copies ($= 2^{(2^{\text{y-axis value}})}$) were calculated as advised in Oncomine instructions.

There are errors in the “*Usmg5* copy number in cancers” section of the Results. It should read:

Usmg5 copy number in cancer cell lines

Since DAPIT over-expression induced EMT and glycolytic switch in HEK293T cells, we tested if DAPIT is over-presented in cancer cell lines. The Oncomine Cancer Genomics database and CCLE revealed a duplication (3–4 copies) of *Usmg5* copy number in a large panel of cell lines (Table 2) Several datasets indicated uniform increase in copy number in various lung (NCI-H1775, NCI-H1993, NCI-H1563, NCI-H1755, VMRC-LCD, SBC-5, NCI-H1703), gastric (HCT116, Hs746T, MKN74, SNU-668), ovarian (OVTOKO, MCAS), liver (SNU-398) and pancreatic (PSN1, PANC-1) cancer cell lines. The copy number was also confirmed in breast (SUM-52PE), endometrial (AN3CA), esophagus (OE33), hematopoietic (MPLM6), kidney (SNU-1272) and lymphoid (Ki-JK) cell lines, being encountered once in the others. These data strongly suggest a role for DAPIT over-expression in cancers.

There are errors in Table 2 and in its caption. Please see the corrected Table 2 and its correct caption below.

There are errors in the last sentence in the penultimate paragraph of the Discussion. It should read: Interestingly, searching in the Oncomine cancer genomics database and Cancer Cell Line Encyclopedia, CCLE, revealed a duplication in *Usmg5* copy number in various cancer cell lines (Table 2), highlighting several lung, gastric, ovarian, liver and pancreatic cancer cell lines by supporting fidelity in duplication. The copy number was also confirmed in some breast, endometrial, esophageal, hematopoietic, kidney and lymphoid cell lines. Despite the link between DAPIT and the tumorigenic capacity has not been sufficiently demonstrated, this result strengthens a correlative involvement of DAPIT in cancer and suggests a possible oncogenic function for it.

There are errors in the References. Please view the correct additional references, which are also corrected in Table 3 and the article text described above.



OPEN ACCESS

Citation: Kontro H, Cannino G, Rustin P, Dufour E, Kainulainen H (2015) Correction: DAPIT Over-Expression Modulates Glucose Metabolism and Cell Behaviour in HEK293T Cells. PLoS ONE 10(10): e0141036. doi:10.1371/journal.pone.0141036

Published: October 15, 2015

Copyright: © 2015 Kontro et al. This is an open access article distributed under the terms of the [Creative Commons Attribution License](https://creativecommons.org/licenses/by/4.0/), which permits unrestricted use, distribution, and reproduction in any medium, provided the original author and source are credited.

Table 2. Cancer cell lines expressing increased genomic *Usmg5* copy number in OncoPrint cancer genomics database and Cancer Cell Line Encyclopedia, CCLE.

Classification	Cancer type	Cell line	DNA copy number	OncoPrint dataset/ CCLE	
Bone	Osteosarcoma	143B	2,76	CCLE [31]	
Brain	Brain glioblastoma	A-172	3,48	Berouchim brain [35]	
	Cerebral glioblastoma	LN-18	2,78	Berouchim brain [35]	
Breast	Breast adenocarcinoma	MCF7	2,62	Nicolosky Breast [32]	
		SUM-52PE	3,60	Nicolosky Breast [32]	
	Breast carcinoma			3,42	Chin breast2 [65]
		CAL-51	3,28	Hu CellLine2 [66]	
		MDA-MB-468	2,96	Hu CellLine2 [66]	
		CAL-120	2,81	Hu CellLine2 [66]	
		Hs 578T	2,74	Hu CellLine2 [66]	
		MDA-MB-361	2,72	Hu CellLine2 [66]	
		HCC1806	2,62	CCLE [31]	
	Ductal breast carcinoma	T-47D	3,18	Nicolosky Breast [32]	
		MFM-223	2,85	Nicolosky Breast [32]	
	Squamous cell breast carcinoma, Acantholytic variant	HCC1806	2,88	Hu CellLine2 [66]	
Central nervous system	Cannabinoid receptor	CB1	2,69	CCLE [31]	
	Glioma	KSN60	2,59	CCLE [31]	
Endometrium	Endometrial adenocarcinoma	JHUEM2	2,60	CCLE [31]	
		AN3CA	2,60	CCLE [31]	
Esophagus	Eesophageal adenocarcinoma		2,59	Rothenberg CellLine [38]	
		JHESOAD1	2,61	CCLE [31]	
		OE33	2,77	CCLE [31]	
Gallbladder	Barrett's adenocarcinoma		2,65	Wooster CellLine [N/A]	
Gallbladder	Biliary tract cancer	SNU478	3,49	CCLE [31]	
Gastric	Cecum adenocarcinoma	LS411N	2,70	Lu colorectal [67]	
		NCI-H498	2,61	Lu colorectal [67]	
		NCI-H747	2,60	Lu colorectal [67]	
	Colon adenocarcinoma	SW620	2,88	Lu colorectal [67]	
		HCT-15	2,77	Lu colorectal [67]	
		LS180	2,72	Lu colorectal [67]	
	Colon carcinoma	HCT116		2,94	CCLE [31]
				2,78	Berouchim multicancer [34]
				2,78	Lu colorectal [67]
				2,77	Rothenberg CellLine [38]
	Gastric cancer	Hs 746T		3,54	Rothenberg CellLine [38]
				2,90	Palanisamy gastric [N/A]
		NCI-N87	3,41	Palanisamy gastric [N/A]	
		KATO111	3,34	Palanisamy gastric [N/A]	
		YCC-16	3,21	Palanisamy gastric [N/A]	
		HUG1N	3,02	CCLE [31]	
		YCC-9	3,00	Palanisamy gastric [N/A]	
YCC-6		2,85	Palanisamy gastric [N/A]		
Gastric tubular adenocarcinoma	SNU520	2,69	CCLE [31]		
	MKN74	2,74	CCLE [31]		
Gastrointestinal stromal tumor		2,57	Rothenberg CellLine [38]		
	GIST 882X	2,97	Berouchim multicancer [34]		
Signet ring cell gastric adenocarcinoma	SNU-668	2,93	CCLE [31]		
		2,80	Barretina CellLine 2 [31]		

(Continued)

Table 2. (Continued)

Classification	Cancer type	Cell line	DNA copy number	Oncomine dataset/ CCLE		
Hematopoietic tissue	Acute Myeloid Leukemia	CMK115	2,90	CCLE [31]		
		KASUMI1	2,85	CCLE [31]		
		CMK	2,67	CCLE [31]		
	M2-type of Myeloid Leukemia	KASUMI6	2,78	CCLE [31]		
	Blast phase cronic myelogenous leukemia	MOLM6	2,78	CCLE [31]		
			2,60	Barretina CellLine 2 [31]		
	Chronic myeloid leukemia	BV173	2,55	CCLE [31]		
	Leukemia	NCO2	2,53	CCLE [31]		
Erythroleukemia	TF-1	2,60	Barretina CellLine 2 [31]			
Kidney	Clear cell renal carcinoma	SNU-1272	3,13	CCLE [31]		
			2,77	Barretina CellLine 2 [31]		
	Renal carcinoma	UOK101	2,87	CCLE [31]		
	Human proximal tubular cell line, immortalized	HK2	2,67	CCLE [31]		
	Renal adenocarcinoma	ACHN	2,55	CCLE [31]		
Liver	Hepatocellular adenocarcinoma	SNU-398	2,84	CCLE [31]		
			2,75	Rothenberg CellLine [38]		
			2,72	Wooster CellLine [N/A]		
			2,59	Barretina CellLine 2 [31]		
	Hepatocellular carcinoma	LI7	3,40	CCLE [31]		
Lung	Lung adenocarcinoma	C3A	2,62	CCLE [31]		
			2,62	CCLE [31]		
		NCI-HI435	3,15	CCLE [31]		
			2,73	CCLE [31]		
		NCI-H1775	2,62	Lu lung [67]		
				NCI-H1993	2,79	Lu lung [67]
				2,72	Sos CellLine [69]	
		NCI-H1563	2,68	2,62	Wooster CellLine [N/A]	
				2,74	CCLE [31]	
		NCI-H1838	2,63	2,68	Lu lung [67]	
	2,63			Lu lung [67]		
	NCI-H1755	2,58	2,86	Sos CellLine [69]		
			2,58	Rothenberg CellLine [38]		
	VMRC-LCD	2,57	2,67	CCLE [31]		
			2,57	Rothenberg CellLine [38]		
	LU65A	2,75	Rothenberg CellLine [38]			
	Large cell lung carcinoma	Calu-6	2,59	Lu lung [67]		
	Giant cell lung carcinoma	LU65B	3,03	Rothenberg CellLine [38]		
	Small cell lung carcinoma	NCI-H510	2,83	CCLE [31]		
			DMS53	2,69	Olejniczak CellLine 2 [68]	
SBC-5		2,69	CCLE [31]			
		2,64	Rothenberg CellLine [38]			
DMS114		2,55	CCLE [31]			
Non-small cell lung carcinoma	NCI-H1581	2,67	CCLE [31]			
Squamous cell lung carcinoma	HCC1897	3,53	CCLE [31]			
		NCI-H1703	2,63	CCLE [31]		
	2,61	Wooster CellLine [N/A]				
Lung carcinoma	EPLC272H	2,56	CCLE [31]			

(Continued)

Table 2. (Continued)

Classification	Cancer type	Cell line	DNA copy number	Oncomine dataset/ CCLE
Lymphoid tissue	Anaplastic large cell lymphoma	Ki-JK	3,21	CCLE [31]
			2,80	Barretina CellLine 2 [31]
	Non-Hodking B cell Lymphoma	JM1	2,79	CCLE [31]
	Non-Hodking T cell Lymphoma	SR786	2,78	CCLE [31]
		SUDHL1	2,65	CCLE [31]
Splenic marginal zone B-cell lymphoma	SLVL	2,63	Rothenberg CellLine [38]	
Ovarian	Ovarian adenocarcinoma	TOV21G	2,98	CCLE [31]
		OVK18	2,89	CCLE [31]
		CAO V3	2,62	CCLE [31]
	Ovarian clear cell adenocarcinoma	OVTOKO	4,04	CCLE [31]
			3,20	Barretina CellLine 2 [31]
	Ovarian mucinous custadenocarcinoma	MCAS	3,05	CCLE [31]
			2,92	Rothenberg CellLine [38]
			2,68	Barretina CellLine 2 [31]
	Ovarian carcinoma	OVSAHO	2,72	CCLE [31]
	Ovarian carcinoma	OVK12	2,65	Barretina CellLine 2 [31]
Ovarian granulosa cell tumor	COV434	2,80	CCLE [31]	
Pancreas	Ampulla of Vater adenocarcinoma	SNU-478	3,08	Barretina CellLine 2 [31]
	Pancreatic adenocarcinoma	PSN1	2,75	CCLE [31]
			2,61	Barretina CellLine 2 [31]
			2,64	CCLE [31]
			2,53	Barretina CellLine2 [31]
	Panreatic carcinoma	PK1	2,53	CCLE [31]
			PK45H	2,63
YAPC			2,62	CCLE [31]
Skin	Cutaneous melanoma	A7	2,81	Wooster CellLine [N/A]
	Melanoma	IGR1	2,63	CCLE [31]
	Squamous cell adenocarcinoma	HCC95	2,78	Sos CellLine [69]
		HCC-15	2,59	Sos CellLine [69]
Thyroid	Follicular thyroid carcinoma	ML1	2,53	CCLE [31]

N/A indicating not available

doi:10.1371/journal.pone.0141036.t001

65. Chin SF, Teschendorff AE, Marioni JC, Wang Y, Barbosa-Morais NL, Throne NP et al. High-resolution aCGH and expression profiling identifies a novel genomic subtype of ER negative breast cancer. *Genome Biol.* 2007;8(10):R215. doi: [10.1186/gb-2007-8-10-r215](https://doi.org/10.1186/gb-2007-8-10-r215)

66. Hu X, Stern HM, Ge L, O'Brien C, Haydu L, Honchell CD, Haverty PM et al. Genetic alterations and oncogenic pathways associated with breast cancer subtypes. *Mol Cancer Res.* 2009 Apr;7(4):511–22. doi: [10.1158/1541-7786.MCR-08-0107](https://doi.org/10.1158/1541-7786.MCR-08-0107)

67. Lu X, Zhang K, Van Sant C, Coon J, Semizarov D. An algorithm for classifying tumors based on genomic aberrations and selecting representative tumor models. *BMC Med Genomics.* 2010 Jun 22;3:23. doi: [10.1186/1755-8794-3-23](https://doi.org/10.1186/1755-8794-3-23)

68. Olejniczak ET, Van Sant C, Anderson MG, Wang G, Tahir SK, Sauter G et al. Integrative genomic analysis of small-cell lung carcinoma reveals correlates of sensitivity to bcl-2 antagonists and uncovers novel chromosomal gains. *Mol Cancer Res.* 2007 Apr;5(4):331–9. Doi: [10.1158/1541-7786](https://doi.org/10.1158/1541-7786)

69. Sos ML, Michel K, Zander T, Weiss J, Frommolt P, Peifer M et al. Predicting drug susceptibility of non-small cell lung cancers based on genetic lesions. *J Clin Invest*. 2009; Jun;119(6):1727–40. doi: [10.1172/JCI37127](https://doi.org/10.1172/JCI37127)

Reference

1. Kontro H, Cannino G, Rustin P, Dufour E, Kainulainen H (2015) DAPIT Over-Expression Modulates Glucose Metabolism and Cell Behaviour in HEK293T Cells. *PLoS ONE* 10(7): e0131990. doi: [10.1371/journal.pone.0131990](https://doi.org/10.1371/journal.pone.0131990) PMID: [26161955](https://pubmed.ncbi.nlm.nih.gov/26161955/)

CORRECTION

Correction: DAPIT Over-Expression Modulates Glucose Metabolism and Cell Behaviour in HEK293T Cells

Heidi Kontro, Giuseppe Cannino, Pierre Rustin, Eric Dufour, Heikki Kainulainen

There are errors in the References. Please view the correct additional references here.

31. Barretina J, Caponigro G, Stransky N, Venkatesan K, Margolin AA, Kim S, et al. The cancer cell line encyclopedia enables predictive modelling of anticancer drug sensitivity. *Nature*. 2012;483(7391):603–607. doi: [10.1038/nature11003](https://doi.org/10.1038/nature11003)

32. Nikolsky Y, Sviridov E, Yao J, Dosymbekov D, Ustyansky V, Kaznacheev V, et al. Genome-wide functional synergy between amplified and mutated genes in human breast cancer. *Cancer Res*. 2008;68(22):9532–9540. doi: [10.1158/0008-5472.CAN-08-308](https://doi.org/10.1158/0008-5472.CAN-08-308)

34. Beroukhi R, Mermel CH, Porter D, Wei G, Raychaudhuri S, Donovan J, et al. The landscape of somatic copy-number alteration across human cancers. *Nature*. 2010;463(7283):899–905. doi: [10.1038/nature08822](https://doi.org/10.1038/nature08822)

35. Beroukhi R, Getz G, Nghiemphu L, Barretina J, Hsueh T, Linhart D, et al. Assessing the significance of chromosomal aberrations in cancer: Methodology and application to glioma. *Proc Natl Acad Sci U S A*. 2007;104(50):20007–20012. doi: [10.1073/pnas.0710052104](https://doi.org/10.1073/pnas.0710052104)

38. Rothenberg SM, Mohapatra G, Rivera MN, Winokur D, Greninger P, Nitta M, et al. A genome wide screen for microdeletions reveals disruption of polarity complex genes in diverse human cancers. *Cancer Res*. 2010;70(6):2158–2164. doi: [10.1158/0008-5472.CAN-09-3458](https://doi.org/10.1158/0008-5472.CAN-09-3458)

Reference

1. Kontro H, Cannino G, Rustin P, Dufour E, Kainulainen H (2015) DAPIT Over-Expression Modulates Glucose Metabolism and Cell Behaviour in HEK293T Cells. *PLoS ONE* 10(7): e0131990. doi: [10.1371/journal.pone.0131990](https://doi.org/10.1371/journal.pone.0131990) PMID: [26161955](https://pubmed.ncbi.nlm.nih.gov/26161955/)



OPEN ACCESS

Citation: Kontro H, Cannino G, Rustin P, Dufour E, Kainulainen H (2015) Correction: DAPIT Over-Expression Modulates Glucose Metabolism and Cell Behaviour in HEK293T Cells. *PLoS ONE* 10(11): e0143268. doi: [10.1371/journal.pone.0143268](https://doi.org/10.1371/journal.pone.0143268)

Published: November 12, 2015

Copyright: © 2015 Kontro et al. This is an open access article distributed under the terms of the [Creative Commons Attribution License](https://creativecommons.org/licenses/by/4.0/), which permits unrestricted use, distribution, and reproduction in any medium, provided the original author and source are credited.